DEVELOPMENT AND ANALYSIS OF DYNAMIC MODELS OF THE *LAC* OPERON

By

Mrs. Asma Ahmed Ben Halim

A thesis submitted in partial fulfilment
of the requirements of the
University of Northumbria at Newcastle Upon Tyne
for the degree of
Doctor of Philosophy

Research undertaken in the Faculty of Engineering and Environment

December 2013

Table of Contents

List of Tables

List of Figures

Declaration

I declare that the work contained in this thesis has not been submitted for any other award and that it is all my own work. I also confirm that this work fully acknowledges options, ideas and contributions from the work of others.

Name: Asma Ben Halim

Signature:

Date:

Abstract

In this work, the mathematical models describing the dynamics of the gene regulatory network of the *lac* operon are considered. The *lac* operon is one of the simplest biological systems which involves the regulation network of three genes. The mathematical models of the regulatory mechanisms of the *lac* system, developed in the literature are based on deterministic or fully stochastic approach to the problem. The aim of the thesis is the development of two stochastic models (reduced and full) based on extension of existing deterministic models with noise terms. The two models reflect different level of complexity of the regulatory processes. The advantage of this approach is based on the realistic description of protein concentrations, protein kinetics and time delays.

Furthermore, a time delayed version of the stochastic model does not exist in the literature for the *lac* operon. Time delays are important for biological systems as the reaction to changes in the system are always with some delays. The full and reduced models of the *lac* regulation, considered in this work, have three and two time delays respectively.

The noise is another essential component of the *lac* model as it regulatory processes are probabilistic. Adding noise to the determinstic model mimics the stochastic behaviour of the system.

The research considers first order stochastic delayed differential equations (SDDEs) and their solutions. Stability properties of the stochastic models are investigated by linearization of the systems of SDDEs. New sufficient conditions of mean square

stability are obtained analytically for these models using Lyapunov function. Additionally, the threshold values for SDDEs are derived. These conditions and threshold values are applied to find analytical solutions of the two models of nonlinear SDDE. Further, numerical solutions of these equations are obtained using Euler Maruyama method. A detailed analysis of the stability regions of the models is performed, analytically and numerically. A specific attention is given to the bistable region as it reflects important biological features of the system linked to the positive regulatory mechanism. It is concluded that the stochasticity can change the boundaries of the bistable region which cannot be obtained in the case of the deterministic model of the *lac* operon.

The issue of modifying the behaviour of the regulatory network is by controlling the input to the system is another important problem considered in this work. First, the variables of the system that are not directly measurable or the measurement is very difficult or expensive, are estimated using the observer method. For the reduced *lac* system, these variables are mRNA and β-galactosidase. In this context, an observer is employed instead of using hardware solutions (such as sensors) which normally are used in the experiment. For the *lac* operon, the available measurement of lactose and allolactose are used to provide an estimate of mRNA and β-galactosidase. A feedback controller is designed to regulate the concentration of allolactose. The main motivation for using an observer is because it is a cheaper alternative solution compared to hardware solution.

This thesis provides a thorough investigation of the stochastic stability of two *lac* operon models and demonstrates that the system behaviour is very sensitive to protein concentrations. It also provides a novel way for estimating such concentrations.

Chapter 1

Introduction

Every cell in living organisms contains a set of genes. A gene network consists of one or more input genes. Its components are genes and proteins and the interactions between them, which, collectively, carry out some cellular functions. A genetic regulatory network is an interaction between DeoxyriboNucleic (DNA), Ribonucleic acid (RNA) and proteins. Gene regulatory network has been well studied in the bacterium Escherichia coli (*E. coli*) [3, 4]. *E. coli* lives in the human body and can be represented as a sequence of genes (DNA) that metabolize lactose in its environment. The genes turned on to beak down lactose are regulatory genes, so called the lactose operon (*lac* operon). *lac* operon was studied by Jacques Monod and Fracois Jacob in 1959 [5]. *E. coli* also produces the aminoacid tryptophan (protein) and is characterized by experiments that detect the behaviour of full molecular systems.

There is a long history of a mathematical modelling of gene regulatory networks. In this work the mathematical models are considered that explain a gene regulatory network constructed from chemical rate rules [6]. The set of chemical reactions can lead to detailed deterministic (ordinary differential equations) and stochastic differential equation models, describing the reaction kinetics of the constituent parts. One goal of the development of mathematical models is to analyze the behaviour of the systems in order to obtain experimentally testable predictions [7, 8].

The *lac* operon is a well-known gene regulatory network, and there are many models

focusing on different regulation mechanisms of the *lac* operon. The first model is by Griffith [4]. However, model that describes the potential for bistability (two stable steady states in a system) in the *lac* operon is by Babloyantz and Sanglier [9]. Some recent works, such as the model of Ozbudak et al. [10], observed that bistability has been experimentally observed on artificial genes but not on natural (lactose). Yildirim and Mackey [11, 12] developed two deterministic models of the *lac* operon represented by two systems of nonlinear delay differential equations, known as the full and reduced models respectively. They found that both models are capable to show bistable behaviour.

The stability of the *lac* operon model is an important feature to show the behaviour of the model and to determine the fate of the model. This work investigates the stability of the full and reduced model of the *lac* operon with stochastic perturbation.

More recently, deterministic differential equations with a noise term (stochastic differential equations) were subjected to a number of studies [13, 14, 15]. The noise term could be presented as a random function and could induce many important effects on the model. However, all reported in the literature studies the stochastic model of the *lac* operon are without time delays and do not investigate the stochastic stability in the bistable region.

A stochastic stability is introduced in this work by adding perturbations to the deterministic models of Yildirim and Mackey [11, 12]. Thus, the stability behaviour for the full and reduced stochastic delay differential equations models are investigated in this research depending on the level of lactose. This allows to investigate very specific question, namely are what the differences between stochastic and deterministic behaviour of the *lac* system.

The problem of modifying the behaviour of the regulatory network by controlling the input to the system is also considered. For this, some of the essential variables of the system are estimated first that are not accessible to measurement. In this context, an observer design is employed. For the *lac* operon, the available measurements of proteins is used to provide an estimate of unmeasurable proteins. the issue of modifying the behaviour of the regulatory network is also considered by controlling

the input to the system.

As a case study, the *lac* operon model for gene regulatory networks with the existence of a feedback loop has chosen. The *lac* operon is an interesting model and a well-described example of a gene regulatory system with a good set of experimentally measured parameters.

1.1 Research motivation

Stability plays a significant role in some of the basic processes of an organism. The model of the *lac* operon can be investigated by focusing on the equilibria points and investigating the stability of a system of delay differential equations. The stability behaviour of the *lac* operon has been the subject of a number of studies [16, 17]. Bistability was observed by Novick [18], whereas Griffith [4] developed the inherent positive feedback in the *lac* operon model that can cause bistability under certain conditions. The recent models to match bistability data are from [11, 12, 19, 20].

The *lac* operon consists of three genes. A stochastic model is more appropriate for the small system, such as the *lac* operon model in *E.coli* [21, 22]. The stochastic behaviour can be considered by adding perturbations to the deterministic model and understanding of the probabilities for a protein to be switched on or off [15, 6].

The investigations of bistability in deterministic and stochastic ordinary differential equations models have been looked at separately. Thus, this study answers the need to investigate the stability and bistability of the system by stochastic delay differential equations.

The stochastic stability can be very useful for showing asymptotic behaviour corresponding to a noise term. It shows the effect of stochasticity and different behaviour of the model within and outside the bistable region.

Another key challenge of the research is the evaluation of difficult to measure proteins of the *lac* operon system by using the measurement of the input and output proteins.

The existing and the proposed models and solutions for the *lac* operon can be summarized in two figures (Figure 1.1 and Figure 1.2).

Figure 1.1 is related to the full and reduced deterministic and stochastic delay differential equations models corresponding to different regulation mechanisms. Figure 1.2 introduces the observer and controller design method for the reduced model.

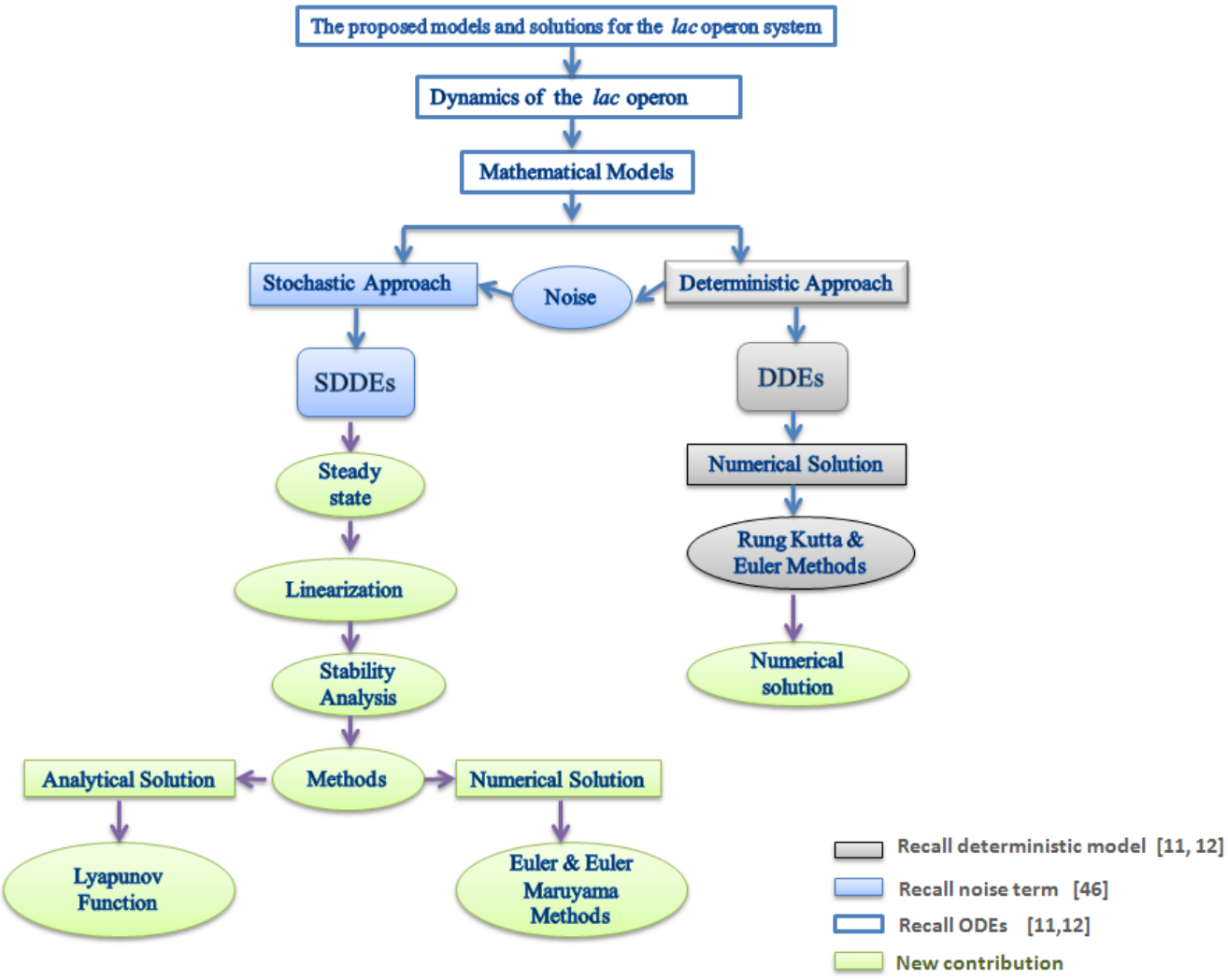

Figure 1.1: Modelling Framework: the grey and blue colours indicate work done in [11], [12] and [46] respectively. Green colour indicates new contribution of this work.

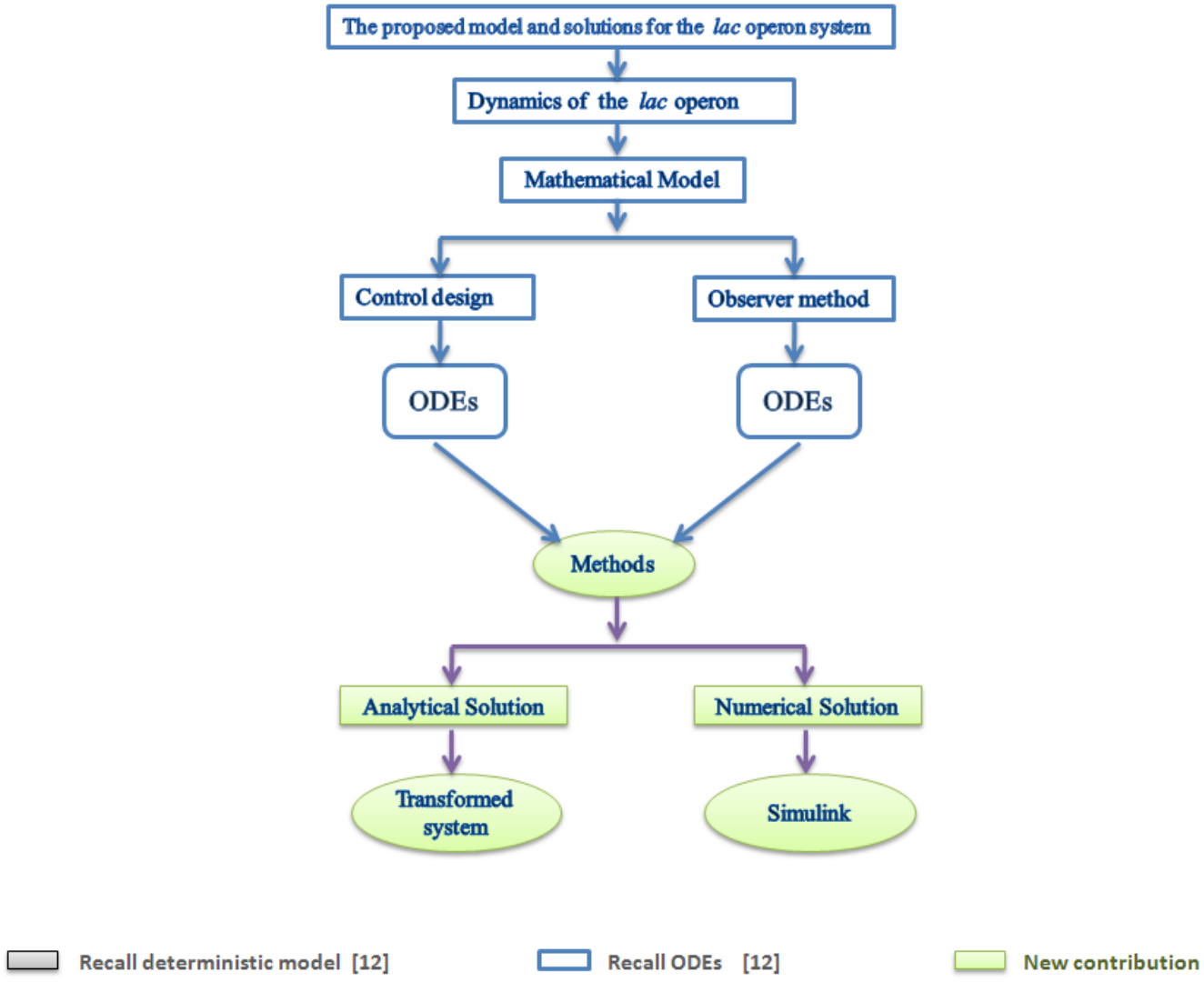

Figure 1.2: Modelling Framework: the blue colour indicates work done in [12]. Green colour indicates new contribution of this work.

1.2 Problem definition

To understand the functions of the gene regulatory network, a mathematical is needed that can capture correctly the complexity of the interactions between the elements of the networks. Ordinary differential equations (ODEs) are a tool known to model the dynamics of gene regulatory networks. As the ODEs are nonlinear, analytical methods and advanced software is required. Stability analysis is an appropriate method for investigating the nonlinear dynamic systems and both, analytical and numerical simulations are used to study their behaviour.

The stochastic process of a continuous time variable used in a very precise context of gene regulatory networks models is now widely applied to describe any phenomenon where the presence of noise in a nonlinear system of ODEs provides an efficient approximation of the behaviour of system under consideration at the particular stationary equilibrium point. However, most of the stochastic models currently proposed for the *lac* operon do not investigate the stochastic behaviour within bistablility region of the *lac* operon with time delay. Thus, the stochastic stability of the full and reduced models of the *lac* operon consisting of five and three delay differential equations respectively, are investigated in the thesis, using Ito stochastic approach involving mean square stability with Lyapunov function. Numerically the models are investigated using dde23 and Euler Maruyama methods. Also, an observer design of the dynamic of the *lac* operon model is employed that uses experimentally measured input and output of the model, to estimate proteins that cannot be easily measured experimentally. In addition, a control design is built to the model to amend the behaviour of the model of the *lac* operon. Numerically the system is analysed using simulink (Matlab) for both observer and control designs.

1.3 Objectives and aims

The aim of this thesis is to study the dynamics of genetic regulatory networks of the *lac* operon and to contribute to the understanding of the mechanisms of genes

interactions that organize such simple biological systems like the *lac* operon. Tow positive feedback mechanism of lactose regulation in the *lac* operon are studied in the thesis, described by stochastic. Extensions of previously developed deterministic models.

The stochastic behaviour is described by adding noise term to the deterministic systems of ODEs with delays. The meaningful solutions that describe the system's behaviour are the stable solutions for the models of the *lac* operon at the particular stationary equilibrium point. For regulatory networks, even in the case of simple system the values of the parameters cannot always be measured accurately and, in practice, the parameters have to be estimated numerically. The methods for evaluating the parameters that provide stable solutions are investigated, in this work.

The thesis has the following objectives:

- Provide an overview mathematical models of the gene regulatory network (GRN) of the *lac* operon. Review the current state of the art for *lac* operon mathematical modelling techniques relating.
- Study an existing deterministic model of the *lac* operon with differential equations with time delay, and perform a stability analysis of the system.
- Study the need for stochastic corrections and introduce noise to the model.
- Investigate the effects of stochastic stability on the *lac* operon models of stochastic differential equations with time delay.
- Analyse stochastic stability of the full and reduced models, of the *lac* operon.
- Investigate the stochastic stability within and around the bistable region.
- Investigate the available of experimental measurements of the inputs and outputs of the *lac* operon model in order to estimate the unmeasured proteins, using observer design.
- Investigate a control design of the *lac* operon model to modify the behaviour of the model and show the behaviour in a required time.

1.4 Thesis contribution

As a result of the study, the following original contributions have been made:

1. A numerical solution for the full and reduced deterministic of the *lac* operon models has been reproduced in order to study the behaviour of the deterministic system (Chapter 4,5).

2. The stochastic stability of the reduced model of the *lac* operon has been formulated and investigated. A full analysis has been carried out to study the effect of noise (Chapter 6).

3. The stochastic stability of the full model of the *lac* operon has been formulated and investigated (Chapter 7).

4. A numerical solution for the reduced stochastic model has been obtained and investigation of the bistable region has been presented (Chapter 6).

5. A numerical solution for the full stochastic model has been obtained and investigation of the bistable region has been presented (Chapter 7).

6. A study of the behaviour of full and reduced stochastic models on the edges of the bistable region has been made (Chapter 6,7).

7. An Investigation has been conducted into the unmeasured state of the reduced model of the *lac* operon, using observer design (Chapter 8).

8. A control design of the reduced model of the *lac* operon has been presented (Chapter 8).

1.5 Structure of the thesis

The thesis is organised in nine chapters. The background of mathematical biology is given in Chapter 2. The chemical kinetic equations and the literature review of

mathematical models that describe gene regulation of the *lac* operon is summarised in Chapter 3. Chapter 4 contains an overview of a published in the literature mathematical model that describe the full model of the *lac* operon with deterministic differential equations with time delays. A reduced deterministic model of the *lac* operon regulation published in the literature with the numerical and analytical solutions is given in Chapter 5. The stochastic stability is introduced and analysis carried out to study the effect of perturbations around equilibrium points for the reduced model of the *lac* operon in Chapter 6. This includes results of the investigation using computer simulations and investigation of the bistable region. The stochastic stability of the full model is introduced and analysis carried out in Chapter 7. The analytical and numerical solution are obtained and investigated in same chapter. A nonlinear closed-loop observer is designed in Chapter 8 to provide estimates of variables that are not measured experimentally for the reduced model of the *lac* operon. It includes a control design of the model and full investigation. Chapter 9 summarizes the research undertaken and the results of the investigation and provides further recommendations for future work. The concepts of stability for the solution of nonlinear ordinary differential equations (ODEs) and some methods used to prove the stability of the dynamical system are described and some tools of the stability are reviewed in Appendix A.

Chapter 2

Biological background

2.1 Biological concepts

For a long time biologists have scientifically investigated how parts of the cell work: they have studied the biochemistry of molecules, such as the structures of DNA, RNA, proteins, and function of membranes, they have developed theoretical concepts about the interaction of elements in different types of genetic networks.

A system biology begins with the study of genes and proteins in an organism using high throughput techniques to quantify the change in response to a given perturbation. These techniques include microarrays to measure the changes in mRNAs, and mass spectrometry, which is used to identify proteins, detect protein modifications, and quantify protein levels. The development of a more methodical view of biological processes is based on the revolution in experimental techniques and methodologies. The biology of a living organism begins with the study of genes and protein. In this section a review of the main biological concepts, relevant to this thesis, is given.

2.1.1 Concept of the gene

System biology begins with the genes in an organism. Each cell in every living thing on earth contains thousands of genes, which carry information that goes toward determining the traits of the living organisms. These traits are described by the genetic information carried by the DNA molecule. Each strand of DNA contains many genes. Genes are coded information in every living organisms for making what is necessary, especially making proteins. Proteins are chains of aminoacids and form the structure of organisms.

DNA acid is the genetic material of a cell, it is a nucleic acid usually in the form of a double helix joined by hydrogen bonds. It is two strands coiled round each other and contains the genetic instructions. Each strand is a chain of chemical structures (nucleotides). The four bases found in DNA are adenine (A), cytosine (C), guanine (G) and thymine (T). These allowable base components of nucleic acids can be polymerized in any order, giving the molecules a high degree of uniqueness. Between the two strands, each base can only pair with one single predetermined other base. The double-stranded structure of DNA provides a simple mechanism for DNA replication. The base on the old strand dictates which base will be on the new strand, and the cell ends up with an extra copy of its DNA.

Transcription, translation, and replication are the essential mechanisms to produce a complex group of proteins. Starting from DNA, the genetic information is transcribed to messenger RNA, and then translated into proteins. There is a single copy of DNA and there may be multiple copies of RNA.

The eukaryotic cells have a nucleus, the DNA is located in the nucleus, but prokaryotic cells do not have a nucleus. DNA is not separated from the cytoplasm by a nuclear envelop, so it is occupies any part of the cell. These two cells, eukaryotic and prokaryotic, are important for determining which kinds of models are appropriate. Prokaryotic cell transcription occurs in the cytoplasm alongside translation, eukaryotic transcriptional regulatory mechanisms are much more complicated than

the prokaryotic ones. For instance, in eukaryotes, promoters may have large numbers of binding sites more or less clustered. Also, in eukaryotes, the genetic material (DNA), and, therefore, transcription, is primarily localized to the nucleus, where it is separated from the cytoplasm (where translation occurs) by the nuclear membrane. DNA is also present in mitochondria; eukaryotes have three nuclear RNA polymerases which transcribe ribosomal RNA (rRNA), messenger RNA (mRNA) and small nuclear RNAs (snRNAs), transfer RNA (tRNA) and other small RNAs.

The translation of mRNA binds to a ribosome, whose function is to create proteins. This process is in eukaryotic cells, where the transcription processes in the nucleus, so mRNA is transported to the cytoplasm, where the translation processes occur and mRNA binds to ribosomes which is move along the mRNA. A sequence of codons in part of mRNA molecule. Each codon consists of three base nucleotides, usually translated into a single amino acid. As the amino acids are linked into the growing peptide chain, they begin folding into the polypeptide chains. This folding continues until the nascent polypeptide chains are released from the ribosome as a mature protein. In some cases, the new polypeptide chain requires additional processing to make a mature protein. In prokaryotic cells, which have no nuclear compartment, the process of transcription and translation may be linked together. Finally, replication is carried out by a complex group of proteins, and using DNA polymerase and its associated proteins, these copy or replicate the master template itself [19, 23].

2.1.2 Gene regulatory networks

A gene network is an image of gene interactions between DNA, RNA, proteins, and small molecules. The investigation of genetic networks has been accelerated by the development of microarray technology. For any organism, gene regulation (regulation of gene expression) is the cellular control of the amount and timing of appearance (induction) of the functional product of a gene.

The gene consists of a coding region and a regulatory region. The coding region is the part of the gene that will be transcribed into messenger RNA (mRNA) and translated

into protein. The regulatory region is the part of DNA that contributes to the control of the gene.

In prokaryotes, there are repressor and activator genes which bind to regions called operators that are generally located near the promoter region which are both are regulatory regions of DNA , where repressors impede RNA polymerase progress along the strand, thus impeding the expression of the gene, and activators encourage the expression of the gene and enhance the interaction between RNA polymerase and a promoter. In eukaryotes, transcriptional regulation tends to involve combinatorial interactions between several transcription factors. In particular, it contains binding sites for transcription factors, which operate by binding to the DNA and affecting the initiation of transcription. Figure 2.1 represents general transcription; P1,..., P4, are promoters and G1,..., G4, are genes. Genes can be viewed as binds in such a network, where TFs are proteins that bind with DNA at promoters. TFs are responsible for regulating when a certain gene is expressed.

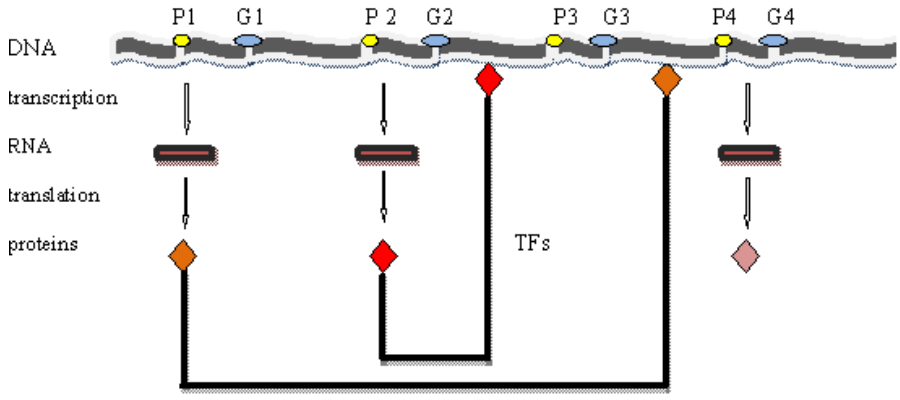

Figure 2.1: General transcription in gene network.

2.1.3 Operon

The operon consists of a group of genes preceded by an operator, a promoter and one or more structural genes controlled to produce mRNA. Operon is one or more genes transcribed on the same mRNA. The operon may also contain regulator genes, such

as a repressor gene which codes for a protein that binds to the operator, shutting a gene down (off) or turning it (on) and inhibits transcription. Operon regulation can be either negative or positive.

The operon occurs in prokaryotes, the prokaryotic cells are parts encode multiple protein pathways that are grouped together and controlled by the same regulation. This process is called an operon. In comparison, the eukaryotic parts contain information from only one gene with one protein.

2.1.4 Operon regulation

In negative inducible operons, a regulatory repressor protein is normally bound to the operator and it prevents the transcription of the genes on the operon.
In positive inducible operons, activator proteins are normally unable to bind to the pertinent DNA. However, certain substrate molecules can bind to the activator proteins and change their conformations so that they can bind to the DNA and enable transcription to take place [19].

2.1.5 Operons in *E.coli*

There are three systems, the phage λ, *trp* operon and *lac* operon, in molecular biology that are most studied in *E.coli* (a simple prokaryote) and that contain all the information about the genes and their interaction.

- The phage λ is a paradigm for molecular switches; it is a virus that infects the cells of the *E.coli* bacteria. The genes of phage λ constitute a single DNA molecule, its chromosome wrapped in a protein coat. The coat is a structure with a head and a tail, all encoded by the chromosome. A phage infects *E. coli* by injecting its DNA into the host, the phage λ injects its genome inside the bacterium and leaves the protein coat outside. The lambda's DNA may behave in a lytic cycle, where phages eventually cause lysis of the host cell, or a lysogenic cycle, where DNA integrates into the host DNA [24].

- The tryptophan operon (*trp* operon) is a paradigm for a repressible operon, and it is an essential amino acid for the synthesis of all proteins composed of a DNA sequence involved in the regulation of gene activity in response to tryptophan. The *trp* operon contains five structural genes encoding tryptophan synthetase, a promoter which binds to RNA polymerase, and an operator which blocks transcription when bound to the protein synthesized by the repressor gene that binds to the operator. This process is different in the *lac* operon. In the *trp* operon, tryptophan binds to the repressor protein and enables it to repress gene transcription products, mRNA then there is translation into five enzymes, that constitutes *trp* operon [25].

- The *lac* operon is activated (turned on) when a high level of lactose available and a low level of glucose; causing a positive feedback loop. The most recent discoveries of the *lac* operon behaviour in the development of molecular and systems biology are briefly reviewed. The *lac* operon is one of the best understood organisms in *E.coli* and is a paradigm for inducible operons. The *lac* operon, shown in Figure 2.2, is a genetic region of the *E.coli* consisting of three adjacent structural genes, a promoter, a terminator, and an operator, required for the metabolism of glucose. The three structural genes in the *lac* operon are: *lacZ*, *lacY*, and *lacA*. *lacZ* encodes β -galactosidase, an intracellular enzyme that catalyzes the breakdown of lactose into glucose and galactose. Gene *lacY* encodes β-galactoside permease, a membrane bound transport protein that pumps lactose into the cell. *lacA* encodes β-galactoside transacetylase, an enzyme that transfers an acetyl group to β-galactosides. Only *lacZ* and *lacY* appear to be necessary for lactose metabolism. Transcription of *lac* structural genes starts with the binding of the enzyme RNA polymerase (RNAP) to the *lac* promoter. The three structural genes are transcribed into a single messenger RNA (mRNA). The *lacI* gene encoding repressor lies near the *lac* operon and is always expressed [19].

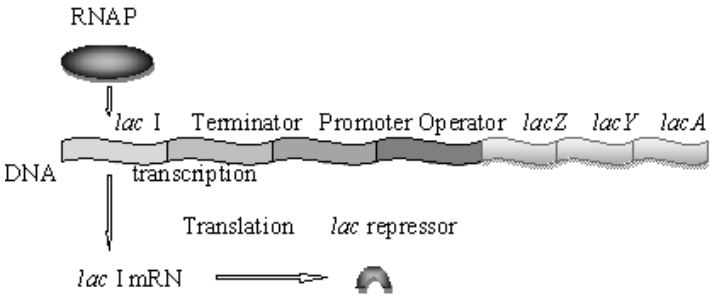

Figure 2.2: Diagram of the *lac* operon, where lactose is not present, *lacI* always transcribed then translated into repressor.

When *E.coli* cells are growing in the presence of lactose, some of the lactose is converted to allolactose (a lactose metabolite) and binds to the repressor, then the repressor is unable to bind to the operator, enabling RNAP from transcription to the *lacZYA* (mRNA) (Figure 2.3). If lactose is absent from the growth medium, the repressor binds to the operator region and prevents the transcription of the *lac* genes Figure (2.4). Therefore, the regulation of mRNA depends on the *lac* repressor, which is controlled by the presence and absence of lactose.

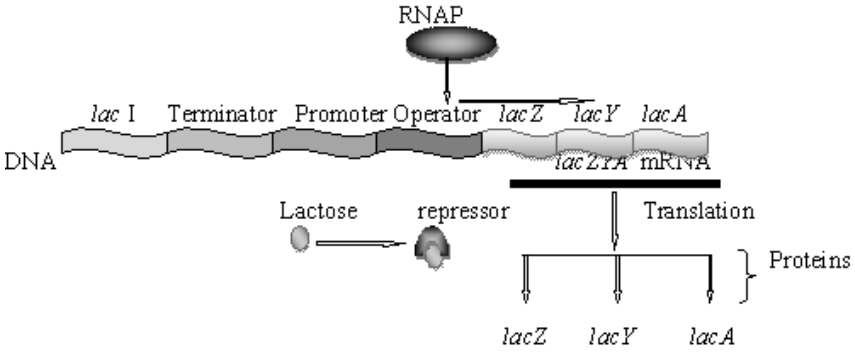

Figure 2.3: Diagram of the *lac* operon with lactose present, inactive repressor, transcription of *lacZYA*.

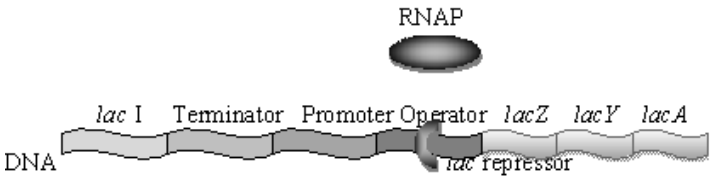

Figure 2.4: Diagram of the *lac* operon with lactose absent, repressor active and no *lacZYA* transcription.

In this thesis the case study of *lac* operon is chosen to illustrate the stochastic delay differential equations used for the description of gene regulation of the *lac* network model.

Chapter 3

An overview of the mathematical models of the *lac* operon

3.1 Introduction

All living organisms involve proteins (enzymes), which act as remarkably efficient catalysts. Substrates are enzymes that react selectively on definite compounds. To understand the role of enzymes regulation in biology processes, one need to study rate of reactions (enzyme kinetics). A more detailed level of explanation is used in the chemical kinetics approach, in which the variables of significance are the concentrations of individual proteins within the cell, and the dynamics describe the rates of production and decomposition of these proteins.

As most genetic regulatory networks of interest involve many components connected through interlocking positive and negative feedback loops, an intuitive understanding of their dynamics is hard to obtain. As a consequence, formal methods and computer tools for the modeling and simulation of genetic regulatory networks will be indispensable. Numerous levels of detail have conventionally been used in modelling gene regulation, and the dynamics describe how groups of genes activate to change one another is states over time.

Modeling gene regulation networks has, in some cases, enabled biologists to predict

cellular behaviour long before such behavior can be experimentally validated. The extent to which biologists can take advantage of the modelling techniques is limited by the computational complexity of gene regulatory network simulation algorithms and efficiency of the numerical methods utilised in the models.

The model of the *lac* operon was described by delay differential equations [11] which are constructed from chemical rate rules. All cells have the same genomic data, but proteins synthesized in each cell differ according to cell type, environmental and time with network of interactions. This chapter reviews previous works of the *lac* operon models. Next section will describe the mathematical description.

3.2 Mathematical description of regulation

Mathematics has played important roles in many fields of biology.
To study system biology one important step is to understand biochemical reactions and networks of genes in cells. Chemical concentrations and variables are converted to differential equations. Some approaches based on gene regulatory networks are being developed by computational biologists, statisticians, mathematicians, computer scientists, engineers and physicists are necessary to obtain experimentally testable predictions. New computer simulations have started analyzing the simplest genetic networks, which are found in bacteria demonstrated network behaviours, such as the *lac* operon [26, 19].

3.2.1 Chemical kinetics

Chemical reactions are important in the description of biological systems. In the simplest terms, a reaction requires reactants and products. Chemical reactions provide unifying notation by which to express arbitrarily complex chemical processes, either quantitatively or qualitatively. Chemical reactions can lead to different computational models (deterministic or stochastic models). The chemical equation definiens

how the state of the system changes. For example, a generic chemical reaction is,

$$n_1A + n_2B \xrightarrow{k} m_1C + m_2D.$$

This means that the reactants between some molecules of types A and B are products formed by reaction and transformed to molecules of types C, D. The coefficients n_1, n_2, m_1 and m_2 are called stoichiometric coefficients and are small integers. The value k is a rate constant (change in concentration in time), which depends on temperature, which is usually given by the Arrhenius equation [27]:

$$k = Ae^{-\frac{E_a}{RT}},$$

where E_a is the activation energy, R is the gas constant, T is the absolute temperature, A is the frequency factor, the value for A and E_a being dependent on the reaction. The state of a system is a snapshot and an important concept in dynamical systems and contains enough information to predict the behaviour of the system for all future times. Different models of gene regulation provide a depiction of the state. Those different models have some similarities: each model predicts which state or states can occur next, it gives just the current state.

3.2.2 Chemical reaction and Michaelis-Menten kinetics

The reaction rate (enzyme kinetics) for a reactant and product in a particular reaction is defined as the amount of the molecule [6]. For a typical chemical reaction consider:

$$n_1A + n_2B \underset{k_-}{\overset{k_+}{\rightleftarrows}} C + D.$$

where A, B, C and D are active masses, $n_1,\ n_2$ are the number of molecules for A and B respectively, and k_+, k_- are affinity constant. The forward and backward reaction rates w_+, w_- are

$$w_+ = k_+[A]^{n_1}[B]^{n_2}, \qquad w_- = k_-[C][D],$$

here [] denotes concentration. If the chemical reaction is in equilibrium, the affinities and reaction rates for forward and backward reaction rates are equal, then

$$K = \frac{k_+}{k_-} = \frac{[C][D]}{[A]^{n_1}[B]^{n_2}}.$$

where K is the reaction dissociation. This equation is known as the law of mass action [19].

Michaelis-Menten kinetics describes the rate of enzyme reactions for many enzymes, involving a substrate S reacting with an enzyme E to form a complex SE, which, in turn, is converted into a product P and the enzyme E.

$$S + E \underset{\longleftarrow}{\overset{k_+}{\longrightarrow}} SE \xrightarrow{k_2} P + E. \tag{3.2.1}$$

The first two arrows indicate that the reaction is reversible, while the single arrow indicates that the reaction can go only one way. k_+, k_- and k_2 are constant parameters associated with the rates of reaction. The mechanism is: one molecule of S combines with one molecule of E to form one of SE, which eventually produces one molecule of P and one molecule of E again. Under certain assumptions, such as the enzyme concentration being much less than the substrate concentration, the rate of velocity of the enzymatic reaction is

$$\frac{d[P]}{dt} = k_2[SE] = k_2 E_t \frac{S}{S + k_m} = V_{max} \frac{S}{S + k_m},$$

where V_{max} is the maximum velocity, E_t is a E_{total} where $E_t = [E] + [SE]$ and $\frac{d[P]}{dt}$ is the product rate of formation. When $[S]$ substrate equals k_m, $\frac{S}{S+k_m}$ equals 0.5, the rate of product is half of the maximum velocity rate, but if S is larger than k_m, $\frac{S}{S+k_m}$ approaches 1, then the rate of product is equal to $k_2[E_t]$ [6, 19, 8].

The model for Michaelis-Menten kinetics takes the form of an equation describing the rate of enzymatic reactions, by relating reaction rate $\frac{d[P]}{dt}$ to S, the concentration of a substrate S, given by

$$\frac{d[P]}{dt} = V_{max} \frac{S}{S + k_m}.$$

3.2.3 System state

The state of a system at a given time should contain enough information to predict the behaviour of the system for all times [8].

A model is a plan, representation, or description designed to show the structure or dynamic of a system. However, a model can also be abstract or conceptual, when ordinary or technical languages are used to represent something in the real world.

The following types of models are used in literature to describe gene regulation networks: Boolean network models, differential equations models and stochastic models are most widely used for the description of gene regulation [23, 8, 26].

- Boolean network models

  Boolean models consider each gene to be in one of two states, as either expressed (on/1) or not expressed (off/0) which are represented as activated and inhibited. There are several ways in this model. From a given state for the system of genes, the system moves deterministically to a next state (Boolean state), to express this is to write out a truth table, which specifies what the next state is for each current state. Boolean functions provide an alternative representation of truth tables. Each variable is written as a function of the others. Truth table and Boolean functions are equivalent in the sense that one can convert from one to the other using standard techniques. Some authors have developed a technique based on information theory that has been applied to biological systems. The kinetic logic and the continuous logical networks are more complex and more related to the detailed biology than are Boolean networks [23].

- Kinetic logic models

  This formalism has greater predictive value and more granularity than Boolean networks. It considers levels; for example, when there is no expression, this is indicated by 0, low expression is indicated by 1, medium expression is indicated by 2, and high expression is indicated by 3. However, different genes may have a different granularity; one gene may only have states 0 and 1, while another may have multiple intermediate levels. In order to determine which model is suitable for the system, one must consider first two changes of state with two constraints: continuity and asynchronicity. The meaning of continuity can be explained by the following: if the current state of a gene is 0 and its desired next state is 3, then its actual next state will be 1; that is, it takes one step at a time

toward its final goal. In biological terms, this means a gene is not expressed. One can see the difference between kinetic logic formalism and Boolean network models, where all genes change their states at the same time; in addition, the functions describing the changes of state are more complicated than in Boolean networks, so more data is needed to find the function. The predictions of this model are more tied to the biology than Boolean networks.

- Differential equation models

  Differential equation models provide a general framework in which gene regulation processes are considered. By making certain assumptions, one can transform essentially any system of chemical reactions and physical constraints into a system of ordinary differential equations. It has to be noted that not all systems can be modelled with differential equations. The changes of state in differential equations assume that the interactions in the system are continuous or deterministic. Discontinuous transitions in deterministic systems can be modelled with various hybrids between discrete and continuous dynamics, including continuous time logic, special kinds of grammars, and discrete event systems. Nondeterministic systems, where the same state can lead to different possible outcomes, must generally be modelled in a different framework; one example taken from physics is the Langevin approach (approximations, of the stochastic model), which will be reviewed in the next part.

  To solve a differential equation or a system of differential equations, one needs the initial values condition. In most cases, equations of gene regulatory networks can be solved numerically and there are many tools to solve differential equations.

- Langevin and Fokker-Planck approaches

  The langevin approach is an approach for the mathematical modelling of the dynamics of system biology and is a system of differential equations, where a noise term is added to each equation. The noise term is the random function and can induce many important effects on the dynamic systems [23]. The Langevin

equation can be reformulated as a FokkerPlanck equation that regulates the probability distribution of the random variable.

Fokker-Planck equations are approximations of the stochastic model. One starts from a probabilistic framework and writes a full set of equations that describes the change in probability distribution as a function of time, while the probability distribution is a continuous function of concentration. This leads to a certain partial differential equation of the probability distribution [23].

- Stochastic models

  Stochastic models consider the individual molecules involved in gene regulation, rather than using concentrations and making the continuity assumption of differential equations. The state in stochastic models indicates how many molecules of each type are present in the system. The state changes discretely, but which change occurs and when it occurs is probabilistic, the rate constant specify the probability per unit time of a discrete event happening. For example, consider the simple chemical equation:

$$A \xrightarrow{k} \tilde{A}$$

  where the reactant A is the molecule transformed into the product $\tilde{A}$. The probability of this event happening to a given molecule of A in a given time dt is given by kdt. Hence, the probability of some molecule of A being transformed in a small time is $k\{n_a\}dt$, where $\{n_a\}$ indicates the number of molecules of A present. For small systems, the list of the numbers of molecules is a configuration, the state is the probability distribution over all configurations; if the number of configurations is small, then the numbers of probability is also small. For reactions with more than one reactant, the probability per unit time is given by the rate constant times the number of molecules of each reactant, this is completely similar to the differential equations. The chemical equilibrium in the stochastic framework is not possible to define, as any reaction that occurs changes the number of molecules. Thus, in stochastic models, there is an equilibrium probability distribution, a set of probabilities that the system has

certain numbers of molecules [23].

Table 3.1 shows a comparison between different models. Hence, the deterministic and stochastic models are appropriate for gene regulation network (GRN) of the *lac* operon model.

Table 3.1: Comparison between different models for gene regulatory networks.

The modeling approaches	Suitability	Advantages	Weaknesses
Boolean models	Suitable for describing large GRN because it is not required kinetic parameters.	Are simple theoretical model and is a simplest description of a biological system. Easily to recognize the equilibrium states.	The model Assuming that all genes change state at the same time. Can not represent necessary biological details.
Kinetic logic models	Suitable for describing large GRN because it is not required kinetic parameters.	These models allow genes change state at independent rates and try adjusting the rate at which the system goes from one state to another. The prediction of this model are more closely to the biology.	Required more data to find the function. The description of the state changes are more complicated than in Boolean networks.
Differential equations models	The model assuming that the state changes are continuous and deterministic.	Provided a general framework in which to consider the processes of gene regulation. Given the transition rates between all states. Many method exist to solve and analyze systems of differential equations.	Can not model discontinuous transitions in deterministic systems.
Stochastic models	Consider non-deterministic small systems and making the county assumption of differential equations.	Stochastic model described by either Langevin equation or by Fokker-Planck equation, both are give very good approximations. The difference between approximation and exact solution is much smaller than the variance of the approximation. Many computational methods exist to solve stochastic systems.	The solution is particulary difficult if the number of states is infinite and not small (high number of molecules and long time steps).

3.3 Overview of the Mathematical models of the *lac* operon

The study of living organisms involves many mathematical ideas; the most basic of these is the idea of a dynamics of genetic network. The biological systems are formed by variables that describe the state of the system. Many models in biology (see Section 3.2.3) have been prepared using deterministic or stochastic ordinary differential equations with time delays.

Deterministic models are based on the approximation of an infinitely large population size. There are different ways of computational methods for modelling genetic networks [23]. Differential equation models provide a general framework in which to consider gene regulation processes. By making certain assumptions, one can describe the reaction kinetics of the constituent parts that can transform into a system of differential equations, considering the transition rates between all microscopic states. The concentrations of products are modelled by continuous functions of time, regulated by differential equations. When the number of states becomes too large, the genetic network can be described well as a continuous system and differential equations model is a good approximation.

A number of models were developed to describe the *lac* system essentially using Jacob Monod's description [3] and several of deterministic models have been developed with different goals. Farina [28] proposed the *lac* operon as a hybrid model of the regulatory mechanism dependable on the action of lactose by the bacterium *E.coli*. There are two different parts in this system: parts that are involved into the regulation at the genetic level, and parts that take into account the metabolism of the cell, involving the kinetics of enzymatic catalyse reactions. The model consists of two linear equations establishing the dynamics of the RNA and of the enzymes. In any hybrid system, the biological switches are modeled by instantaneous switches. This set of variables offers several advantages: the equations can be solved formally, and it allows an analytical analysis that makes possible a qualitative interpretation of the curves obtained.

Introduce the work of Almaas et al [29] is used Flux balance analysis (FBA is a mathematical approach for analyzing the flow of metabolites through a metabolic network). The authors implemented a FBA of the *E.coli* metabolism. Whereas, most metabolic reactions have low fluxes, the overall activity of the metabolism is dominated by several reactions with very high fluxes. *E.coli* responds to changes in growth conditions by reorganizing the rates of selected fluxes predominately within this high flux backbone. The interplay between the underlying of the metabolic network of *E.coli* and its functional organization involves the global features of potentially able to be achieved flux states. The cellular metabolism has been assumed in a steady state and optimized for the maximal growth rate which offer experimentally verifiable predictions on the flux states of the cell, FBA have been used to calculate the flux for each reaction using linear optimization, which provides a measure of relative activity of each reaction and provides successful in analyzing the capabilities of cellular metabolism, the ability to calculate the relative flux values of metabolic reactions and the properties of alternate optimal growth states in a wide range of simulated.

An important feature that was studied in gene regulatory network models is bistability. The bistability of the *lac* operon was observed more then fifty years ago by Novick and Weiner [18]. The positive feedback loop creates the potential for bistability [4, 30] which means that for certain extracellular inducer concentrationsis that two stable steady states exist for the *lac* operon in a different perspective, referred to as induced and uninduced states for high and low induction respectively.

The model of Ozbudak et al. [10] describes a set of experiments that allowed them to quantify the *lac* operon expression level in single bacteria. Their results confirmed the existence of bistability in the *lac* operon. However, when Ozbudak et al. repeated their experiments using lactose as a natural inducer, they found no evidence for bistability. This provided new quantitative data that raised questions which were answered in the papers of [19, 20, 31] and concluded that the bistability does not disappear because of lactose metabolism. From the model of Jacob- Monod [3] for the *lac* operon Nikolov et al. [32] have analyzed the dynamical role of time delays in protein cross talk. They have considered the time delay as a bifurcation parameter.

Yildirim and Mackey developed and analyzed, analytically and numerically, two sets of models [11, 12], for the regulation of the *lac* operon in *E.coli*. The first model is based on first order differential equation [11] that describes the positive feedback mechanism of the operon, consisting of two loops (Figure 4.1). The simplified model [12], is based on the inner feedback loop only (Figure 5.1). The authors assumed equilibration of internal and external lactose and there is a constant permease concentration. The justification for this assumptions is to know that the positive feedback regulation of mRNA production by allolactose is sufficient to display bistability which is important dynamic characteristics of the *lac* operon. Both models were investigated analytically and numerically using published parameter values [1, 2] and demonstrated that the steady state displays bistability depending on the lactose concentration and growth rate.

The continuation of this model, [17], develops a more detailed mathematical model of the lactose operon which includes catabolite repression, inducer exclusion, lactose hydrolysis to glucose and galactose, and synthesis and degradation of allolactose. For catabolite repression two models have been tested: cAMP synthesis inversely correlated with the external glucose concentration, and synthesis inversely correlated with the glucose transport rate. In addition, two models for the phosphorylation of the glucose produced from lactose hydrolysis have been tested: phosphorylation by intracellular hexokinase, and secretion of glucose and subsequent phosphorylation upon transport back into the cell. The former two models resulted in no significant differences between them being observed, the latter two models resulted in weak catabolite repression when the glucose produced from lactose was transported out of the cell, whereas the former model showed no catabolite repression during growth on lactose. Parameter sensitivity analysis indicates the importance of key parameters to *lac* operon expression and cell growth. The model equations are numerically solved using Runge Kutta method to investigate the influence of glucose dependent regulatory mechanisms (catabolite repression and lactose uptake) on the system bistable behaviour, there is good agreement between the simulation predictions and the experimental data. The model is reliable enough to numerically analyze the system bistable

behaviour and explore the individual effects of catabolite repression and inducer exclusion. Furthermore, this model helps to understand the dynamic response via the mechanisms of catabolite repression and inducer exclusion, of the lactose operon to extracellular glucose, and provides quantitative predictions.

The stochastic model describes the probabilistic processes in finite size populations. Namely, stochastic models transform reaction rates into probabilities and concentrations into numbers of molecules, allowing understanding how noise influences a system. The probability that the next state consists of a certain number of molecules given the current state, can be expressed in a straightforward way, so various computational methods have been developed to deal with this framework.

Deterministic differential equations with a stochastic noise term is a way of modelling regulatory networks that has been used successfully for description of some biological systems and has its origin in physical and chemical. It describes a continuous system, given by a differential equation, with added stochastic noise term where the same state can lead to different possible outcomes. This is known in the literature as the Langevin approach [6]. A Langevin model is given by a system of differential equations, where a noise term (random function) is added to each equation [7, 33].

The noise is another essential component of the *lac* model as it regulatory processes are probabilistic. Adding noise to the determinstic model mimics the stochastic behaviour of the system. The stochastic model can be considered by adding perturbations to the deterministic model based on reaction kinetics rules. In the paper of Mettetal et al [34], a deterministic model is used to predict the measure of population distributions of protein numbers as a function of time in the *E.coli* lactose uptake network (*lac* operon), first they construct a deterministic model which is composed of three equations. It is shown that the system can have either a monostable or bistable, depending on the concentration of extracellular thiomethyl β-D-galactoside (TMG), the numerical results are calculated using Euler method. The paper has introduced a dynamic stochastic model which consists of this processes: mRNA production and mRNA degradation, protein degradation, and global noise. The authors show that prediction of dynamic distributions requires only a few noise parameters in addition

to the rates that characterize a deterministic model. It is important to note that the stochastic model predicts the experimental dynamics without any fit parameters.

Stochastic models allow understanding of the probabilities for a gene to be on or off or in a process to be turned on, associated with time to extinction [15]. Within this framework, Santillan et al. [19] developed a model of the *lac* operon for the regulatory pathway in a system of three differential equations and they introduced a stochastic term to account for the noise in the system due to extracellular glucose and lactose concentrations. The model studies the origin of bistability and indicates that bistability can help guarantee that *E.coli* consumes glucose and lactose in the most efficient possible way. The model of Johan [35] discussed some analytical studies of constitutive expression between theoretical description, focusing on gene mRNA protein model (feedback analysis excluded) in the stochastic modelling of these processes. The analysis in the paper of McAdams and Arkin [36] emphasizes the mechanisms of protein production. Simulation of the process of gene expression shows that proteins are produced from activated promoter in short bursts of proteins that occur at random time intervals. The random expression can produce probabilistic outcomes in switching mechanisms that select between alternative regulatory paths.

In the paper of Vilar et al [13] three different level of description the *lac* operon in *E.coli* are used to illustrate that the current state, applicability, and limitation of cellular processes: molecular, cellular, and that of cell population into a single model. They model the dynamics of the induction process using four ordinary differential equations, which can be solved numerically, and the results show some differences between experimental and simulation results. In the simulations all the cells eventually become induced. In the experiments, the production of β-galactosidase for suboptimal inducer concentrations, which is an indication of the coexistence of the induced and uninduced cells, cause that the induced and uninduced cells grow at a different rate. In addition, Vilar et al do not explain what makes the cell switch from the uninduced to the induced state. Furthermore, how the intrinsic randomness of molecular events affects the system, and how induction depends on the molecular aspects of gene regulation.

Recently, a number of studies of the *lac* operon have been developed with different noise types. Experimentally, the work [22] have measured the amount of intrinsic noise (generated by transcription and translation) and extrinsic noise (from the cell cycle) of the *lac* repressible in different *E.coli* strains. On the other hand, a theoretical framework was presented in [37] that can interpret the experimental measurements [22] of stochasticity in gene expression and verified that the intrinsic and extrinsic noise can often be of similar measurement.

Stochastic gene expression can cause switching between high and low inductions in a bistable region. The study of the ODEs of the *lac* operon [38], induced by lactose metabolism, showed a bistable switch shifted from inducer to low inducer, and vice versa. Nevertheless, [39] concluded that the stochastic nature of gene expression in the *lac* operon cannot avoid the inherent disadvantages of bistability and showed that bistability is even more harmful in the stochastic then in deterministic system. The same authors concluded [40] that in silico evolved *lac* operon exhibits bistability for artificial inducers but not for lactose. However, the model [41] showed that the noise enables switching from induced to uninduced state, and from uninduced to induced state only when external lactose is either at the beginning or at the end of the bistable region. Despite the differences between the kinetics of systems [41] and [10], the author [42] has modelled both systems by adding small noise and found that the behaviour of both models is qualitatively similar. The study [43] found that noise in protein production is minimized in genes for which it is likely to be most harmful. The authors [44] presented a comparative analysis of correspondent deterministic and stochastic models for the *lac* operon system. The incorporation of biological information into the models revealed the effect of biomolecular parameters in the presence and absence of stochasticity. The stochastic system of the *lac* operon was investigated in [45] with and without circuit design method under process molecular noises for the improvement of robust stability and molecular noise filtering ability of nonlinear gene network to attenuate molecular noises. The author is used linear matrix inequalities (LMI) technique (that gives a procedure for determining the stability bound) and fuzzy interpolation scheme.

The stochastic models currently proposed for the *lac* operon do not investigate the stochastic stability with mean square stability with time delay which is one of the aims of this research. The basic theory of stochastic stability of dynamical systems can be found in [46, 47, 48, 49].

Next two chapters 4 and 5 recalls the models of Yildirim and Mackey and confirm the results obtained in [11, 12] to developed a stochastic version of it.

3.4 Summary

The purpose of the mathematical models is to simplify the network in an appropriate way and provide solutions that can explain biological findings, a lot of methods exist for this propose (Section 3.2.3). The dynamic of the biological systems studied may only be known approximately. Thus, the notion of a stablility is a useful tool for studying the dynamics of the systems, the stability of the dynamical system includes that initial conditions for which the trajectory (the solution curve that get tracked out in state space) would be balanced or equivalent. This chapter described a survey of the *lac* operon model, contains a review of the current state of art for the *lac* operon mathematical modelling technics and current results.

Chapter 4

The full deterministic model of the *lac* operon

4.1 Introduction

As known in Chapter 3, many different mathematical models of gene regulatory have been formulated depending on the mechanisms of a system's dynamics. In this chapter the mathematical model of the *lac* operon in *E.coli* ([11]) is presented. This model is based on five delay differential equations which are proposed and solved numerically and analytically in [11] using published parameter values. The result are reviewed here and numerical solutions within bistable region are shown.

4.2 Yildirim and Mackey model

The *lac* operon consists of a promoter, operator region and three larger structural genes *lacZ*, *lacY*, and *lacA*. The a preceding regulatory operon is responsible for producing a repressor R protein. In the absence of glucose available for cellular metabolism, but in the presence of external lactose, L_e, lactose is transported into the cell by a permease, P. Intracellular lactose, L, is then broken down into allolactose, A, first and then glucose and galactose by the enzyme β-galactosidase, B. The allolactose

feeds back to bind with the lactose repressor and enables the transcription process to proceed. One possible dynamics of this control mechanisms is illustrated in Figure 4.1. This section considers the dynamic models proposed by Yildirim and Mackey's model [11] and recalls the results of this works.

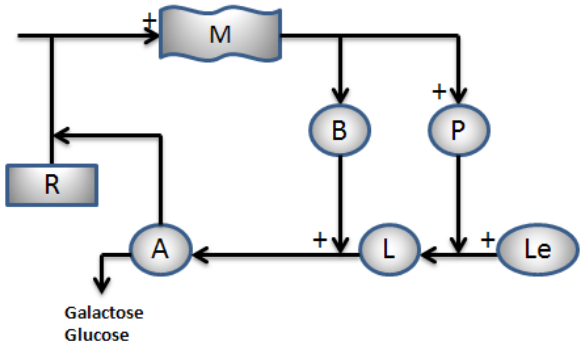

Figure 4.1: One possible mechanism for control of the *lac* operon

Development of the full model Yildirim and Mackey's model [11] consists of five delay ordinary differential equations (DDEs) given as follows:

$$\frac{dM}{dt} = \alpha_M \frac{1 + K_1(e^{-\mu\tau_M} A_{\tau_M})^n}{K + K_1(e^{-\mu\tau_M} A_{\tau_M})^n} - \widetilde{\gamma}_M M \tag{4.2.1}$$

$$\frac{dB}{dt} = \alpha_B e^{-\mu\tau_B} M_{\tau_B} - \widetilde{\gamma}_B B \tag{4.2.2}$$

$$\frac{dA}{dt} = \alpha_A B \frac{L}{K_L + L} - \beta_A B \frac{A}{K_A + A} - \widetilde{\gamma}_A A \tag{4.2.3}$$

$$\frac{dL}{dt} = \alpha_L P \frac{L_e}{K_{L_e} + L_e} - \beta_{L_1} P \frac{L}{K_{L_1} + L} - \beta_{L_2} B \frac{L}{K_{L_2} + L} - \widetilde{\gamma}_L L \tag{4.2.4}$$

$$\frac{dP}{dt} = \alpha_P e^{-\mu\tau_P} M_{\tau_P} - \widetilde{\gamma}_P P. \tag{4.2.5}$$

The equations represent the dynamics for all of mRNA, M, production, β- galactosidase, allolactose, lactose, and the permease respectively. The delays, τ_M, τ_B, are due to the transcription and translation process. Here $A_{\tau_M} = M(t-\tau_M)$, $M_{\tau_B} = M(t-\tau_B)$ and $M_{\tau_P} = M(t-\tau_P)$ are the value of variable A delayed with τ_M, the value of variable M delayed with τ_B and the value of variable M delayed with τ_P respectively. Whereas, $\widetilde{\gamma}_i = (\gamma_i + \mu)$, $i = M, B, L, A, P$ are the rates of loss term and α_i, $i = M, B, L, A$ and P

are the production terms required to produce M, B, A, L, P. In the equation above μ is the growth rate dependent on allolactose dilution during the transcriptional period. In this model, the total operator and repressor concentrations are assumed constant and it is assumed that the amount of repressor bound to the operator region is small compared to the total repressor concentration.

Yildirim and Mackey [11] showed that this system of five equations is capable of bistable steady-state behaviour when the value of L_e is between $27.5 - 60\ \mu M$, and this corresponds to a bifurcation in the model's dynamics.

The system (4.2.1-4.2.5) have been numerically solved in [11] using published parameter values [1, 2], given in Table 4.1. The authors showed that the bistable steady states behaviour depending on the extracellular lactose concentration.

Parameter	Value	Parameter	Value
γ_M	$0.411 min^{-1}$	γ_B	$8.33 \times 10^{-4} min^{-1}$
γ_A	$1.35 \times 10^{-2} min^{-1}$	γ_L	$1.6043 min^{-1}$
γ_P	$0.65 min^{-1}$	α_M	$0.997 \mu M$
α_B	$1.66 \times 10^{-2} min^{-1}$	α_A	$1.76 \times 10^{4} min^{-1}$
α_L	$2908.8 min^{-1}$	α_P	$10 min^{-1}$
K	7200	K_1	$2.52 \times 10^{-2} \mu M$
K_A	$1950 \mu M$	K_L	$970 \mu M$
K_{L_2}	$972 \mu M$	K_{L_1}	$1810 \mu M$
K_{L_e}	$260 \mu M$	β_A	$2.15 \times 10^{4}\ min^{-1}$
β_{L_1}	$2.65 \times 10^{3} min^{-1}$	β_{L_2}	$7.614 \times 10^{3} min^{-1}$
μ	$3.03 \times 10^{-2} min^{-1}$	μ_{max}	$3.47 \times 10^{-2} min^{-1}$
τ_M	$0.1 min$	τ_B	$2\ min$
τ_P	$2.38 min$	n	2

Table 4.1: The parameters for the *lac* operon regulatory system from [1, 2]

4.3 Numerical simulation of the full model

The Numerical solution of (4.2.1- 4.2.5) was derived with Matlab using routine dde23. It reproduces the numerical solution proposed by Yildirim and Mackey [11]. The range of external lactose concentrations over which three steady states exist (bistable region) is given in [11, Figure 2]. The numerical simulation of M, B, A, L and P

with three time delays are shown in Figure 4.2. It represents the solution of the deterministic model with initial values taken from the steady state values. The steady state $(M_\star, B_\star, A_\star, L_\star, P_\star)$ point obtained by solving the system when the left hand side of (4.2.1- 4.2.5) are zero, namely $\frac{dM}{dt} = \frac{dB}{dt} = \frac{dA}{dt} = \frac{dL}{dt} = \frac{dP}{dt} = 0$. the following steady states numerically obtained $(M_\star = .154\mu M, B_\star = 0.104\mu M, A_\star = 142\mu M, L_\star = 139\mu M, P_\star = 2.16\mu M)$ when $L_e = 30\mu M$.

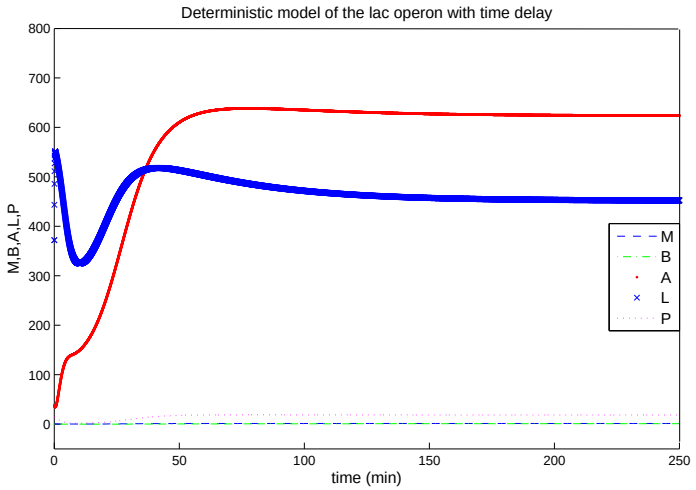

Figure 4.2: Full deterministic model of the *lac* operon with time delays, $M, B, A, L, P\,(\mu M)$ concentration versus time (min).

Next table (4.2) shows the level of external lactose concentrations of the *lac* operon.

external lactose	0-27 μM	One steady state	Stable
external lactose	27.46 μM	Two steady states	Two stable
external lactose	27.5- 62 μM	Three steady states	Two stable and one unstable
external lactose	62.4 μM	Two steady states	Two stable
external lactose	62.5-80 μM	One steady state	Stable

Table 4.2: External lactose level when there are one, two and three steady states solutions

Stable and unstable steady states Figure 4.3 illustrated the evolution with time of the three steady states for allolactose when $L_e = 30\mu M$ (Table 4.2). $A1, A2, A3$ will be referred to as follows: The lower position of the state $\overrightarrow{\mathbf{S}} = (M, B, A, L, P)$

containing the coordinate $A1$, is stable and uninduced (repressible), the middle position, containing $A2$ is unstable and the upper position including $A3$ is stable and induced.

The numerical solutions for the full model either converged to the lower or upper coordinate for various initial conditions as shown in Figure 4.3. For this simulation, two initial allolactose levels were chosen close to the coordinate $A2$ in middle position (unstable) and all other variables M, B, L, P kept at their steady state values (Table 4.3). Corresponding to the values on the coordinate $A2$ in middle position for initial allolactose values are bigger or less then $A_\star$ ($A2 \gtrless A_\star$), the simulated curve converged to the value on the uninduced or to the value on induced curve (Figure 4.3) respectively. However, the boundary initial values on unstable curve separate the behaviour where the states are attracted to the uninduced or induced steady state.

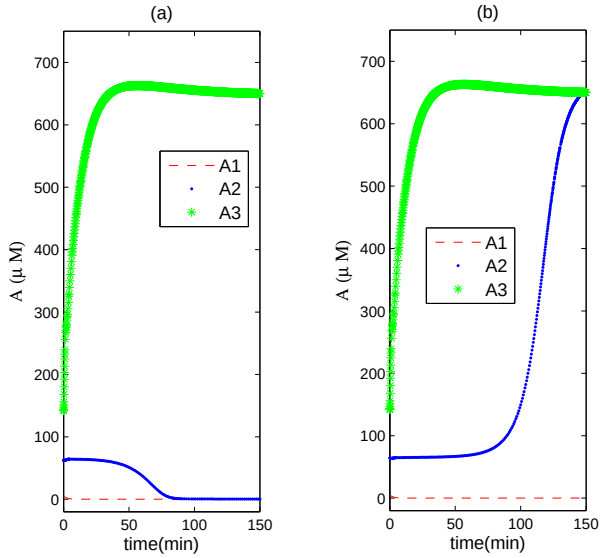

Figure 4.3: Deterministic (full) model of the *lac* operon showing allolactose when $L_e = 30\mu M$. The initial values are given in the text.

Below is a table of multiple steady states and their numerical values when $L_e = 30\mu M$.

ON	Interposition	OFF
induced	(induced or uninduced)	uninduced
stable	unstable	stable
(upper branch)	(middle branch)	(lower branch)
(M3,B3,A3,L3,P3)	(M2,B2,A2,L2,P2)	(M1,B1,A1,L1,P1)
$(.154, 0.104, 142, 139, 2.16)\mu M$	$(0.0346, 0.0234, 64.3, 136, 0.438)\mu M$	$(0.00214, 0.00144, 4.31, 101, 0.0298)\mu M$

Table 4.3: Three steady states values when $L_e = 30\mu M$.

4.4 Summary

The dynamic behaviour of the lactose regulation system of the *E.coli* bacteria [11] is reviewed. The mathematical model of the *E.coli* bacteria of Yildirim and Mackey, which consists of a system of five delay differential equations is recalled. The model verified that this system is capable of bistable behaviour depending on the external lactose. However, when there are three coexisting steady states, the simulated solutions show that the unstable solution converged to either the induced or uninduced coordinate depending on the initial values. Next chapter, studies a simplified model of the *lac* operon, which ignores the feedback loop including the permease. This allows a rigorous analytical solution that shows bistable solution without permease.

Chapter 5

The reduced deterministic model of the *lac* operon

5.1 Introduction

Yildirim and Mackey simplified the model in Chapter 4 using the inner feedback loop only on Figure 4.1. Thus, the dynamics of L and P is not considered which simplifies the model to three differential equations with two time delays [12]. In this chapter, the analytical and numerical results of this model are recalled and the stable and unstable regions are specified.

5.2 Reduced model of Yildirim and Mackey

Yildirim and Mackey [12] proposed a model assuming a constant quantity of lactose inside the cell (equilibrium of internal and external cellular lactose). The simplified model allows to understand better the functionality of M, B, A in the regulation mechanism (Figure 5.1). This led to a reduced model based on a system of three differential equations with two time delays. This model ignored the permease dynamics and assumed a constant permease concentration.

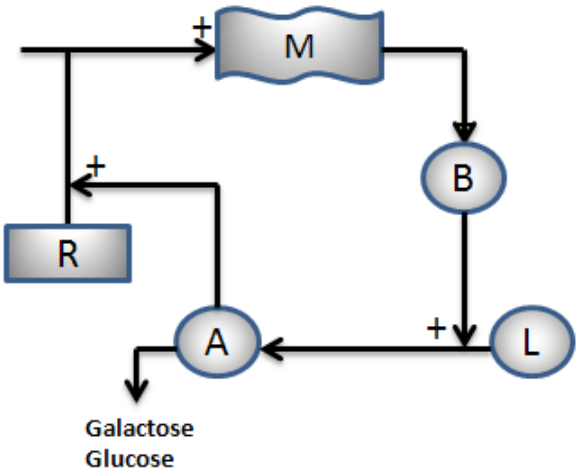

Figure 5.1: Reduced model of the *lac* operon

The system of two delay differential equations (DDEs) is:

$$\frac{dM}{dt} = \alpha_M \frac{1 + K_1(e^{-\mu\tau_M} A_{\tau_M})^n}{K + K_1(e^{-\mu\tau_M} A_{\tau_M})^n} - \widetilde{\gamma}_M M \tag{5.2.1}$$

$$\frac{dB}{dt} = \alpha_B e^{-\mu\tau_B} M_{\tau_B} - \widetilde{\gamma}_B B \tag{5.2.2}$$

$$\frac{dA}{dt} = \alpha_A B \frac{L}{K_L + L} - \beta_A B \frac{A}{K_A + A} - \widetilde{\gamma}_A A. \tag{5.2.3}$$

where all parameters are the same as in the full model (see Chapter 4).

The reduced model of the *lac* operon was numerically solved by Yildirim and Mackey in 2004 using published parameter values [1, 2] given in Table 4.1. It was shown that the steady states behaviour for the reduced model is similar to the full model and the model exhibits bistability, depending on the lactose concentration.

5.2.1 Analytical and numerical solution

Finding the equilibrium for nonlinear dynamical systems may help determine the possible initial conditions that makes sense biologically. Then one can study the properties of the dynamical system near the equilibria. The nonlinear system can be understood by characterizing the behavior of the system linearized near equilibrium points. This behavior is determined by the eigenvalues of the linearized system to show whether the behaviour of the system is close to the equilibrium points [50].

Steady state for the *lac* operon model The steady state point (M_*, B_*, A_*) for the reduced model is defined as the point where,

$$\frac{dM}{dt} = 0, \frac{dB}{dt} = 0, \frac{dA}{dt} = 0$$

Thus, we obtain a definition of the steady state as the state (M_*, B_*, A_*) by

$$f(A_*) = \chi \frac{A_*}{[h(L) - \frac{\beta_A}{\alpha_A} g(A_*)]}, \tag{5.2.4}$$

where the functions are defined as follows,

$$f(A_*) = \frac{1 + K_1(e^{-\mu\tau_M} A_{*\tau_M})^n}{K + K_1(e^{-\mu\tau_M} A_{*\tau_M})^n}, \quad h(L) = \frac{L}{K_L + L},$$

$$g(A_*) = \frac{A_*}{K_A + A_*}, \quad \chi = \frac{\widetilde{\gamma}_M \widetilde{\gamma}_B \widetilde{\gamma}_A e^{\mu\tau_B}}{\alpha_M \alpha_B \alpha_A}. \tag{5.2.5}$$

The solution can be found graphically by plotting with Matlab the left and right hand sides of Equation (5.2.4) and is given on Figure 5.2. The red curve represents the left hand side (LHS), and the other three curves represent the right hand side (RHS) for three different values of L. The intersection between the two curves RHS and LHS gives the location of the steady state.

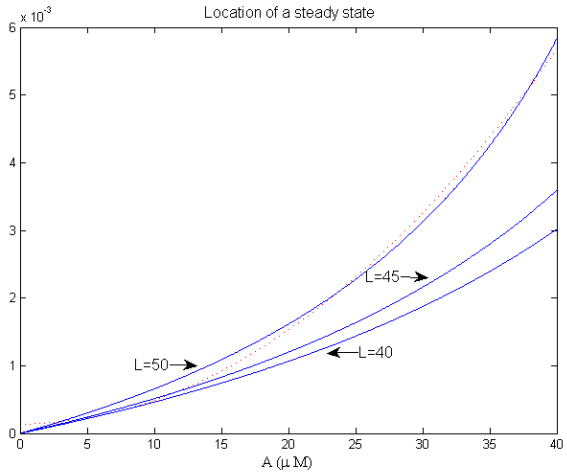

Figure 5.2: Steady states of the *lac* operon as function of allolactose $A\,(\mu M)$ for different values of intercellular lactose $L\,(\mu M)$.

Linearization for the *lac* operon model To check the stability one must linearize the reduced model in the neighbourhood of a steady state by using the following change of variables $s_1 = M - M_*, s_2 = B - B_*, s_3 = A - A_*$. In the new variables, following system is obtained,

$$\frac{ds_1}{dt} = \alpha_M f'(A_*) - \widetilde{\gamma}_M s_1 \tag{5.2.6}$$

$$\frac{ds_2}{dt} = \widetilde{\alpha}_B s_{1\tau_B} - \widetilde{\gamma}_B s_2 \tag{5.2.7}$$

$$\frac{ds_3}{dt} = \widetilde{\alpha}_A s_2 - \widetilde{\beta}_A s_3. \tag{5.2.8}$$

where $\widetilde{\alpha}_A = \alpha_A h(L) - \beta_A g(A_*), \quad \widetilde{\beta}_A = \beta_A B_* g'(A_*) + \widetilde{\gamma}_A, \quad \widetilde{\alpha}_B = \alpha_B e^{-\mu\tau_B}$, and $f'(A_*) = \frac{2(K-1)}{(K+e^{-2\widetilde{\mu}\tau_M}A^2)^2}$. The steady state coordinates are obtained as,

$$M_* = \frac{\widetilde{\gamma}_B}{\alpha_B}B_*, \quad B_* = \frac{\widetilde{\beta}_A A_*}{\widetilde{\alpha}_A}, \quad A_* = f(A_*)\frac{\widetilde{\alpha}_A\alpha_M\alpha_B\alpha_A}{\widetilde{\gamma}_M\widetilde{\gamma}_B\widetilde{\gamma}_M}.$$

This reduces the system around the steady state to

$$Y' = ZY,$$

where

$$Y' = \begin{pmatrix} \frac{ds_1}{dt} \\ \frac{ds_2}{dt} \\ \frac{ds_3}{dt} \end{pmatrix}$$

$$Y = \begin{pmatrix} M - M_* \\ B - B_* \\ A - A_* \end{pmatrix}$$

$$Z = \begin{pmatrix} -\widetilde{\gamma}_M & 0 & \alpha_M f'(A_*) \\ \alpha_B & -\widetilde{\gamma}_B & 0 \\ 0 & \widetilde{\alpha}_A & -\widetilde{\beta}_A \end{pmatrix}.$$

The eigenvalues of Z are the roots of the characteristic polynomial of this matrix given by $det(\lambda I - Z) = 0$, where I is the unit matrix and

$$det(\lambda I - Z) = \begin{pmatrix} \lambda + \widetilde{\gamma}_M & 0 & \alpha_M f'(A_*) \\ \alpha_B & -\widetilde{\gamma}_B & 0 \\ 0 & \widetilde{\alpha}_A & -\widetilde{\beta}_A \end{pmatrix}.$$

Solving the equation for eigenvalues gives

$$P(\lambda) + Q(\lambda)e^{-\lambda\tau} = 0, \quad \tau = \tau_M + \tau_B, \tag{5.2.9}$$

where $P(\lambda)$ is a polynomial of the form,

$$P(\lambda) = \lambda^3 + \lambda^2(\Upsilon_2) + \lambda(\Upsilon_1) + \Upsilon_0, \tag{5.2.10}$$

where $\Upsilon_0 = \widetilde{\gamma}_M\widetilde{\gamma}_B\widetilde{\beta}_A$, $\Upsilon_1 = \widetilde{\gamma}_M\widetilde{\gamma}_B + \widetilde{\gamma}_B\widetilde{\beta}_A + \widetilde{\gamma}_M\widetilde{\beta}_A$,$\Upsilon_2 = \widetilde{\gamma}_M + \widetilde{\gamma}_B + \widetilde{\beta}_A$. The function $Q(\lambda)$ is

$$Q(\lambda) = -\Theta, \tag{5.2.11}$$

where $\Theta = -\alpha_M\alpha_B\widetilde{\alpha}_A f'(A_*)$.

The system has unstable and stable steady states in the domain $\widetilde{\alpha}_A > 0$. $P(\lambda)$ has the form given in Equation (5.2.10), where $\widetilde{\gamma}_M > 0$, $\widetilde{\gamma}_B > 0$, $\widetilde{\beta}_A > 0$ and $f'(A_*)$ is an increasing function. If $\Theta > P(0)$ then all the roots of $P(\lambda) - \Theta < 0$ have negative real part. On the other hand, all the roots have positive real part when $\Theta < P(0)$, $P(\lambda) - \Theta > 0$. It is shown in [6] by the Routh- Hurwitz criteria that all roots have negative real part if and only if:

$\widetilde{\gamma}_M\widetilde{\gamma}_B\widetilde{\beta}_A > 0$, $\widetilde{\gamma}_M + \widetilde{\gamma}_B + \widetilde{\beta}_A > 0$, $\widetilde{\gamma}_M\widetilde{\gamma}_B\widetilde{\beta}_A < (\widetilde{\gamma}_M + \widetilde{\gamma}_B + \widetilde{\beta}_A)(\widetilde{\gamma}_M\widetilde{\gamma}_B + \widetilde{\gamma}_B\widetilde{\beta}_A + \widetilde{\gamma}_M\widetilde{\beta}_A)$.

5.3 Numerical simulation of the reduced model

Using routine dde23 in Matlab. Figure 5.3 shows the stable and unstable regions (Section 5.2.1) in the lactose-allolactose space. The S-shaped curve on Figure 5.3 depicts the steady states, their number clearly depends on L. The notation ($\bullet$) indicates the location of the stable steady states. For example, there is one steady state for $L = 30\mu M$, three steady states for $L = 50\mu M$ and two steady states when $L = 38.5\mu M$, positioned on the lower, middle and upper branch of the S-shaped curve, henceforth referred to as lower (uninduced), middle and upper (induced) coordinates of the steady state $\overrightarrow{\mathbf{S}} = (M, B, A)$. The Table 5.1 shows the level of lactose as induced in the *lac* operon.

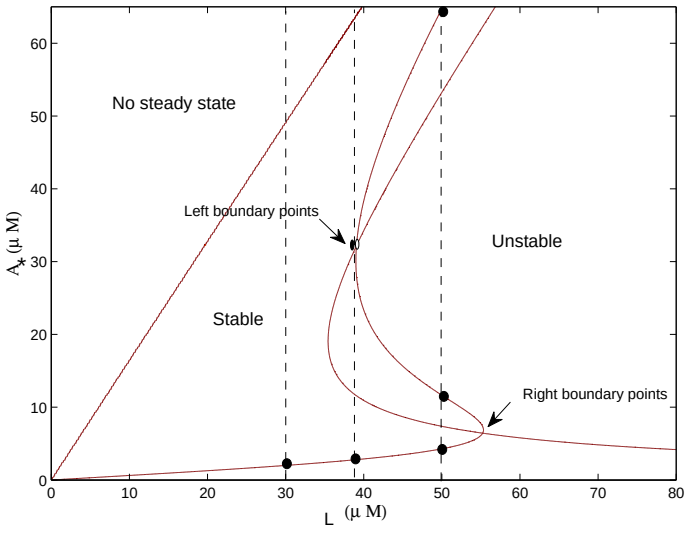

Figure 5.3: Stable and unstable regions for the deterministic reduced *lac* operon model. (•) indicates steady states coordinates on the S-shape curve.

Lactose	0-38 μM	One steady state	Stable
Lactose	38.5 μM	Two steady states	Two stable
Lactose	39.1- 55.43 μM	Three steady states	Two stable and one unstable
Lactose	55.45 μM	Two steady states	Two stable
Lactose	55.55-60 μM	One steady state	Stable

Table 5.1: Lactose level when there are one, two and three steady states solutions

Stable and unstable steady states The evolution of the three steady states for allolactose (Table 5.1) is illustrated on Figure 5.4. It is clear that upper state coordinate $A3$ is stable and induced, the lower state coordinate $A1$, is stable and uninduced (repressed) and the middle state coordinate $A2$ is unstable.

Depending whether the initial values of the coordinate of the middle steady state for allolactose, A, is bigger or less then $A_\star$ ($A2 \gtrless A_\star$), the simulated curve converged to the coordinate of the upper steady state (induced) or the lower steady state (uninduced) respectively (Figure 5.4). The initial values are steady states $(M_\star, B_\star, A_\star)$ for $L = 50\mu M$.

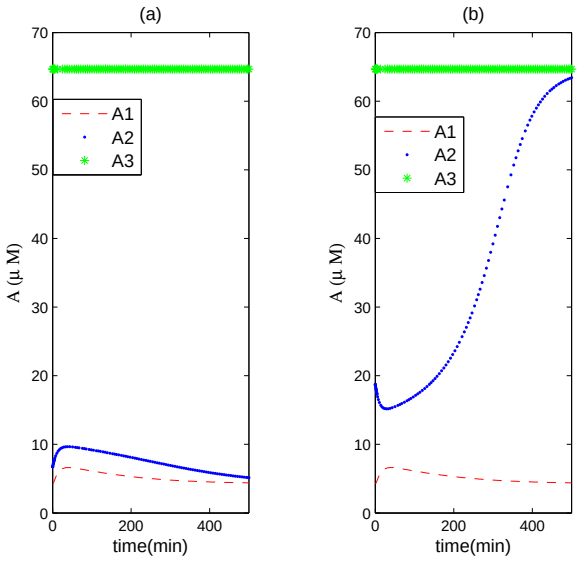

Figure 5.4: Deterministic (reduced) model of the *lac* operon showing allolactose when $L = 50\mu M$. The initial values are given in the text.

Below is a table of multiple steady states and their numerical values when $L = 50\mu M$.

ON	Interposition	OFF
induced	(induced or uninduced)	uninduced
stable	unstable	stable
(upper branch)	(middle branch)	(lower branch)
(M3,B3,A3)	(M2,B2,A2)	(M1,B1,A1)
$(0.032710, 0.01642, 64.68)\mu M$	$(0.00139, 0.0007, 11.73)\mu M$	$(0.00046, 0.00023, 4.21)\mu M$

Table 5.2: Three steady states values when $L = 50\mu M$.

5.4 Summary

The dynamic behaviour of the lactose regulation system of the *E.coli* bacteria [11] is reviewed. The mathematical model of Yildirim and Mackey, which consists of a system of two delay differential equations is explained. The linearization of the model around the steady states and the characteristic equation of the system is reviewed. The stable and unstable solution regions of the system of the *lac* operon were found depending on lactose concentration. Whereas, the reduced model consists of just the

inner feedback loop the behaviour of the system is not significantly different from those of the full model. Thus, the reduced model with the feedback by allolactose can be used to show that the behaviour of the system and investigate the regulation mechanisms and shows bistable behaviour.

Chapter 6

The reduced stochastic model of the *lac* operon

6.1 Introduction

The deterministic model, in [12] assumed equilibrium of internal and external lactose, and therefore, ignored the positive feedback loop involving permease. Thus, the positive feedback for the mRNA, β-galactosidase and allolactose (reduced model) is only by allolactose.

To describe the stochastic behaviour of the reduced system, the reduced deterministic model of Chapter 5 is considered with a noise term. Studying, the stochastic stability of the reduced model is to figure out whether the noise term can change the behaviour in the bistable region due to the lactose concentration.

The stochastic stability framework is useful in understanding the relative stability of equilibria point and allows to define more adequate description of the dynamics. In this chapter, the stability properties of the stochastic model of the *lac* operon system ([12]) are investigated by linearization of the system of stochastic delay differential equations (SDDEs) and using Lyapunov functional. The sufficient conditions for mean square stable state of the trivial solution of linearized stochastic system around positive equilibrium are obtained. The trivial solution of an equation is the solution

in which the value of every variable of the equations is equal to zero. For instance, for the reduced model, $M(t) = B(t) = A(t) = 0$, is a solution of the system which is called the trivial solution. The stochastic stability properties of the model are investigated both analytically and numerically (by using Euler Maruyama method) in order to obtain the solution of stochastic differential equations.

6.2 Stochastic stability of the reduced model

Consider the system of Equations (5.2.1-5.2.3) and include stochastic perturbations of the variables M, B, A from the equilibrium M_*, B_*, A_*, respectively, gives the following Ito problem.

$$dM = [\alpha_M f(A_{\tau_M}) - \widetilde{\gamma}_M M]dt + \sigma_1(M - M_*)dw_1(t), \tag{6.2.1}$$

$$dB = [\alpha_B e^{-\widehat{\mu}\tau_B} M_{\tau_B} - \widetilde{\gamma}_B B]dt + \sigma_2(B - B_*)dw_2(t), \tag{6.2.2}$$

$$dA = [\alpha_A B h(L) - \beta_A B g(A) - \widetilde{\gamma}_A A]dt + \sigma_3(A - A_*)dw_3(t), . \tag{6.2.3}$$

where

$$f(A) = \frac{1 + K_1(e^{-\mu\tau_M} A_{\tau_M})^n}{K + K_1(e^{-\mu\tau_M} A_{\tau_M})^n}, \quad g(A) = \frac{A}{K_A + A}, \quad h(L) = \frac{L}{K_L + L}$$

Here $(w_1(t), w_2(t), w_3(t))$ be a three- dimensional standard Wiener process on the probability space $[\Omega, \xi, \mathbf{P}]$ with the filtration $\{\xi_t\}_{0 \le t < \infty}$ and $\overrightarrow{\boldsymbol{\sigma}} = (\sigma_1, \sigma_2, \sigma_3)$ are real constants. The initial values are $M(0) = M_*$, $B(0) = B_*$, $A(0) = A_*$. Note that the equilibrium point $(M_*,\ B_*,\ A_*)$ of the deterministic system from Chapter 5 (Equations 5.2.1-5.2.3) is being used.

The mean square stability of the trivial solution of the linearized system (Equations (6.2.1-6.2.3) is investigated around equilibrium point by using the Lyapunov method with two time delays τ_M, τ_B. There stability play an essential role on the behaviour of the model of the *lac* operon. As a result, the following theorem is formulated:

Theorem 6.2.1. *Let the model parameters in Equations (6.2.1-6.2.3) are such that coordinate of the steady state* $A_* \in (0, (K_A - K_L))$ *and* $h(L) < \frac{\beta_A}{\alpha_A}$ *is satisfying,*

$$\tau_{M*} = \frac{1}{2\mu} \log[\frac{\xi_7 \alpha_M}{2\widetilde{\beta}_A - \widetilde{\alpha}_A}], \qquad \tau_{B*} = \frac{1}{2\mu} \log[\frac{\xi_5 \alpha_B}{2\widetilde{\gamma}_M - \xi_4 \widetilde{\gamma}_B}]. \tag{6.2.4}$$

Let the time delays $\tau_{M*} < \tau_M$, $\tau_{B*} < \tau_B$. Then for any constants $\sigma_1, \sigma_2, \sigma_3$ satisfying the conditions

$$\sigma_1^2 < 2\widetilde{\gamma}_M - \widetilde{\alpha}_M\xi_4 - \widetilde{\alpha}_B\xi_5,\ \sigma_2^2 < 2 - \widetilde{\gamma}_B - \widetilde{\alpha}_B - \widetilde{\alpha}_A\xi_6,$$
$$\sigma_3^2 < 2\widetilde{\beta}_A - \widetilde{\alpha}_A - \widetilde{\alpha}_M\xi_7, \tag{6.2.5}$$

the trivial solution of the linearized system around equilibrium is exponentially mean square stable.

Proof. Let $s_1 = M - M_*, s_2 = B - B_*, s_3 = A - A_*$ be the change of variables for the reduced model (6.2.1-6.2.3) and linearizing the system around the positive equilibrium gives,

$$ds_1 = [-\widetilde{\gamma}_M s_1 + \widetilde{\alpha}_M s_3(t-\tau_M)]dt + \sigma_1 s_1 dw_1 \tag{6.2.6}$$
$$ds_2 = [-\widetilde{\gamma}_B s_2 + \widetilde{\alpha}_B s_1(t-\tau_B)]dt + \sigma_2 s_2 dw_2 \tag{6.2.7}$$
$$ds_3 = [-\widetilde{\beta}_A s_3 - \widetilde{\alpha}_A s_2]dt + \sigma_3 s_3 dw_3, \tag{6.2.8}$$

where

$$\widetilde{\alpha}_A = \beta_A g(A_*) - \alpha_A h(L), \quad \widetilde{\beta}_A = \beta_A B_* g'(A_*) + \widetilde{\gamma}_A, \quad \widetilde{\alpha}_B = \alpha_B e^{-\widehat{\mu}\tau_B},$$
$$\widetilde{\alpha}_M = \alpha_M e^{-2\widehat{\mu}\tau_M} f'(A_*),$$
$$f'(A_*) = \frac{2(K-1)}{(K + e^{-2\widehat{\mu}\tau_M}A^2)^2}.$$

Let,

$$ds(t) = [\nu s(t) - \upsilon s(t-\tau)]dt, \tag{6.2.9}$$

where $\nu = [\frac{\partial f}{\partial s_j}]_{s=0}$, $\upsilon = [\frac{\partial f}{\partial s_j(t-\tau)}]_{s=0}$, $j = 1, 2, 3$ and

$$\nu = \begin{pmatrix} -\widetilde{\gamma}_M & 0 & 0 \\ 0 & -\widetilde{\gamma}_B & 0 \\ 0 & -\widetilde{\alpha}_A & -\widetilde{\beta}_A \end{pmatrix},$$

$$\upsilon = \begin{pmatrix} 0 & 0 & \widetilde{\alpha}_M \\ \widetilde{\alpha}_B & 0 & 0 \\ 0 & 0 & 0 \end{pmatrix}.$$

Consider the Lyapunov functional:

$$V = V_1 + V_2. \tag{6.2.10}$$

Where V_1 chosen as follows

$$V_1(s(t)) = \frac{1}{2}(\xi_1 s_1^2 + \xi_2 s_2^2 + \xi_3 s_3^2). \tag{6.2.11}$$

The constants $\xi_1, \xi_2, \xi_3 > 0$ and V_2 will be chosen later.
For all $t \geq 0$, the first and second derivatives with respect to s are continuous, and the first derivative with respect to t is continuous and bound. Then, the definition of the differential operator $\mathbf{L}$ associated with Equation (A.3.3) (see Appendix A) yields,

$$\mathbf{L} = \frac{\partial}{\partial t} + \sum_{i=1}^{m} f_i(t,s))\frac{\partial}{\partial s_i} + \frac{1}{2}\sum_{k=1}^{m} \mathrm{Tr}[g^T(t,s)g(t,s)]_k \frac{\partial^2}{\partial s_i^2}\,.$$

For $V \in C([0,\infty) \times R^m; R_+)$,

$$\mathbf{L}(V) = \frac{dV_2}{dt} + f^T(s, s(t-\tau))\frac{\partial V_1}{\partial s} + \frac{1}{2}\mathrm{Tr}[g^T(t,s)\frac{\partial^2 V_1}{\partial s^2}g(t,s)].$$

The operator $\mathbf{L}(V)$ can be written as,

$$\mathbf{L}(V) = \frac{dV_2}{dt} + \mathbf{L}(V_1), \tag{6.2.12}$$

where

$$\begin{aligned}\mathbf{L}(V_1) = {} & -\xi_1\widetilde{\gamma}_M s_1^2 + \xi_1\widetilde{\alpha}_M s_1 s_3(t-\tau_M) - \xi_2\widetilde{\gamma}_B s_2^2 + \xi_2\widetilde{\alpha}_B s_2 s_1(t-\tau_B) - \xi_3\widetilde{\alpha}_A s_2 s_3 \\ & -\xi_3\widetilde{\beta}_A s_3^2 + \frac{1}{2}\mathrm{Tr}[g^T(t,s)\frac{\partial^2 V_1}{\partial s^2}g(t,s)],\end{aligned} \tag{6.2.13}$$

and

$$\frac{\partial^2 V_1}{\partial s^2} = \begin{pmatrix} \xi_1 & 0 & 0 \\ 0 & \xi_2 & 0 \\ 0 & 0 & \xi_3 \end{pmatrix}.$$

This gives,

$$g^T\frac{\partial^2 V_1}{\partial s^2}g(t,s_t) = \begin{pmatrix} \xi_1\sigma_1^2 s_1^2 & 0 & 0 \\ 0 & \xi_2\sigma_2^2 s_2^2 & 0 \\ 0 & 0 & \xi_3\sigma_3^2 s_3^2 \end{pmatrix}.$$

Therefore,

$$\frac{1}{2}\mathrm{Tr}[g^T\frac{\partial^2 g(t,s_t)}{\partial s^2}g(t,s_t)] = \frac{1}{2}[\xi_1\sigma_1^2 s_1^2 + \xi_2\sigma_2^2 s_2^2 + \xi_3\sigma_3^2 s_3^2],$$

which implies that

$$\begin{aligned} L(V_1) &= -\xi_1\widetilde{\gamma}_M s_1^2 + \xi_1\widetilde{\alpha}_M s_1 s_3(t-\tau_M) - \xi_2\widetilde{\gamma}_B s_2^2 + \xi_2\widetilde{\alpha}_B s_2 s_1(t-\tau_B) - \xi_3\widetilde{\alpha}_A s_2 s_3 \\ &\quad -\xi_3\widetilde{\beta}_A s_3^2 + \frac{1}{2}\xi_1\sigma_1^2 s_1^2 + \frac{1}{2}\xi_2\sigma_2^2 s_2^2 + \frac{1}{2}\xi_3\sigma_3^2 s_3^2\,. \end{aligned} \tag{6.2.14}$$

In Equation (6.2.14) the parameter ξ_1 is chosen as $\xi_1 = \frac{K}{n}$ where K, n are constants, normally determined from the experiment and in the case of the *lac* operon are given in Table 4.1. It is known that $f(A_*)$ is linear around the steady state which leads to $f'(A_*) \backsimeq 1$, for all $\tau_M > 0$ and $A_* \in (0, (K_A - K_L))$. This gives $\widetilde{\alpha}_M = \alpha_M e^{-2\widehat{\mu}\tau_M}$.

By using standard inequalities,

$$|s_2 s_1(t-\tau_B)| \leq \frac{1}{2}(s_2^2 + s_1^2(t-\tau_B)), \quad |s_2 s_3| \leq \frac{1}{2}(s_2^2 + s_3^2),$$

$$|s_1 s_3(t-\tau_M)| \leq \frac{1}{2}(s_1^2 + s_3^2(t-\tau_M)), \quad |s_1 s_3| \leq \frac{1}{2}(s_1^2 + s_3^2),$$

from Equation (6.2.14) is obtained,

$$\begin{aligned} L(V_1) &\leq -[\xi_1\widetilde{\gamma}_M - \frac{1}{2}\widetilde{\alpha}_M - \frac{1}{2}\xi_1\sigma_1^2]s_1^2 - [\xi_2\widetilde{\gamma}_B - \frac{1}{2}\xi_2\widetilde{\alpha}_B - \xi_3\frac{1}{2}\widetilde{\alpha}_A - \frac{1}{2}\sigma_2^2]s_2^2 \\ &\quad -[-\xi_3\widetilde{\beta}_A - \frac{1}{2}\xi_3\widetilde{\alpha}_A - \frac{1}{2}\xi_1\sigma_3^2]s_3^2 + \frac{1}{2}\widetilde{\alpha}_M s_3^2(t-\tau_M) \\ &\quad +\frac{1}{2}\xi_2\widetilde{\alpha}_B s_1^2(t-\tau_B)\,. \end{aligned} \tag{6.2.15}$$

Now, let the function V_2 is defined as

$$V_2 = \frac{1}{2}\widetilde{\alpha}_M\int_{t-\tau_M}^{t} s_3^2(\omega)d\omega + \frac{1}{2}\xi_2\widetilde{\alpha}_B\int_{t-\tau_B}^{t} s_1^2(\omega)d\omega\,.$$

Thus

$$\frac{dV_2}{dt} = \frac{1}{2}[\widetilde{\alpha}_M s_3^2 + \xi_2\widetilde{\alpha}_B s_1^2 - \widetilde{\alpha}_M s_3^2(t-\tau_M) - \xi_2\widetilde{\alpha}_B s_1^2(t-\tau_B)]. \tag{6.2.16}$$

From the generating operator (6.2.12) using (6.2.15, 6.2.16) and after some algebra, it is obtained,

$$\begin{aligned}\mathbf{L}(V) \;\leq\; & -[\xi_1\widetilde{\gamma}_M - \frac{1}{2}\widetilde{\alpha}_M - \frac{1}{2}\xi_2\widetilde{\alpha}_B - \frac{1}{2}\xi_1\sigma_1^2]s_1^2 - [\xi_2\widetilde{\gamma}_B - \frac{1}{2}\xi_2\widetilde{\alpha}_B - \frac{1}{2}\xi_3\widetilde{\alpha}_A - \frac{1}{2}\xi_2\sigma_2^2]s_2^2 \\ & -[\xi_3\widetilde{\beta}_A - \frac{1}{2}\xi_3\widetilde{\alpha}_A - \frac{1}{2}\widetilde{\alpha}_M - \frac{1}{2}\xi_3\sigma_3^2]s_3^2\,. \qquad (6.2.17)\end{aligned}$$

Using the values of the parameters given in Table 4.1, $\xi_1 = \frac{K}{n}$ and $\xi_2, \xi_3 > 0$, the Equation (6.2.17) gives,
$(2\widetilde{\gamma}_M - \widetilde{\alpha}_M\xi_4 - \widetilde{\alpha}_B\xi_5) > 0$, $(2\widetilde{\gamma}_B - \widetilde{\alpha}_B - \widetilde{\alpha}_A\xi_6) > 0$, $(2\widetilde{\beta}_A - \widetilde{\alpha}_A - \widetilde{\alpha}_M\xi_7) > 0$,

where $\xi_4 = \frac{1}{\xi_1}$, $\xi_5 = \frac{\xi_2}{\xi_1}$, $\xi_6 = \frac{\xi_3}{\xi_2}$, $\xi_7 = \frac{1}{\xi_3}$.
Thus, $\sigma_i \;\; i = 1, 2, 3$, are positive real numbers if $\tau_M* < \tau_M$, $\tau_B* < \tau_B$.

This completes the proof of Theorem 6.2.1.

6.3 Numerical solution and investigation of the dynamic behaviour with stochastic noise

The Ito system (6.2.1-6.2.3) has been solved numerically by Euler Maruyama methods [51, 48] with constant stepsize. According to the conditions given in Theorem 6.2.1, the mean square stability of the positive steady state depends on σ_i, $i = 1, 2, 3$ and time delays. Using conditions (6.2.4 , 6.2.5) of Theorem 6.2.1 and parameters from Table 4.1, the system is exponentially mean square stable for:

$\sigma_1 < 0.028$, $\sigma_2 < 0.013$, $\sigma_3 < 0.038$ and $\tau_M > 0.032$, $\tau_B > 1.08$. These are the threshold values for the model. For convenance, in what follows one introduces noise as $\overrightarrow{\boldsymbol{\sigma}} = (\sigma_1, \sigma_2, \sigma_3)$.
For the allolactose, A, the displacement from the equilibrium by the noise term, depends on the initial conditions. Figure 6.1 illustrated the case when the initial conditions are changed from the steady state by Δ to the left and the right.

In Figure 6.1, one has to find a limit value for Δ such that the variable close to it must be in the region where steady state exits (S-shape curve) and this depends on

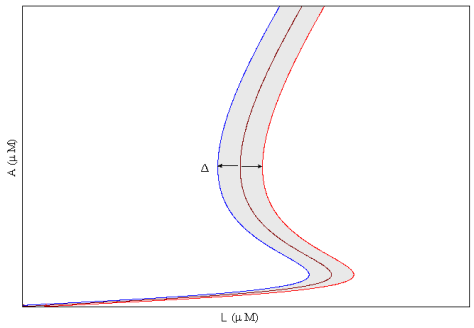

Figure 6.1: Steady state displacement (S-shape curve) due to the distance between the initial value and equilibrium point for allolactose (Δ).

the value of L. Introducing $\frac{\boldsymbol{\sigma}}{\Delta}$, where Δ is the distance between the initial values and equilibrium points which assured that Δ is small enough not affect the S-shape curve. The values of $\frac{\boldsymbol{\sigma}}{\Delta}$ are compered with the noise values which is obtained from the theorem 6.2.1. There are different cases, no change in the S-shape curve (Figure 6.1) when $\frac{\boldsymbol{\sigma}}{\Delta} \geq 1$ (the value of Δ is smaller or same the value of $\boldsymbol{\sigma}$). Whereas, in the case when the value of Δ is larger than the value of $\boldsymbol{\sigma}$, the S-shape curve changes (displacement) within the steady states values when $1 < \Delta \leq 8\,\mu M$ and concluded that $\frac{\boldsymbol{\sigma}}{\Delta} < 1$.

6.3.1 Stable behaviour

The numerical simulation shows the behaviour of the system (6.2.1-6.2.3) around the equilibrium subjected to the perturbation $\boldsymbol{\sigma} = (\sigma_1, \sigma_2, \sigma_3)$. All three coordinates change in a synchronized way and the system shows identical behaviour in the two stable states. For instance, in this model of the *lac* operon if the coordinate A_* belongs to uninduced state, M_*, B_* will also belong to the same uninduced state. This is shown in Figure 6.2 and Figure 6.3, for coordinates of an induced state at $L = 60\ \mu M$ or uninduced state at $L = 33\ \mu M$. Since the scale of allolactose is much larger than mRNA and $\beta-$ galoctosidase the behaviour is shown in two figures.

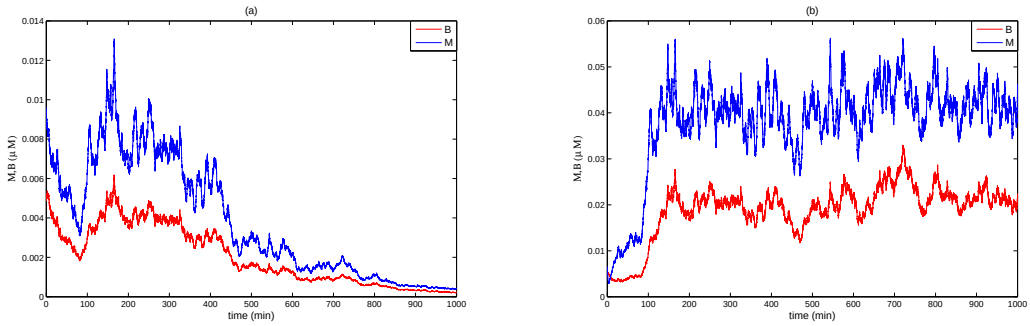

Figure 6.2: $M, B\,(\mu M)$ concentration versus time (minutes) $\sigma_1 = \sigma_2 = \sigma_3 = 0.01$, a) uninduced state $L = 33\ \mu M$ b) induced state $L = 60\ \mu M$.

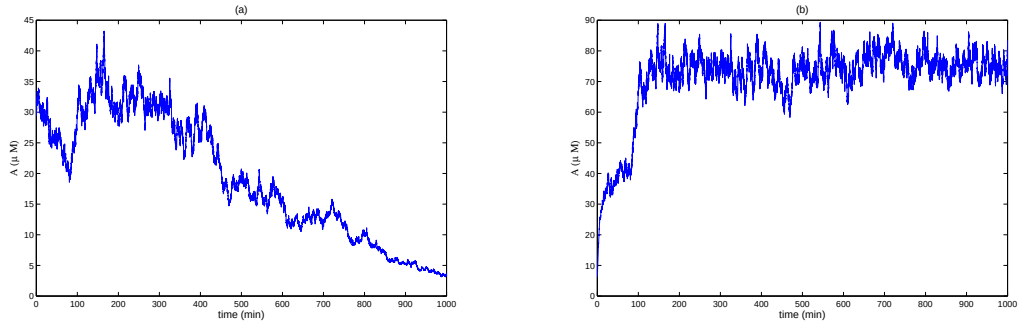

Figure 6.3: $A\,(\mu M)$ concentration versus time (minutes) $\sigma_1 = \sigma_2 = \sigma_3 = 0.01$, a) uninduced state $L = 33\ \mu M$ b) induced state $L = 60\ \mu M$.

6.3.2 Inside bistable region

The numerical simulation of mRNA, $\beta-$ galoctosidase and allolactose with time delays is shown in Figure 6.4 for three values of the noise term when $L = 50\mu M$, where there are an opportunity for multi-stable behaviour. The induced (upper) state $\mathbf{S}= (M, B, A)$ is stable for coordinates $\overrightarrow{\mathbf{S3}}= (M3, B3, A3)$, uninduced (lower) for coordinates $\overrightarrow{\mathbf{S1}}= (M1, B1, A1)$ and the middle state $\overrightarrow{\mathbf{S2}}= (M2, B2, A2)$ is unstable. The most significant changes are observed for the allolactose A, where the concentration is significantly higher compared to B and M. This is expected as the values of A is larger than the values of the other variables M and B. The figure illustrates two cases of perturbation $\boldsymbol{\sigma} = (\sigma_1, \sigma_2, \sigma_3)$, (a) equal noise terms $\sigma_1 = \sigma_2 = \sigma_3 = 0.005$, (b) different noise terms $\sigma_1 = 0.02, \sigma_2 = 0.01, \sigma_3 = 0.03$. Time delays have been chosen $\tau_M = 0.1$ min, $\tau_B = 2$ min as these two time delays are the maximal time delays for the system as suggested in [12] (see Table 4.1) and also satisfy the conditions of Theorem 6.2.1.

For very small perturbation reflected by the values of $\boldsymbol{\sigma} = (\sigma_1, \sigma_2, \sigma_3)$, the unstable state with a coordinate $A2$, is converges to the stable induced state with coordinate $A3$, while with increased noise $\boldsymbol{\sigma}$ the solution converges to the lower uninduced state with coordinate $A1$. Similar behaviour is observed for the concentrations M and B versus time as shown in Figure 6.6 and Figure 6.5 respectively. The stochastic system is bistable and the noise affects mainly the upper (induced) state for all concentrations M, B, A, while the lower (uninduced) state for M and B are almost unchanged by noise around the equilibrium. The initial values for Figures 6.4-6.6 are given in Table 5.2 ($L = 50\mu M$). The stochastic system is bistable and the noise affects mainly the middle unstable solution for all concentrations M, B, A, while lower (uninduced) and upper (induced) solutions for M, B are almost unchanged by noise around the equilibrium.

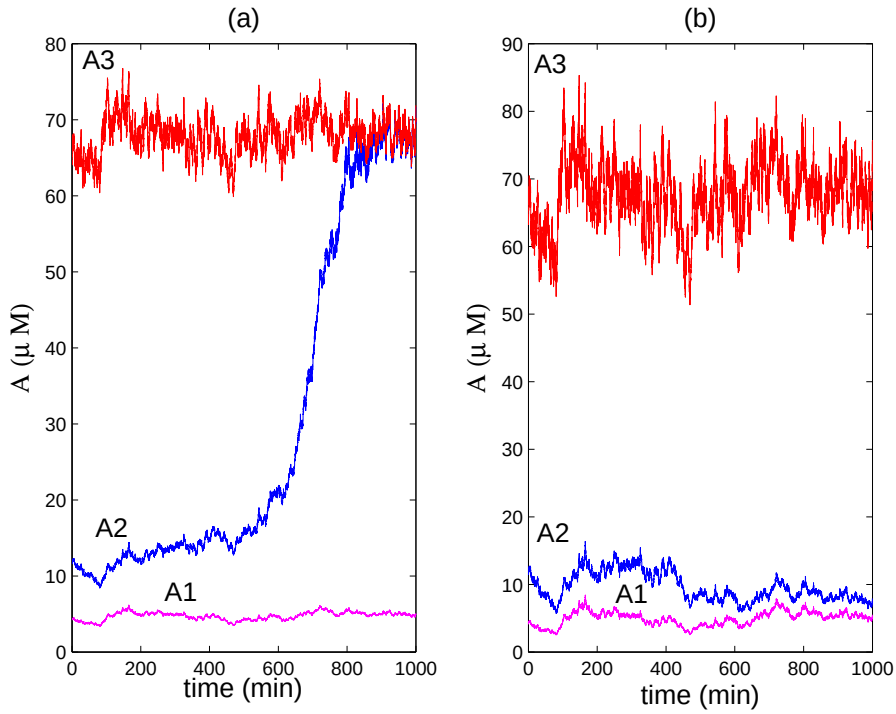

Figure 6.4: Stochastic model showing $A(\mu M)$ concentration versus time (minutes) in bistable region, $L = 50\ \mu M$, $A1, A2, A3$ are the coordinates of the lower, middle and upper states of the model. Time delays $\tau_M = 0.1$, $\tau_B = 2$, and the noise term is (a) $\sigma_1 = \sigma_2 = \sigma_3 = 0.005$, (b) $\sigma_1 = 0.02, \sigma_2 = 0.01, \sigma_3 = 0.03$.

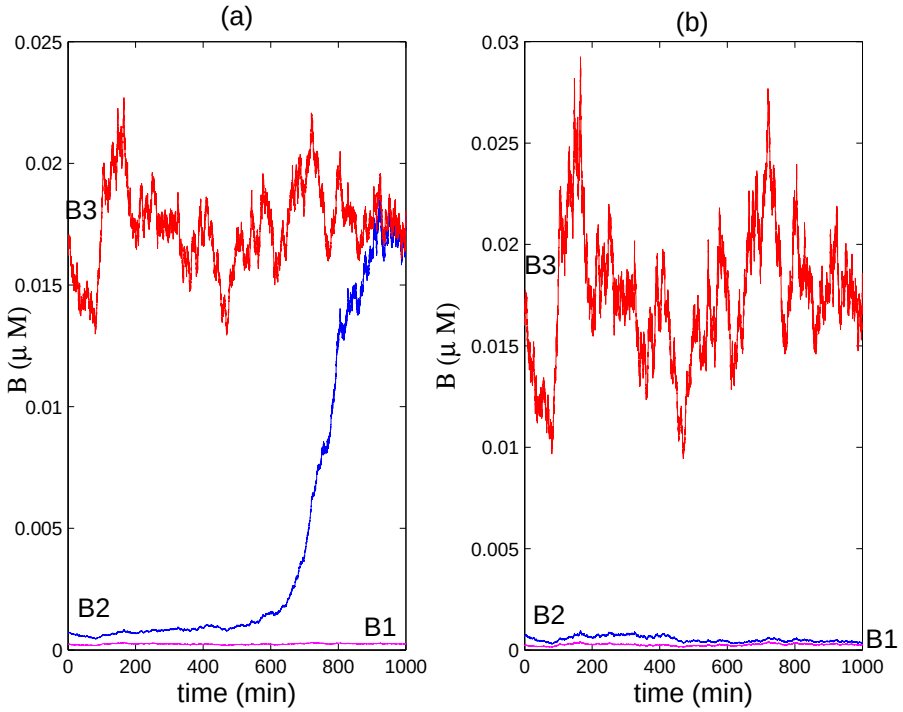

Figure 6.5: Stochastic model showing $B(\mu M)$ concentration versus time (minutes) in bistable region, $L = 50\ \mu M$, $B1, B2, B3$ are the coordinates of the lower, middle and upper states of the model. Time delays $\tau_M = 0.1$, $\tau_B = 2$, and the noise term is (a) $\sigma_1 = \sigma_2 = \sigma_3 = 0.005$, (b) $\sigma_1 = 0.02, \sigma_2 = 0.01, \sigma_3 = 0.03$.

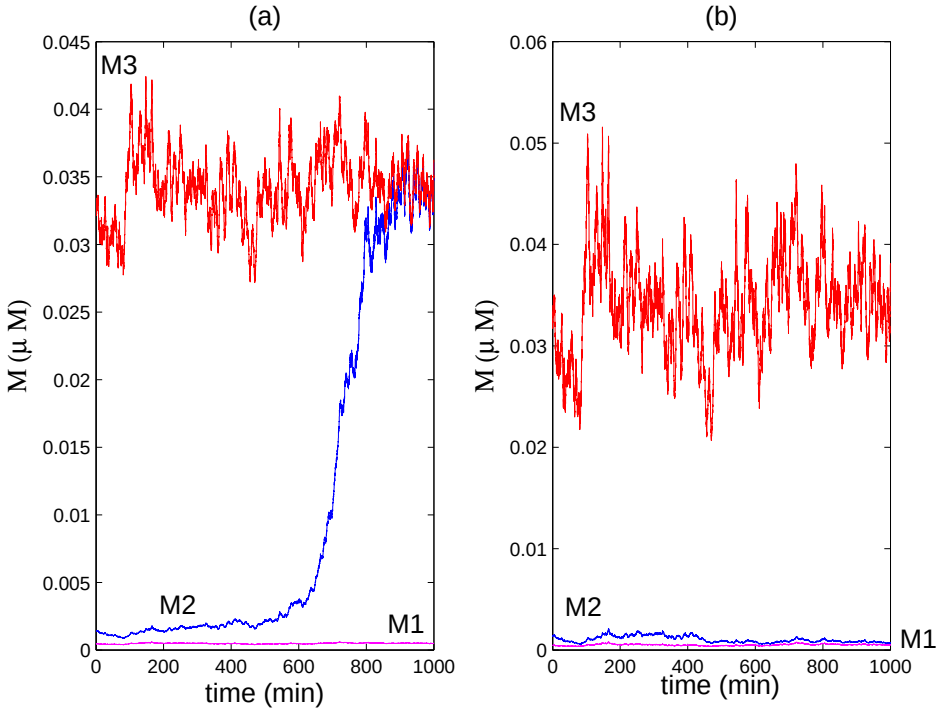

Figure 6.6: Stochastic model showing $M(\mu M)$ concentration versus time (minutes) in bistable region, $L = 50\ \mu M$, $M1, M2, M3$ are the coordinates of the lower, middle and upper states of the model. Time delays $\tau_M = 0.1$, $\tau_B = 2$, and the noise term is (a) $\sigma_1 = \sigma_2 = \sigma_3 = 0.005$, (b) $\sigma_1 = 0.02, \sigma_2 = 0.01, \sigma_3 = 0.03$.

6.3.3 Around the boundary of bistable region

The left and right boundary points depicted in the S-shape curve are shown in Figure 5.3. Here the stochastic behaviour is investigated at the left and right end of the bistable region corresponding to $L = 39.1\ \mu M$ and $L = 55.4\ \mu M$ respectively. The behaviour at the boundary points of the bistable region for different regulation mechanisms of the reduced *lac* operon (with ordinary differential equations) without time delays was studied in [41]. Figure 6.7 a), shows that when the system is at the left boundary point, $L = 39.1\mu M$, the effect of noise is that allolactose in upper state (induced) can switch to lower state (uninduced) after approximately 1000 minutes. However, when the system is at the right boundary point $L = 55.4\ \mu M$, the switch from lower (uninduced) to upper (induced) states appears after approximately 150 minutes and the system remains in the induced state (Figure 6.7 b). Similar behaviour for all the coordinates M and B are shown in Figures 6.8 a) and b) ,6.9 a) and b) respectively.

The following interesting features are observed in the reduced model: In the bistable region close to the left boundary point $L = 39.7\ \mu M$, the the upper state (induced) switches to lower state (uninduced) (Figure 6.7 c). Close to the right boundary point, $L = 54\ \mu M$, the lower state switches to upper state even when the noise very small (Figure 6.7 d). Similar behaviour is observed around the boundary points for M and B and is shown in Figure 6.8 c) and d) and Figure 6.9 c) and d) respectively. The Simulations in this thesis show that fluctuations can cause switching from uninduced to induced solution, also observed the opposite around the left boundary point.

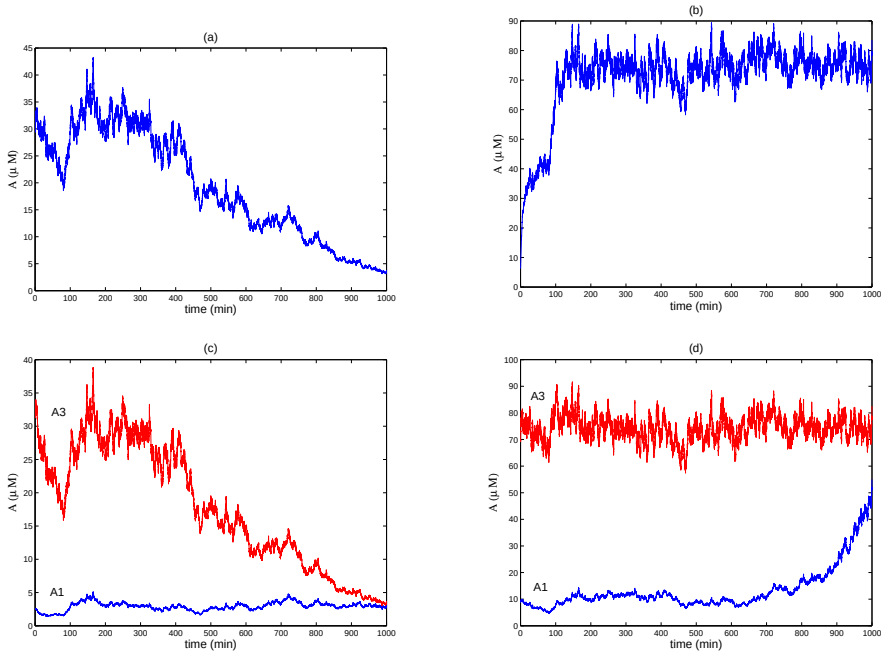

Figure 6.7: $A\,(\mu M)$ concentration versus time (minutes) $\sigma_1 = \sigma_2 = \sigma_3 = 0.005$, a) left boundary point $L = 39.1\ \mu M$, b) right boundary point $L = 55.4\ \mu M$, c) around left boundary point $L = 39.7\ \mu M$, d) around right boundary point $L = 54\ \mu M$.

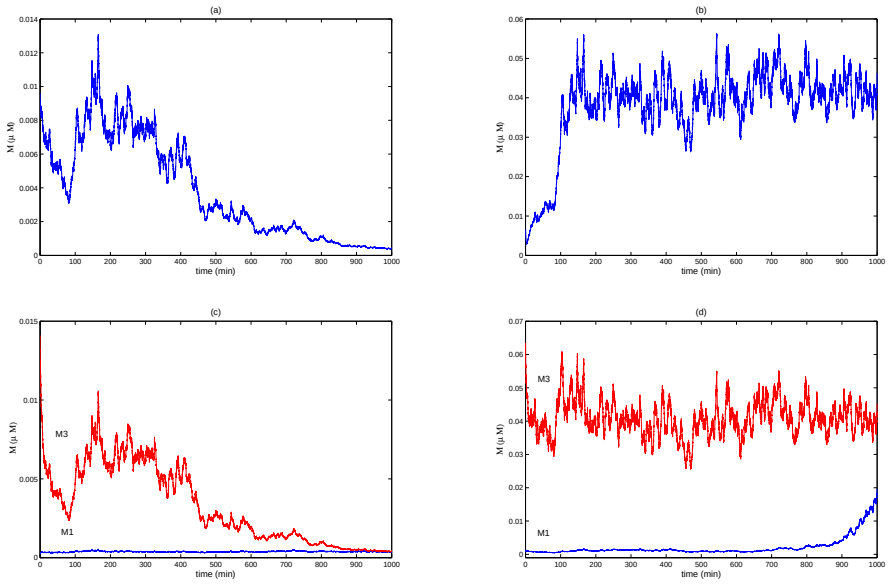

Figure 6.8: $M\,(\mu M)$ concentration versus time (minutes) $\sigma_1 = \sigma_2 = \sigma_3 = 0.005$, a) left boundary point $L = 39.1\ \mu M$, b) right boundary point $L = 55.4\ \mu M$, c) around left boundary point $L = 39.7\ \mu M$, d) around right boundary point $L = 54\ \mu M$.

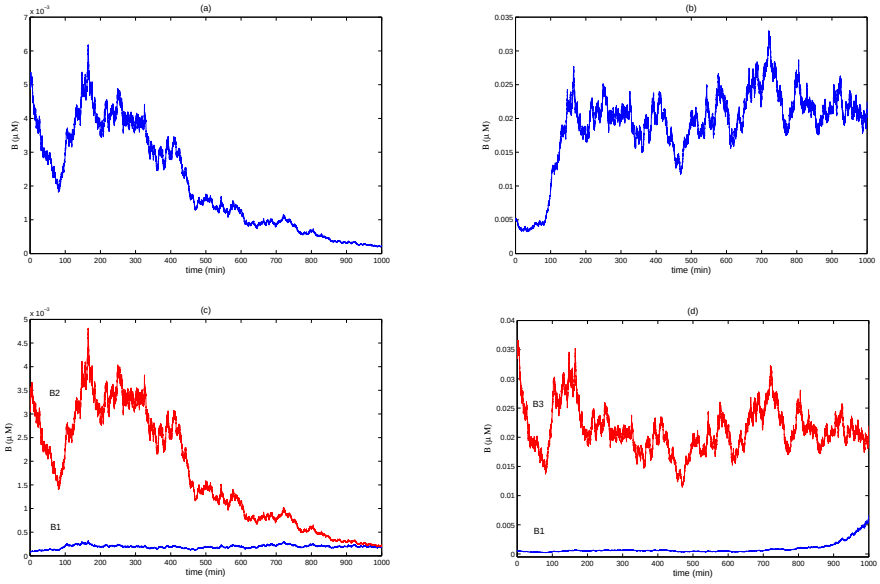

Figure 6.9: $B\,(\mu M)$ concentration versus time (minutes) $\sigma_1 = \sigma_2 = \sigma_3 = 0.005$, a) left boundary point $L = 39.1\ \mu M$, b) right boundary point $L = 55.4\ \mu M$, c) around left boundary point $L = 39.7\ \mu M$, d) around right boundary point $L = 54\ \mu M$.

6.4 Stable and bistable behaviour due to perturbation of allolactose

The analysis of the stochastic system represented by the equations (6.2.1-6.2.3) indicates that the changes in allolactose, A, are more significant, compared to mRNA, M, and $\beta-$ galoctosidase, B. Here, the behaviour of the system is investigated numerically when noise is added to the equation (6.2.3) for allolactose A, only.

If the system is at a single uninduced or induced state it oscillates around this state $\mathbf{S}= (M, B, A)$ when noise is added. This is illustrated for A in Figure 6.10 a), when $L = 30\ \mu M$ and Figure 6.10 b) when $L = 60\ \mu M$. Note that when $\sigma_3 > 0.038$ the system is not mean square stable. In the bistable region, large noise ($\sigma_3 = 0.2$) can switch from uninduced to induced state and vice versa. This is illustrated for A in Figure 6.11 when $L = 50\ \mu M$ and the system is initially in the induced state, the system switches after approximately 700 minutes to coordinate of uninduced state. Perturbing A leads to similar switching in M and B. However, when large noise

is added to all three concentrations, switching inside bistable region has not been observed.

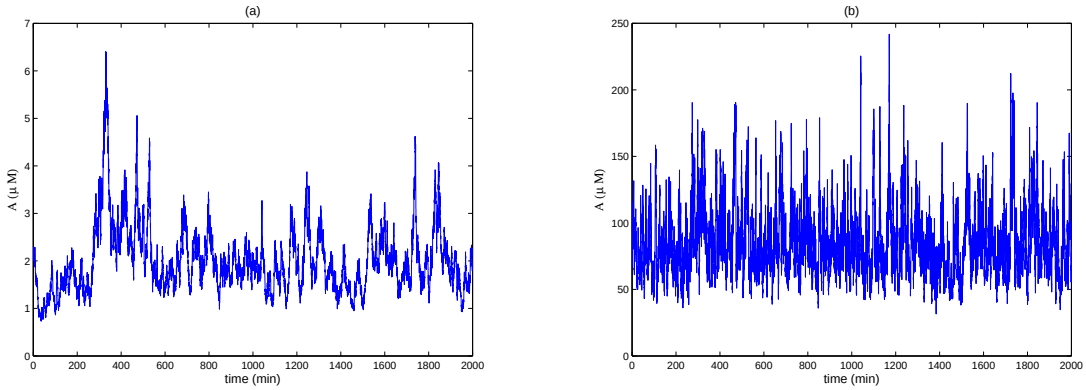

Figure 6.10: A (μM) concentration versus time (minutes). a) Initial values $L = 30$ μM, $\sigma_3 = 0.07$. b) Initial values $L = 60$ μM, $\sigma_3 = 0.2$.

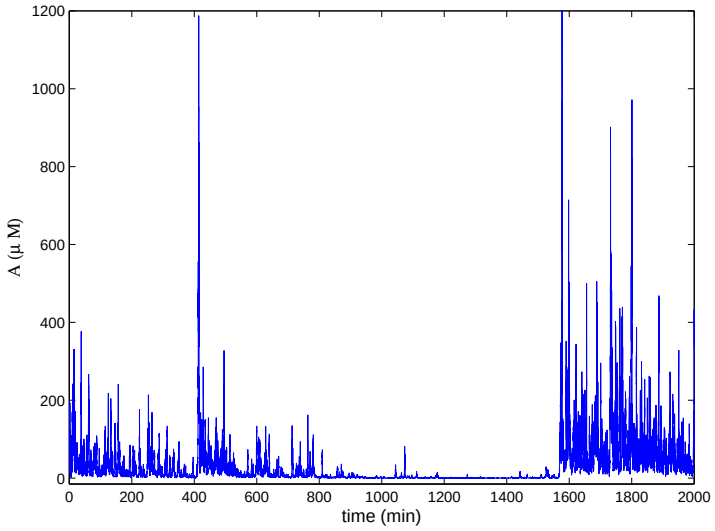

Figure 6.11: A (μM)) concentration versus time (minutes). Initial values $L = 50$ μM, upper state, $\sigma_3 = 0.2$. As seen allolactose switches between two stable .

6.5 Summary

The stability for the reduced stochastic model around equilibrium in the presence of noise and time delays has been studied in this Chapter. The sufficient conditions of exponential mean square stability have been derived giving threshold values for the noise terms. The numerical solution of the Ito stochastic differential equations (6.2.1-6.2.3) by the Euler Maruyama method has verified that the stability of the positive equilibrium depends on the values of the noise terms, time delays and the parameters of the system. If L lies in the bistable region the concentrations of allolactose, β-galoctosidase and mRNA can co-exist in two steady states. When there is an unstable steady state (for $L = 50\ \mu M\ M$ for example), it evolves to induced or uninduced state for the small or larger noise respectively. The model has shown that changes are most significant in allolactose when all three concentrations M, B and A were perturbed with the same noise term. The behaviour has been investigated within the bistable region. Near to equilibrium, when noise terms are below threshold values, the numerical simulations confirm that if the system is in uninduced or induced state it remains in such state in presence of perturbation. However, for values of lactose at or around the right boundary point of the bistable region the system can switch from uninduced to induced state even if the noise is small. Thorough investigation of the stochastic stability of the reduced model of *lac* operon within and outside bistable region with respect to lactose concentration and noise terms demonstrates that the system behaviour is dependent on the lactose levels and perturbations. As such, it has been demonstrated that the stochasticity can change the behaviour in the bistable region, including switching due to the lactose concentration.

Chapter 7

The full stochastic model of the *lac* operon

7.1 Introduction

The full stochastic model of the *lac* operon is considered in this chapter. The full deterministic model of Yildirim and Mackey [12], considered in Chapter 4 studied the lactose operon by including two positive feedback, namely positive feedback regulation of mRNA production by allolactose and positive feedback lactose intake by permease as shown in Figure 4.1. The system has three time delays. The steady states of the full deterministic model display bistability depending on the lactose concentration.

Focusing on the important dynamical features of the *lac* operon model namely, bistability. In chapter 6 the stochastic stability was studied for the reduced model and it was found that the stochasticity can change the behaviour in the bistable region due to lactose concentration. The study of stability of the full model of the *lac* operon allows to figure out wether the noise term can change the dynamic behaviour of the system and in particularly in the bistable region due to the external lactose concentration.

To describe the stochastic behaviour of the full system, the full deterministic model of Chapter 4 is considered with a noise term. In this chapter, the stability properties

of the full stochastic model of the *lac* operon system are investigated by linearization of the system of stochastic delay differential equations (SDDEs) and using Lyapunov functional. The sufficient conditions for mean square stable state of the trivial solution ($M(t) = B(t) = A(t) = L(t) = P(t) = 0$) of linearized stochastic system around positive equilibrium are obtained.

The stochastic stability properties of the model are investigated both analytically and numerically (by using Euler Maruyama method) in order to obtain the solution of stochastic differential equations.

7.2 Stochastic stability of the full model

Consider the system of Equations (4.2.1-4.2.5) and include stochastic perturbations of the variables M, B, A, L, P from the equilibrium M_*, B_*, A_*, L_*, P_*, respectively, gives the following Ito problem.

$$\begin{aligned}
dM &= [\alpha_M f(A_{\tau_M}) - \widetilde{\gamma}_M M]dt + \sigma_1(M - M_*)dw_1(t), && (7.2.1)\\
dB &= [\alpha_B e^{-\widehat{\mu}\tau_B} M_{\tau_B} - \widetilde{\gamma}_B B]dt + \sigma_2(B - B_*)dw_2(t), && (7.2.2)\\
dA &= [\alpha_A B h(L) - \beta_A B g(A) - \widetilde{\gamma}_A A]dt + \sigma_3(A - A_*)dw_3(t), && (7.2.3)\\
dL &= [\alpha_L P h(L_e) - \beta_{L_1} P h_1(L) - \beta_{L_2} B h_2(L) - \widetilde{\gamma}_L L]dt \\
&\quad +\sigma_4(L - L_*)dw_4(t), && (7.2.4)\\
dP &= [\alpha_P e^{-\mu\tau_P} M_{\tau_P} - \widetilde{\gamma}_P P]dt + \sigma_5(P - P_*)dw_5(t). && (7.2.5)
\end{aligned}$$

where

$$h(L) = \frac{L}{K_L + L}, \quad h(L_e) = \frac{L_e}{K_{L_e} + L_e}, \quad h_1(L) = \frac{L}{K_{L_1} + L}, \quad h_2(L) = \frac{L}{K_{L_2} + L}$$

$$f(A) = \frac{1 + K_1(e^{-\mu\tau_M} A_{\tau_M})^n}{K + K_1(e^{-\mu\tau_M} A_{\tau_M})^n}, \quad g(A) = \frac{A}{K_A + A}.$$

Here $(w_1(t), w_2(t), w_3(t), w_4(t), w_5(t))$ be a five- dimensional standard Wiener process on the probability space $[\Omega, \xi, \mathbf{P}]$ with the filtration $\{\xi_t\}_{0 \le t < \infty}$ and $\overrightarrow{\boldsymbol{\sigma}} = (\sigma_1, \sigma_2, ..., \sigma_5)$ are real constants. The initial values are $M(0) = M_*,\ B(0) = B_*,\ A(0) = A_*,\ L(0) =$

$L_*,\ P(0) = P_*$. Note that the equilibrium point $(M_*,\ B_*,\ A_*,\ L_*,\ P_*)$ of the deterministic system from Chapter 4 (Equations 4.2.1-4.2.5) is being used.

The mean square stability of the trivial solution of the linearized system is investigated around equilibrium point by using Lyapunov method. The stochastic full model of the *lac* operon, represented by Equations (7.2.1-7.2.5), is investigated with three time delays τ_M, τ_B, τ_P. As a result, the following theorem is formulated.

Theorem 7.2.1. *Let the model parameters in Equations (7.2.1-7.2.5) are such that* $h(L_*) < \frac{\beta_A}{\alpha_A},\ h(L_e) < \frac{\beta_{L_1}}{\alpha_L}$ *and* $\beta_{L_1} P_* h_1'(L_*) < \beta_{L_2} B_* h_2'(L_*)$. *The three time delays of the system are satisfying*

$$\tau_{M*} = \frac{1}{2\mu}\log[\frac{\varepsilon_3\alpha_M}{2\widetilde{\beta}_A - \widetilde{\alpha}_A - \widetilde{\alpha}_{A_1})}], \qquad \tau_{B*} = \frac{1}{2\mu}\log[\frac{\alpha_B}{2\widetilde{\gamma}_B - \varepsilon_7\widetilde{\alpha}_A - \varepsilon_2\beta_{L2}h_2(L_*)}],$$
$$\tau_{P*} = \frac{1}{2\mu}\log[\frac{\alpha_P}{2\widetilde{\gamma}_P - \varepsilon_4\widetilde{\alpha}_L}] \quad , \tag{7.2.6}$$

let $\tau_{M*} < \tau_M,\ \tau_{B*} < \tau_B,\ \tau_{P*} < \tau_P$. *For any constants* $\sigma_1, \sigma_2, \sigma_3, \sigma_4, \sigma_5$ *such that*

$$\sigma_1^2 < 2\widetilde{\gamma}_M - \varepsilon_1\widetilde{\alpha}_M - \varepsilon_5\alpha_B, \quad \sigma_2^2 < 2\widetilde{\gamma}_B - \widetilde{\alpha}_B - \varepsilon_7\widetilde{\alpha}_A - \varepsilon_2\beta_{L2}g_1(L_*),$$
$$\sigma_3^2 < 2\widetilde{\beta}_A - \widetilde{\alpha}_A + \widetilde{\alpha}_{A_1} - \varepsilon_3\widetilde{\alpha}_M, \quad \sigma_4^2 < 2\widetilde{\beta}_{L1} - \xi_3\widetilde{\alpha}_A - \beta_{L2}h_2(L_*) - \widetilde{\alpha}_L,$$
$$\sigma_5^2 < 2\widetilde{\gamma}_P - \varepsilon_4\widetilde{\alpha}_L - \widetilde{\alpha}_P, \tag{7.2.7}$$

the trivial solution of the linearized system around equilibrium is mean square stable.

Proof. Let $s_1 = M - M_*, s_2 = B - B_*, s_3 = A - A_*, s_4 = L - L_*, s_5 = P - P_*$ be the change of variable for the full model of Equations (7.2.1-7.2.5). The linearized system around the positive equilibrium becomes,

$$\begin{aligned}
ds_1 &= [-\widetilde{\gamma}_M s_1 + \widetilde{\alpha}_M s_3(t-\tau_M)]dt + \sigma_1 s_1 dw_1 \\
ds_2 &= [-\widetilde{\gamma}_B s_2 + \widetilde{\alpha}_B s_1(t-\tau_B)]dt + \sigma_2 s_2 dw_2 \\
ds_3 &= [-\widetilde{\alpha}_A s_2 - \widetilde{\beta}_A s_3 - \widetilde{\alpha}_{A_1} s_4]dt + \sigma_3 s_3 dw_3 \\
ds_4 &= [-\widetilde{\alpha}_L s_5 - \beta_{L_2} h_2(L_*) s_2 - \widetilde{\beta}_{L_1} s_4]dt + \sigma_4 s_4 dw_4 \\
ds_5 &= [-\widetilde{\gamma}_P s_5 + \widetilde{\alpha}_P s_1(t-\tau_P)]dt + \sigma_5 s_5 dw_5.
\end{aligned} \tag{7.2.8}$$

Here

$$\widetilde{\alpha}_{A_1} = \alpha_A B_* h'(L_*)h(L_*), \quad \widetilde{\alpha}_A = \beta_A g(A_*) - \alpha_A h(L), \quad \widetilde{\alpha}_P = \alpha_P e^{-\mu\tau},$$

$$\widetilde{\alpha}_B = \alpha_B e^{-\widehat{\mu}\tau_B}, \quad \widetilde{\alpha}_M = \alpha_M e^{-2\widehat{\mu}\tau_M} f'(A_*), \quad f'(A_*) = \frac{2(K-1)}{(K+e^{-2\widehat{\mu}\tau_M}A^2)^2},$$

$$\widetilde{\alpha}_L = \beta_{L_1} h_1(L_*) - \alpha_L h(L_e), \quad \widetilde{\beta}_{L_1} = \widetilde{\gamma}_A - \beta_{L_1} P_* h_1'(L_*) + \beta_{L_2} B_* h_2'(L_*),$$

$$h_1(L_*) = \frac{L_*}{K_{L_1}+L_*}, \quad h_2(L_*) = \frac{L_*}{K_{L_2}+L_*}, \quad h(L_e) = \frac{L_e}{K_{L_e}+L_e}.$$

All other parameters are known in chapter 4. In general

$$ds(t) = [\nu s(t) - \upsilon s(t-\tau)]dt,$$

where $\nu = [\frac{\partial f}{\partial s_j}]_{s=0}$, $\upsilon = [\frac{\partial f}{\partial s_j(t-\tau)}]_{s=0}$, $j = 1, 2, .., 5$ and

$$\nu = \begin{pmatrix} -\widetilde{\gamma}_M & 0 & 0 & 0 & 0 \\ 0 & -\widetilde{\gamma}_B & 0 & 0 & 0 \\ 0 & -\widetilde{\alpha}_A & -\widetilde{\beta}_A & -\widetilde{\alpha}_{A_1} & 0 \\ 0 & -\beta_{L_2} h_2(L_*) & 0 & -\widetilde{\beta}_{L_1} & -\widetilde{\alpha}_L \\ 0 & 0 & 0 & 0 & -\widetilde{\gamma}_P \end{pmatrix}$$

$$\upsilon = \begin{pmatrix} 0 & 0 & \widetilde{\alpha}_M & 0 & 0 \\ \widetilde{\alpha}_B & 0 & 0 & 0 & 0 \\ 0 & 0 & 0 & 0 & 0 \\ 0 & 0 & 0 & 0 & 0 \\ \widetilde{\alpha}_P & 0 & 0 & 0 & 0 \end{pmatrix}.$$

Consider the Lyapunov functional:

$$V = V_1 + V_2, \tag{7.2.9}$$

where V_1 is chosen as follows

$$V_1(s(t)) = \frac{1}{2}(\xi_1 s_1^2 + \xi_2 s_2^2 + \xi_3 s_3^2 + s_4^2 + \xi_4 s_5^2).$$

The constants $\xi_1, \xi_2, \xi_3, \xi_4 > 0$ and V_2 will be chosen later.

For all $t \geq 0$, the first and second derivatives with respect to s are continuous, and the first derivative with respect to t is continuous and bound. Then, the definition of the differential operator $\mathbf{L}$ associated with Equation A.3.3 (see Appendix A) yields,

$$\mathbf{L} = \frac{\partial}{\partial t} + \sum_{i=1}^{m} f_i(t,s)) \frac{\partial}{\partial s_i} + \frac{1}{2} \sum_{k=1}^{m} \mathrm{Tr}[g^T(t,s) g(t,s)]_k \frac{\partial^2}{\partial s_i^2}.$$

For $V \in C([0,\infty) \times R^m; R_+)$,

$$\mathbf{L}(V) = \frac{dV_2}{dt} + f^T(s, s(t-\tau))\frac{\partial V_1}{\partial s} + \frac{1}{2}\mathrm{Tr}[g^T(t,s)\frac{\partial^2 V_1}{\partial s^2}g(t,s)].$$

The operator $\mathbf{L}(V)$ can be written as,

$$\mathbf{L}(V) = \frac{dV_2}{dt} + \mathbf{L}(V_1), \tag{7.2.10}$$

where

$$\begin{aligned} L(V_1) &= -\xi_1\widetilde{\gamma}_M s_1^2 + \xi_1\widetilde{\alpha}_M s_1 s_3(t-\tau) - \xi_2\widetilde{\gamma}_B s_2^2 + \xi_2\widetilde{\alpha}_B s_2 s_1(t-\tau) \\ &\quad -\xi_3\widetilde{\alpha}_A s_2 s_3 - \xi_3\widetilde{\beta}_A s_3^2 - \xi_3\widetilde{\alpha}_{A_1} s_3 s_4 - \beta_{L_2} h_2(L_*) s_2 s_4 - \widetilde{\beta}_{L_1} s_4^2 \\ &\quad -\widetilde{\alpha}_L s_4 s_5 - \xi_4\widetilde{\gamma}_P s_5^2 + \xi_4\widetilde{\alpha}_P s_5 s_1(t-\tau)\frac{1}{2}\xi_1\sigma_1^2 s_1^2 + \frac{1}{2}\xi_2\sigma_2^2 s_2^2 \\ &\quad +\frac{1}{2}\xi_3\sigma_3^2 s_3^2 + \frac{1}{2}\sigma_4^2 s_4^2 + \frac{1}{2}\xi_4\sigma_5^2 s_5^2. \end{aligned} \tag{7.2.11}$$

Here,

$$\frac{1}{2}\xi_1\sigma_1^2 s_1^2 + \frac{1}{2}\xi_2\sigma_2^2 s_2^2 + \frac{1}{2}\xi_3\sigma_3^2 s_3^2 + \frac{1}{2}\sigma_4^2 s_4^2 + \frac{1}{2}\xi_4\sigma_5^2 s_5^2 = \frac{1}{2}\mathrm{Tr}[g^T\frac{\partial^2 g(t,s_t)}{\partial s^2}g(t,s_t)].$$

In Equation (7.2.11) one can choose $\xi_1 = \frac{K}{n}$ where K, n are constants, normally determined from the experiment and in the case of the *lac* operon are given in Table 4.1. It is known that $f(A_*)$ is linear around the steady state which leads to $f'(A_*) \backsimeq 1$, for all $\tau_M > 0$ and $A_* \in (0, (K_A - K_L))$. This leads to $\widetilde{\alpha}_M = \alpha_M e^{-2\widehat{\mu}\tau_M}$. By using standard inequalities,

$$|s_2 s_1(t-\tau)| \leq \frac{1}{2}(s_2^2 + s_1^2(t-\tau))$$

$$|s_1 s_3(t-\tau)| \leq \frac{1}{2}(s_1^2 + s_3^2(t-\tau))$$

$$|s_5 s_1(t-\tau)| \leq \frac{1}{2}(s_2^2 + s_1^2(t-\tau))$$

$$|s_1 s_3| \leq \frac{1}{2}(s_1^2 + s_3^2)$$

$$|s_2 s_3| \leq \frac{1}{2}(s_2^2 + s_3^2)$$

$$|s_4 s_5| \leq \frac{1}{2}(s_4^2 + s_5^2)$$

$$|s_2 s_4| \leq \frac{1}{2}(s_2^2 + s_4^2)$$
$$|s_3 s_4| \leq \frac{1}{2}(s_3^2 + s_4^2),$$

from Equation (7.2.11) and after algebraic manipulation, it is obtained,

$$\begin{aligned} L(V_1) \leq & -[\xi_1\widetilde{\gamma}_M - \frac{1}{2}\widetilde{\alpha}_M - \frac{1}{2}\xi_1\sigma_1^2]s_1^2 - [\xi_2\widetilde{\gamma}_B - \frac{1}{2}\xi_2\widetilde{\alpha}_B - \frac{1}{2}\xi_3\widetilde{\alpha}_A - \frac{1}{2}\beta_{L2}g_1(L_*) \\ & -\frac{1}{2}\xi_2\sigma_2^2]s_2^2 - [\xi_3\widetilde{\beta}_A - \frac{1}{2}\xi_3\widetilde{\alpha}_A - \frac{1}{2}\xi_3\widetilde{\alpha}_{A1} - \frac{1}{2}\xi_3\sigma_3^2]s_3^2 - [\widetilde{\beta}_{L1} - \frac{1}{2}\xi_3\widetilde{\alpha}_{A_1} \\ & -\frac{1}{2}\beta_{L2}g_1(L^*) - \frac{1}{2}\widetilde{\alpha}_L - \frac{1}{2}\sigma_4^2]s_4^2 - [\xi_4\widetilde{\gamma}_P - \frac{1}{2}\widetilde{\alpha}_L - \frac{1}{2}\xi_4\widetilde{\alpha}_P - \frac{1}{2}\xi_4\sigma_5^2]s_5^2 \\ & +\frac{1}{2}\widetilde{\alpha}_M s_3^2(t-\tau) + \xi_2\frac{1}{2}\widetilde{\alpha}_B s_1^2(t-\tau) + \frac{1}{2}\xi_4\widetilde{\alpha}_P s_1^2(t-\tau) \end{aligned} \quad (7.2.12)$$

Now, define the function,

$$V_2 = \frac{1}{2}\widetilde{\alpha}_M \int_{t-\tau}^{t} s_3^2(\Theta)d\Theta + \frac{1}{2}\xi_2\widetilde{\alpha}_B \int_{t-\tau}^{t} s_1^2(\Theta)d\Theta + \frac{1}{2}\xi_4\widetilde{\alpha}_P \int_{t-\tau}^{t} s_1^2(\Theta)d\Theta,$$

where

$$\begin{aligned} \frac{dV_2}{dt} = & \frac{1}{2}[\widetilde{\alpha}_M s_3^2 + \xi_4\widetilde{\alpha}_B s_1^2 + \xi_4\widetilde{\alpha}_P s_1^2 - \widetilde{\alpha}_M s_3^2(t-\tau) - \widetilde{\alpha}_B s_1^2(t-\tau) \\ & -\xi_4\widetilde{\alpha}_P s_1^2(t-\tau)]. \end{aligned} \quad (7.2.13)$$

From the generating operator (7.2.10) using 7.2.12 and 7.2.13) and considering the Lyapunov functional, $V = V_1 + V_2$, after some algebra, the following is obtained,

$$\begin{aligned} \mathbf{L}(V) \leq & -[\xi_1\widetilde{\gamma}_M - \frac{1}{2}\widetilde{\alpha}_M - \frac{1}{2}\xi_2\widetilde{\alpha}_B - \frac{1}{2}\xi_4\widetilde{\alpha}_P - \frac{1}{2}\xi_1\sigma_1^2]s_1^2 - [\xi_2\widetilde{\gamma}_B - \frac{1}{2}\xi_2\widetilde{\alpha}_B - \frac{1}{2}\xi_4\widetilde{\alpha}_A \\ & -\frac{1}{2}\beta_{L2}h_2(L_*) - \frac{1}{2}\xi_2\sigma_2^2]s_2^2 - [\xi_3\widetilde{\beta}_A - \frac{1}{2}\xi_3\widetilde{\alpha}_A - \frac{1}{2}\xi_3\widetilde{\alpha}_{A1} - \frac{1}{2}\widetilde{\alpha}_M - \frac{1}{2}\xi_3\sigma_3^2]s_3^2 \\ & -[\widetilde{\beta}_{L1} - \frac{1}{2}\xi_3\widetilde{\alpha}_A - \frac{1}{2}\beta_{L2}h_2(L^*) - \frac{1}{2}\alpha_L - \frac{1}{2}\sigma_4^2]s_4^2 - [\xi_4\widetilde{\gamma}_P - \frac{1}{2}\widetilde{\alpha}_L - \frac{1}{2}\xi_4\widetilde{\alpha}_P \\ & -\frac{1}{2}\xi_4\sigma_5^2]s_5^2. \end{aligned} \quad (7.2.14)$$

Using the values of the parameters given in Table 4.1, $\xi_1 = \frac{K}{n}$ and $\xi_2, \xi_3, \xi_4, \xi_5 > 0$, the following is obtained from Equation (7.2.14),

$$2\widetilde{\gamma}_M - \varepsilon_1\widetilde{\alpha}_M - \varepsilon_5\alpha_B > 0, \quad 2\widetilde{\gamma}_B - \widetilde{\alpha}_B - \varepsilon_7\widetilde{\alpha}_A - \varepsilon_2\beta_{L2}g_1(L_*) > 0,$$

$$2\widetilde{\beta}_A - \widetilde{\alpha}_A + \widetilde{\alpha}_{A_1} - \varepsilon_3\widetilde{\alpha}_M > 0, \quad 2\widetilde{\beta}_{L1} - \xi_3\widetilde{\alpha}_A - \beta_{L2}h_2(L_*) - \widetilde{\alpha}_L > 0,$$

$$2\widetilde{\gamma}_P - \varepsilon_4\widetilde{\alpha}_L - \widetilde{\alpha}_P > 0,$$

where $\varepsilon_1 = \frac{1}{\xi_1}$, $\varepsilon_2 = \frac{1}{\xi_2}$, $\xi_3 = \frac{1}{\varepsilon_3}$, $\xi_4 = \frac{1}{\varepsilon_4}$, $\xi_5 = \frac{\xi_2}{\xi_1}$, $\xi_6 = \frac{\xi_4}{\xi_1}$, $\xi_7 = \frac{\xi_4}{\xi_2}$.
Thus, σ_i, $i = 1, 2, 3, 4, 5$, are positive real numbers if $\tau_M* < \tau_M$, $\tau_B* < \tau_B, \tau_P* < \tau_P$.
Therefore the function V satisfies all assumption of Theorem 7.2.1

7.3 Numerical solution and investigation of the dynamic behaviour with stochastic noise

The Ito system (7.2.1-7.2.5) is solved numerically by Euler Maruyama methods with constant stepsize. According to the conditions given in Theorem 7.2.1, the mean square stability of the positive steady state depends on σ_i, $i = 1, 2, 3, 4, 5$, and three time delays. Using conditions 7.2.6 and 7.2.7 of Theorem 7.2.1 and the parameters from Table 4.1, the system is exponentially mean square stable for $\sigma_1 < 0.0207$, $\sigma_2 < 0.045$, $\sigma_3 < 0.042$, $\sigma_4 < 0.0403$, $\sigma_5 < 0.05$ and $\tau_M > 0.0522$, $\tau_B > 0.975$, $\tau_P > 1.21$. These are the threshold values for the model. For convenience, in what follows the notation for perturbation (noise), $\overrightarrow{\boldsymbol{\sigma}} = (\sigma_1, \sigma_2, \sigma_3, \sigma_4, \sigma_5)$. The results in this sub-section will be illustrated in the case when $\sigma_1 = \sigma_2 = \sigma_3 = \sigma_4 = \sigma_5 = \boldsymbol{\sigma}$

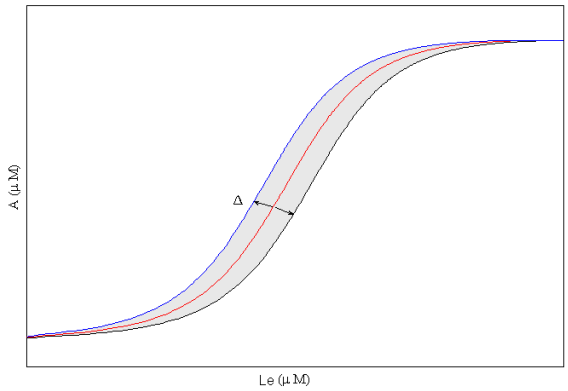

Figure 7.1: Steady state (S-shape curve) displacement due to the distance between the initial value and equilibrium point for allolactose (Δ).

For the allolactose, A, the displacement from the equilibrium by the noise term, depends on the initial conditions. Figure 7.1 illustrated the case when the initial conditions are changed from the steady state by Δ to the left and the right.

In Figure 7.1, one has to find a limit value for Δ such that the variable close to it must be in the region where steady state exits (S-shape curve) and this depends on the value of L_e. Introducing $\frac{\boldsymbol{\sigma}}{\Delta}$, where Δ is the distance between the initial values and equilibrium points which assured that Δ is small enough not affect the S-shape curve. The values of $\frac{\boldsymbol{\sigma}}{\Delta}$ are compered with the noise values which is obtained from the theorem 7.2.1. There are different cases, no change in the S-shape curve (Figure 7.1) when $\frac{\boldsymbol{\sigma}}{\Delta} \geq 1$ (the value of Δ is smaller or same the value of $\boldsymbol{\sigma}$). Whereas, in the case when the value of Δ is larger than the value of $\boldsymbol{\sigma}$, the S-shape curve changes (displacement) within the steady states values when $1 < \Delta \leq 15\,\mu M$ and concluded that $\frac{\boldsymbol{\sigma}}{\Delta} < 1$.

7.3.1 Stable behaviour

The model can display bistability (Chapter 4) depending on the external lactose concentration. Furthermore, the upper solution is stable and induced, the lower is stable and uninduced and the middle solution is unstable are all of the state $\overrightarrow{\mathbf{S}} = (M, B, A, L, P)$. The numerical simulation shows the behaviour of the system (7.2.1-7.2.5) with the perturbation $\overrightarrow{\boldsymbol{\sigma}} = (\sigma_1, \sigma_2, ..., \sigma_5)$. All five coordinates change in a synchronized way. For instance, in this model of the *lac* operon, if A_* belongs to lower state (uninduced) for $L_e = 20\ \mu M$, so will be M_*, B_*, L_*, P_*, as shown in Figures 7.2-7.4 all the components of a state are induced or uninduced ($L_e = 70\ \mu M$) in a synchronization behaviour, Since the scale of allolactose and lactose is much larger than mRNA, $\beta-$ galoctosidase and permease the behaviour is shown in three figures.

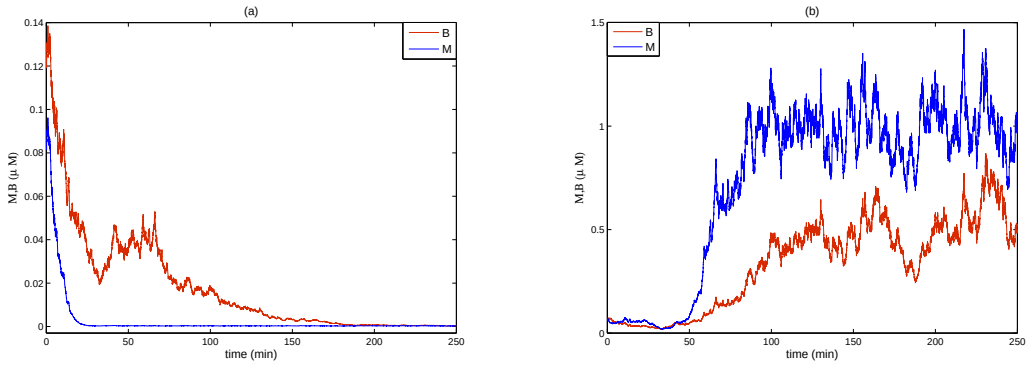

Figure 7.2: $M, B\,(\mu M)$ concentration versus time (minutes) $\sigma_1 = \sigma_2 = \sigma_3 = \sigma_4 = \sigma_5 = 0.03$, a) uninduced state for $L_e = 20\ \mu M$ b) induced state for $L_e = 70\ \mu M$.

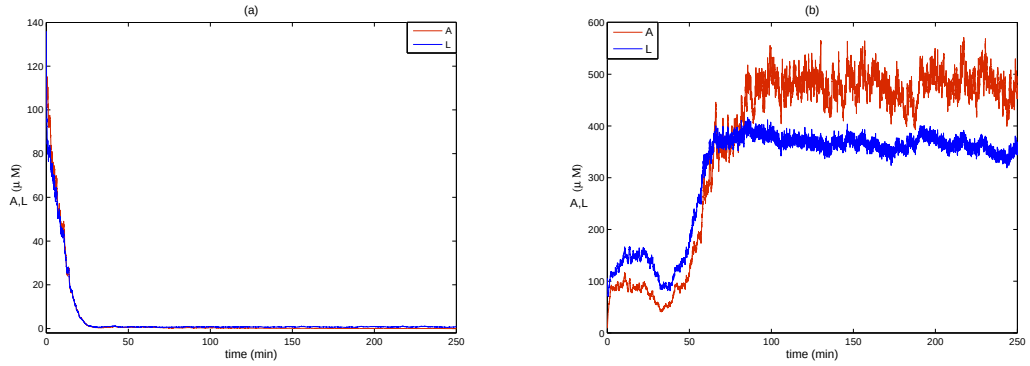

Figure 7.3: $A, L\,(\mu M)$ concentration versus time (minutes) $\sigma_1 = \sigma_2 = \sigma_3 = \sigma_4 = \sigma_5 = 0.03$, a) uninduced state for $L_e = 20\ \mu M$ b) induced state for $L_e = 70\ \mu M$.

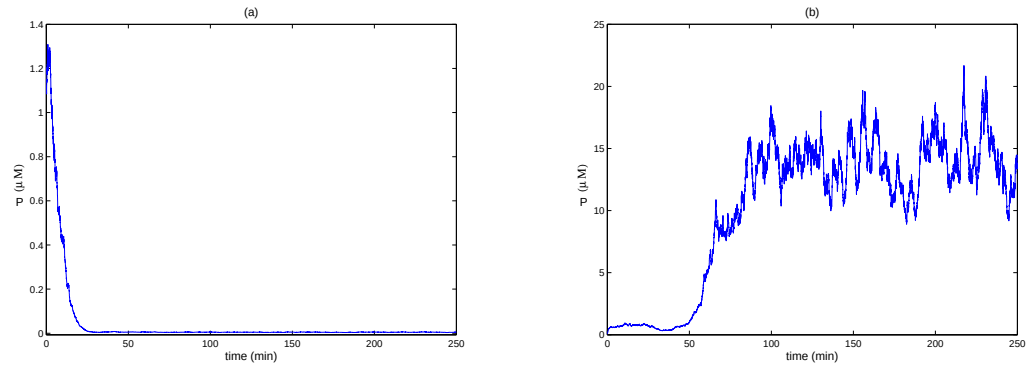

Figure 7.4: $P\,(\mu M)$ concentration versus time (minutes) $\sigma_1 = \sigma_2 = \sigma_3 = \sigma_4 = \sigma_5 = 0.03$, a) uninduced state for $L_e = 20\ \mu M$ b) induced state for $L_e = 70\ \mu M$.

7.3.2 Inside the bistable region

The numerical simulation of mRNA, $\beta-$ galoctosidase, allolactose, lactose and permease (system 7.2.1-7.2.5) with time delays is shown in Figure 7.5 for five values of the noise term. For the case of three possible stable solutions and an opportunity for multi-stable behaviour ($L_e = 30\ \mu M$). The deterministic full model (Chapter 4) is bistable which is only possible when the loop is active by lactose (induced). The stochastic stability framework is useful in understanding the stability of equilibria point and allows to define more adequate description of the dynamics of induced and uninduced states in the bistable region. The most significant changes are observed for the allolactose A and lactose L (see [11, Figure 2]), where the concentrations are significantly higher compared to B, M, L and P. This is expected as the values of A and L are larger than the values of the other three variables M, B and P. Figure 7.5 illustrates the behaviour of the model when $L_e = 30\mu M$ (coexisting three steady states) with perturbation $\boldsymbol{\sigma} = (\sigma_1, \sigma_2, \sigma_3, \sigma_4, \sigma_5)$, (a) $\sigma_1 = \sigma_2 = \sigma_3 = \sigma_4 = \sigma_5 = 0.01$, (b) $\sigma_1 = 0.01, \sigma_2 = 0.02, \sigma_3 = 0.03, \sigma_4 = 0.035, \sigma_5 = 0.04$. Time delays have been chosen as $\tau_M = 0.1$ min, $\tau_B = 2$ min, $\tau_P = 2.38$ min, as these three time delays are the maximal time delays for the system as suggested in [11] (see Table 4.1) and also satisfy the conditions of Theorem 7.2.1.

For very small perturbation, reflected by the values of $\boldsymbol{\sigma} = (\sigma_1, \sigma_2, \sigma_3, \sigma_4, \sigma_5)$, the unstable middle state with coordinate $A2$ converges to $A3$ coordinate, while with increased noise $\boldsymbol{\sigma}$ this solution converges to the lower state with coordinate $A1$. Similar behaviour is observed for M, B, L and P, where the concentrations versus time are shown in Figures 7.7-7.9 respectively. The stochastic system is bistable and the noise affects mainly the middle solution for all concentrations M, B, A, L, P, while lower (uninduced) and upper (induced) solutions for M, B and P are almost unchanged by noise around the equilibrium. The initial values were taken when $L_e = 30\ \mu M$ and are given in Table 4.3.

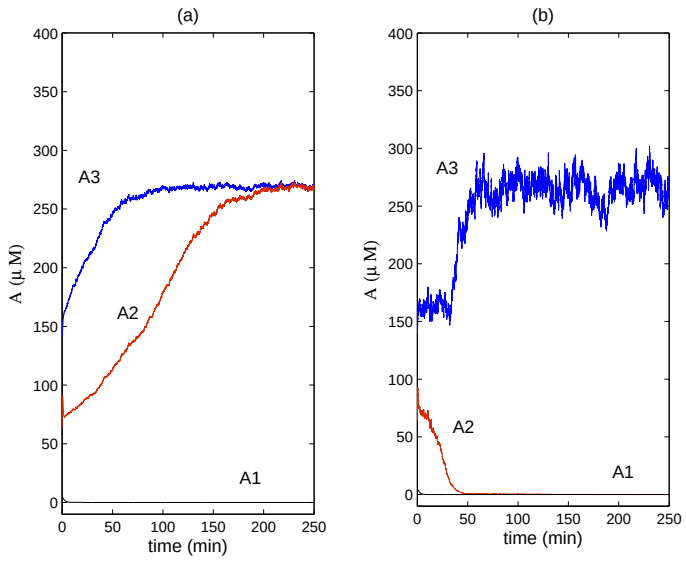

Figure 7.5: Stochastic model showing $A(\mu M)$ concentration versus time (minutes) in bistable region, $L_e = 30\ \mu M$, $A1, A2, A3$ are the coordinates of the lower, middle and upper steady states of the model. Time delays are $\tau_M = 0.1,\ \tau_B = 2,,\ \tau_P = 2.38$ and the noise term is (a) $\sigma_1 = \sigma_2 = \sigma_3 = \sigma_4 = \sigma_5 = 0.01$, (b) $\sigma_1 = 0.01, \sigma_2 = 0.02, \sigma_3 = 0.03, \sigma_4 = 0.035, \sigma_5 = 0.04$.

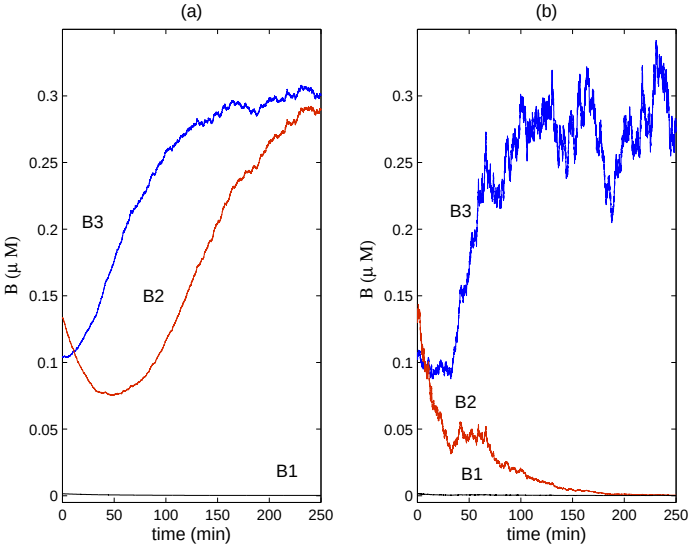

Figure 7.6: Stochastic model showing $B(\mu M)$ concentration versus time (minutes) in bistable region, $L_e = 30\ \mu M$, $B1, B2, B3$ are the coordinates of the lower, middle, upper steady state of the model. Time delays are $\tau_M = 0.1,\ \tau_B = 2,,\ \tau_P = 2.38$ and the noise term is ((a) $\sigma_1 = \sigma_2 = \sigma_3 = \sigma_4 = \sigma_5 = 0.01$, (b) $\sigma_1 = 0.01, \sigma_2 = 0.02, \sigma_3 = 0.03, \sigma_4 = 0.035, \sigma_5 = 0.04$.

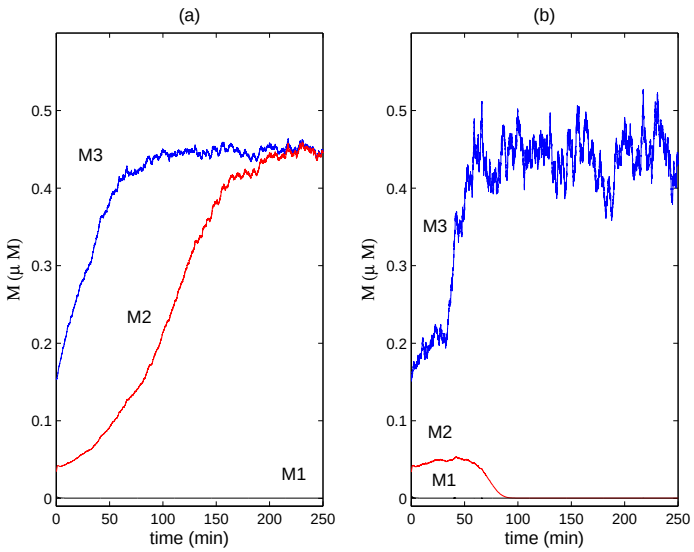

Figure 7.7: Stochastic model showing $M(\mu M)$ concentration versus time (minutes) in bistable region, $L_e = 30\ \mu M$, $M1, M2, M3$ are the coordinates of the lower, middle, upper steady state of the model. Time delays are $\tau_M = 0.1,\ \tau_B = 2,,\ \tau_P = 2.38$ and the noise term is (a) $\sigma_1 = \sigma_2 = \sigma_3 = \sigma_4 = \sigma_5 = 0.01$, (b) $\sigma_1 = 0.01, \sigma_2 = 0.02, \sigma_3 = 0.03, \sigma_4 = 0.035, \sigma_5 = 0.04$.

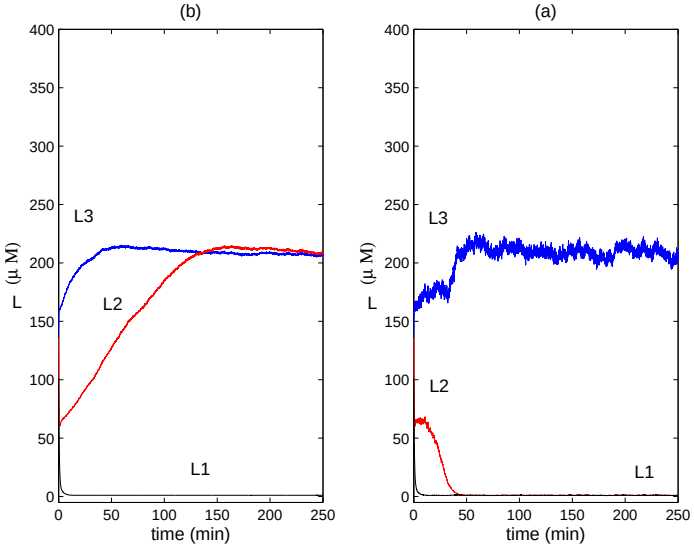

Figure 7.8: Stochastic model showing $L(\mu M)$ concentration versus time (minutes) in bistable region, $L_e = 30\ \mu M$, $L1, L2, L3$ are the coordinates of the lower, middle, upper steady state of the model. Time delays are $\tau_M = 0.1,\ \tau_B = 2,,\ \tau_P = 2.38$ and the noise term is (a) $\sigma_1 = \sigma_2 = \sigma_3 = \sigma_4 = \sigma_5 = 0.01$, (b) $\sigma_1 = 0.01, \sigma_2 = 0.02, \sigma_3 = 0.03, \sigma_4 = 0.035, \sigma_5 = 0.04$.

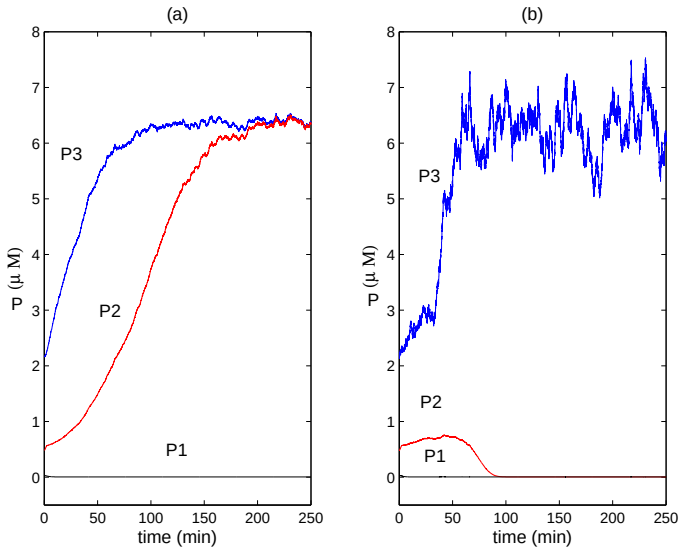

Figure 7.9: Stochastic model showing $P(\mu M)$ concentration versus time (minutes) in bistable region, $L_e = 30\ \mu M$, $P1, P2, P3$ are the coordinates of the lower, middle, upper steady state of the model. Time delays are $\tau_M = 0.1$, $\tau_B = 2,$, $\tau_P = 2.38$ and the noise term is (a) $\sigma_1 = \sigma_2 = \sigma_3 = \sigma_4 = \sigma_5 = 0.01$, (b) $\sigma_1 = 0.01, \sigma_2 = 0.02, \sigma_3 = 0.03, \sigma_4 = 0.035, \sigma_5 = 0.04$.

7.3.3 Around the boundary of bistable region

Here the stochastic behaviour at the left and right end of the bistable region is investigated, corresponding to $L_e = 27.5\ \mu M$ and $L_e = 62\ \mu M$ respectively. This is the first attempt to investigate in details the behaviour in the bistable region for the full stochastic model of the *lac* operon. Figure 7.10 a), shows that when the system is at the left boundary point, $L_e = 27.5 \mu M$, the effect of noise is that allolactose in upper state (induced) can switch to lower state (uninduced) after approximately 30 minutes. However, when the system is at the right boundary point $L_e = 62\ \mu M$, the switch from lower (uninduced) to upper (induced) states appears after approximately 40 minutes and the system remain in the induced (Figure 7.10 b). The same behaviour for all coordinates of B, M, L and P are shown in Figures 7.11 a) and b)-7.14 a) and b) respectively.

The following interesting features are observed: In bistable region close to the left boundary point $L_e = 28\ \mu M$, the upper state (induced) switches to lower state (uninduced) (Figure 7.10 c). Close to the right boundary point, $L_e = 61\ \mu M$, the lower

state switches to upper state even when the noise very small (Figure 7.10 d). Similar behaviour is observed around the boundary points for B, M, L and P are shown in Figures 7.11 c) and d)- 7.14 c) and d) respectively. The simulation result shows that fluctuations can cause switching from uninduced to induced state and observed that the opposite around the left boundary point.

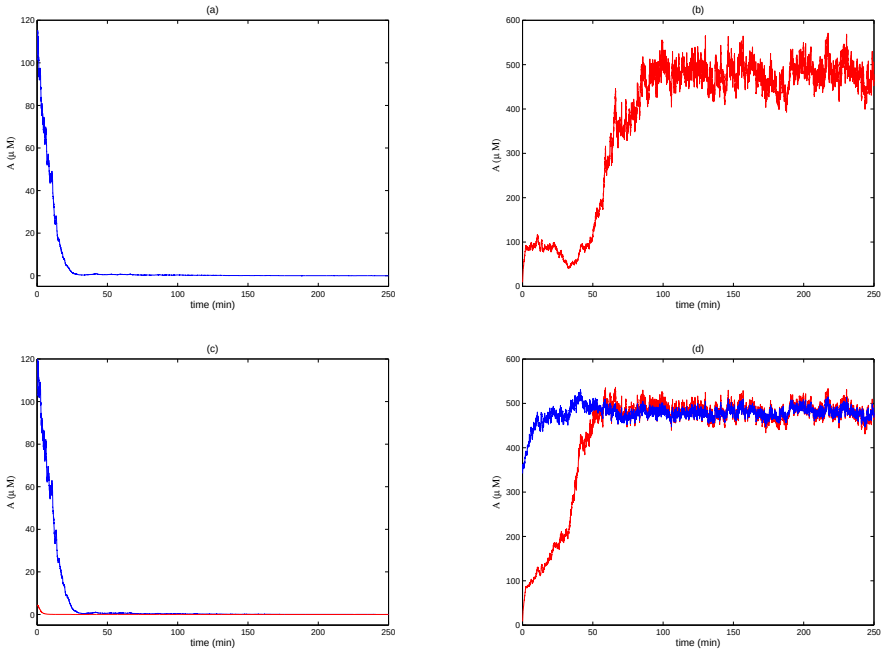

Figure 7.10: $A\,(\mu M)$ concentration versus time (minutes) $\sigma_1 = \sigma_2 = \sigma_3 = \sigma_4 = \sigma_5 = 0.03$, a) left boundary point $L_e = 27.5\ \mu M$, b) right boundary point $L_e = 62\ \mu M$, c) around left boundary point $L_e = 28\ \mu M$, d) around right boundary point $L_e = 61\ \mu M$.

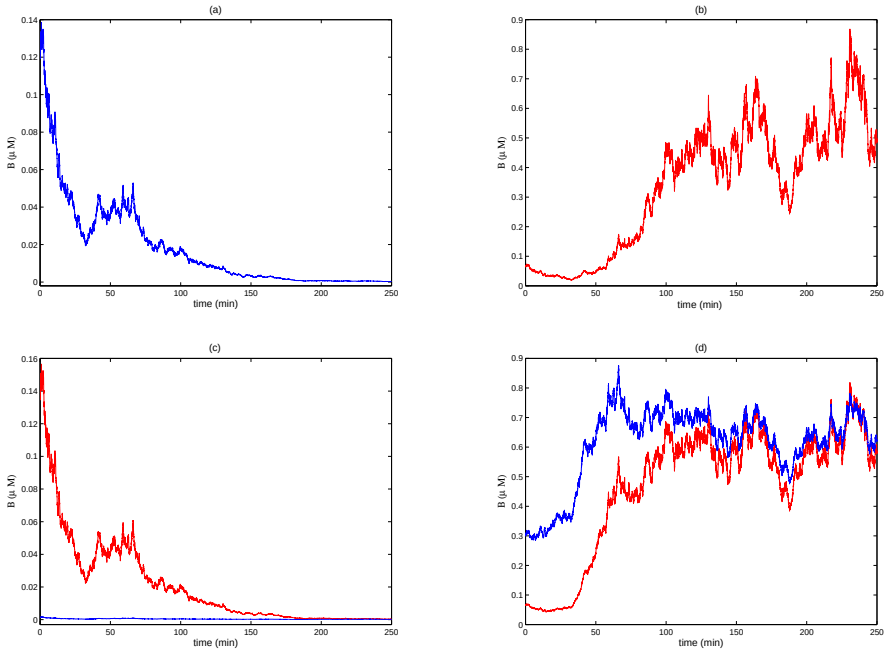

Figure 7.11: $B\,(\mu M)$ concentration versus time (minutes) $\sigma_1 = \sigma_2 = \sigma_3 = \sigma_4 = \sigma_5 = 0.03$, a) left boundary point $L_e = 27.5\ \mu M$, b) right boundary point $L_e = 62\ \mu M$, c) around left boundary point $L_e = 28\ \mu M$, d) around right boundary point $L_e = 61\ \mu M$.

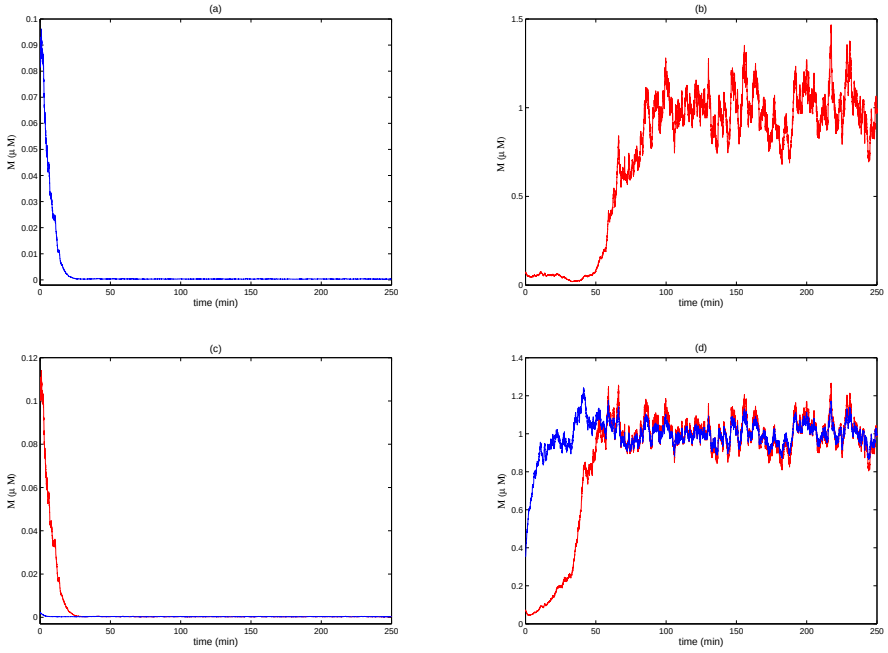

Figure 7.12: $M\,(\mu M)$ concentration versus time (minutes) $\sigma_1 = \sigma_2 = \sigma_3 = \sigma_4 = \sigma_5 = 0.03$, a) left boundary point $L_e = 27.5\ \mu M$, b) right boundary point $L_e = 62\ \mu M$, c) around left boundary point $L_e = 28\ \mu M$, d) around right boundary point $L_e = 61\ \mu M$.

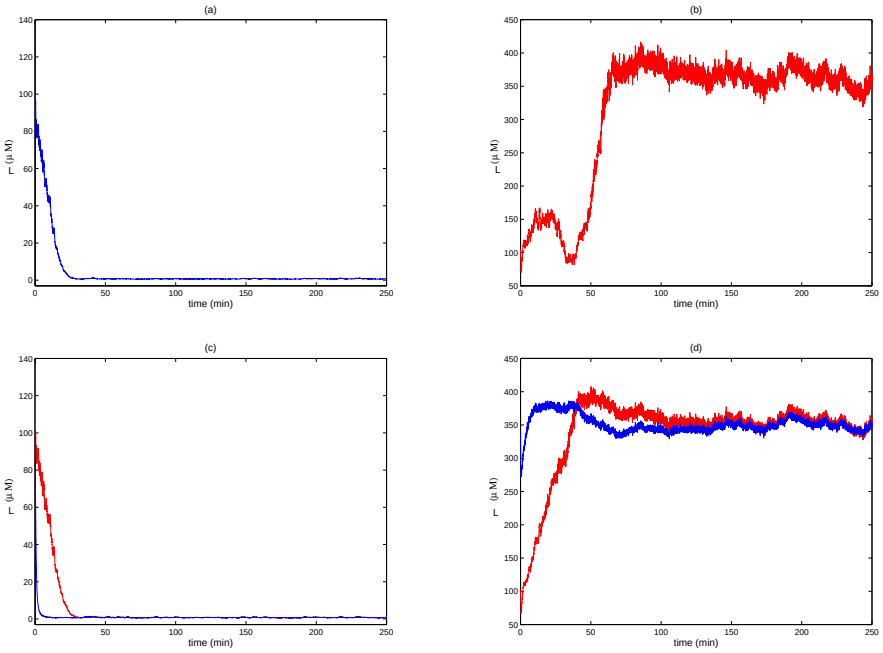

Figure 7.13: $L\,(\mu M)$ concentration versus time (minutes) $\sigma_1 = \sigma_2 = \sigma_3 = \sigma_4 = \sigma_5 = 0.03$, a) left boundary point $L_e = 27.5\ \mu M$, b) right boundary point $L_e = 62\ \mu M$, c) around left boundary point $L_e = 28\ \mu M$, d) around right boundary point $L_e = 61\ \mu M$.

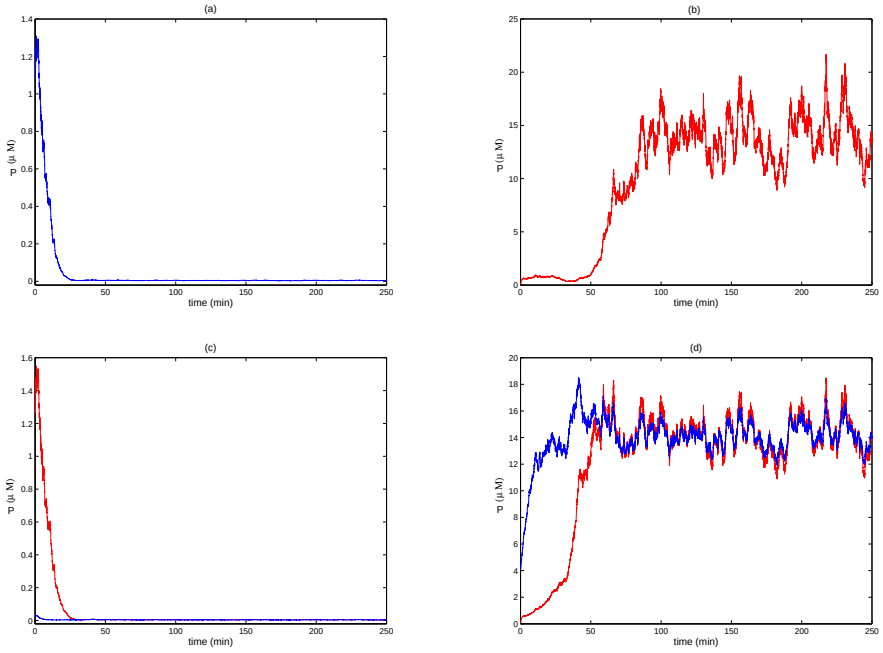

Figure 7.14: $P\,(\mu M)$ concentration versus time (minutes) $\sigma_1 = \sigma_2 = \sigma_3 = \sigma_4 = \sigma_5 = 0.03$, a) left boundary point $L_e = 27.5\ \mu M$, b) right boundary point $L_e = 62\ \mu M$, c) around left boundary point $L_e = 28\ \mu M$, d) around right boundary point $L_e = 61\ \mu M$.

7.4 Stability behaviour due to perturbation of some proteins

The behaviour of the system is investigated numerically when noise is added to the equation (7.2.3) describing the allolactose, A, and equation (7.2.5) for the permease, P. As shown in Chapter 4, the positive feedback regulations of the full model are regulated by allolactose and permease.

In this case, the simulations show that if the system is at a single lower (uninduced) or upper (induced) state it oscillates around this state when noise is added. This is illustrated for P in Figure 7.15 a), when $L_e = 80\ \mu M$ with large noise ($\sigma_3 = \sigma_5 = 0.4, \sigma_1 = \sigma_2 = \sigma_4 = 0$). In the bistable region, large noise ($\sigma_3 = \sigma_5 = 0.4, \sigma_1 = \sigma_2 = \sigma_4 = 0$) can switch from lower to upper state and vice versa. This is illustrated in Figure 7.15 b) when $L_e = 30\ \mu M$ and the system is initially in the upper state. However, when large noise is added to just allolactose or permease, switching inside bistable region has not been observed, even when large noise added to all five concentrations (M, B, A, L, P).

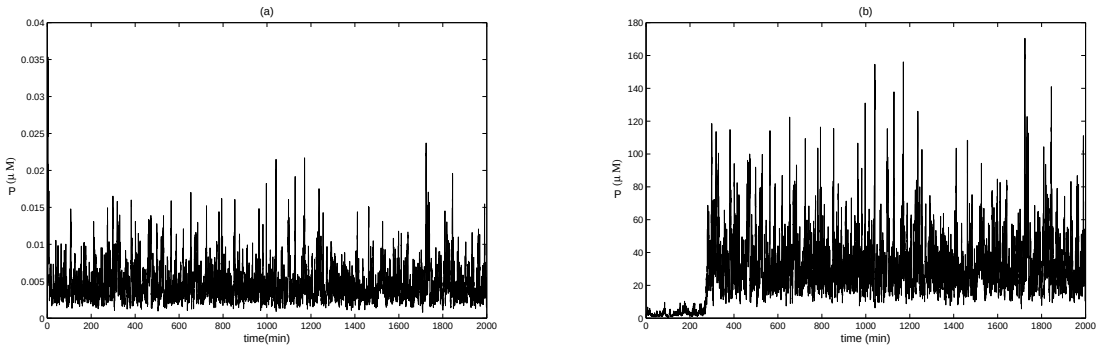

Figure 7.15: P $(\mu M))$ concentration versus time (minutes). a) Initial values $L_e = 80\ \mu M$, $\sigma_3 = \sigma_5 = 0.4$. b) Initial values $L_e = 30$ (μM), $\sigma_3 = \sigma_5 = 0.4$.

7.5 Summary

The stability of the full stochastic model around equilibrium is studied in this chapter in the presence of noise and time delays. The sufficient conditions of exponential mean square stability derived giving threshold values for the noise terms. The numerical solution of the Ito stochastic differential equations (7.2.1-7.2.5) by the Euler Maruyama method verified that the stability of the positive equilibrium depends on the values of the noise terms, time delays and the parameters of the system.

If L_e lies in the bistable region the concentrations of mRNA, β- galoctosidase, allolactose, lactose and permease can co-exist in two steady states. When there is an unstable steady state (for $L_e = 30\ \mu M$, Figure 7.9 for example), it evolves to upper or lower state for the small or larger noise respectively. The model has shown that changes are most significant in allolactose and lactose when all concentrations M, B, A, L and P were perturbed with the same noise term. The behaviour was investigated within the bistable region, near to equilibrium is investigated when noise terms are below threshold values. The numerical simulations confirmed that if the system is in upper (induced) state or lower (uninduced) state it remains in such state in presence of perturbation. However, for values of external lactose at or around the right boundary point of the bistable region the system can switch from uninduced to induced state even if the noise is small. Thorough investigation of the stochastic stability of the full model of *lac* operon within and outside bistable region with respect to external lactose concentration and noise terms demonstrates that the system behaviour is dependent on the external lactose levels and perturbations. As such, it is demonstrated that the stochasticity can change the behaviour in the bistable region but it depends on the value of external lactose. Experimentally, bistablility as a function of lactose levels has been observed for artificial sugars only ([10]).

Chapter 8

The observer method for the *lac* operon

8.1 Introduction

As explained in the previous chapters, the state space representation of the *lac* operon model provides a suitable basis for stability analysis. In addition, from a control theory point of view, it also provides a suitable and necessary basis for designing feedback control laws. In the context of state feedback control design, the following important issues need to be addressed:
1) first, one needs to identify the inputs and outputs (measured variables) of the system. In the case of the *lac* operon, the inputs considered in this work, is the lactose concentration, L, and the output is allolactose concentration, A.
2) next one needs to identify which variables are not measured (or accessible). This is important because if the feedback laws depends on the state variables that are not measured, then one cannot practically implement the control law. In the case of the *lac* operon, the non-measured variables are the mRNA, M, and the β-galactosidase, B, respectively.

It is also important to note that when some state variables are not measured one can either use a sensor or an observer. However, sensors are quite expensive compared to

observers. In effect, observers are basically software sensors. For this reasons they are quite cheap with respect to analyzers used to measure concentrations.

To be more precise, an observer is a dynamical system that uses the measured inputs $u(t)$ and outputs $y(t)$ in order to provide an estimate $\widetilde{x}(t)$ of the non-measured variables $x(t)$ as shown in Figure 8.4. Finally, it is also important to note that it is not always possible to design an observer or any arbitrary system; one has to verify whether the system is observable or not before proceeding to design an observer. Similarly in control design one has to verify whether a system is controllable or not before designing a controller.

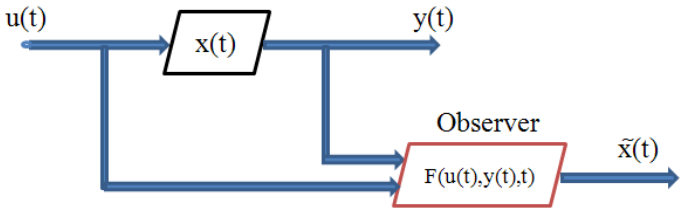

Figure 8.1: Observer design.

There are many observer design methodologies for observer design; see for instance [52, 53, 54, 55] just to mentioned a few.

In this chapter, an observer will be designed in order to estimate the concentration of the mRNA M and the β-galactosidase B respectively. To the best of the author's knowledge, there is no works in the literature that deals with the estimation of the mRNA and the β-galactosidase using observers. In this sense, such work may be seen as a starting point for future development in this area.

As mentioned before, the input is the lactose L and output is the allolactose A shown in Figure 8.2. As a control objective a controller will be designed so that allolactose feeds back to bind with the repressor R and enables the mRNA M to proceed.

Before proceed to study the observer design for the *lac* operon a brief overview about observer and control design method is given.

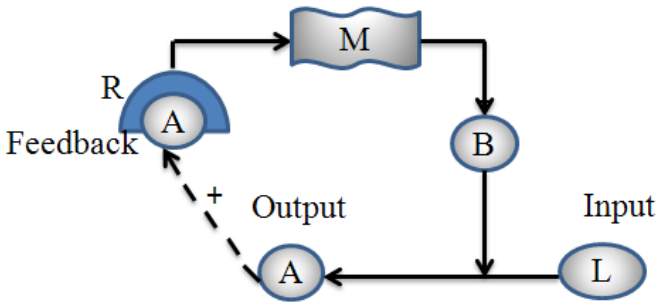

Figure 8.2: Feedback loop for the *lac* operon model.

8.2 Observer design

Consider a dynamic system is described in state space form as

$$\frac{dx(t)}{dt} = \dot{x}(t) = f(x(t), u(t)), \tag{8.2.1}$$

where x is the state variable, $x \in R^n$, and u is the control variable, $u \in R^m$.
The measurement (output) vector y is given by

$$y = h(x(t)), \tag{8.2.2}$$

where $y \in R^p$. Generally, $p < n$, which means that $n - p$ variables are not measured. In the case where $p = n$, an observer is not require because all the variables are being measured by some sensors or other means.

An observer for the above system can be written as:

$$\dot{\widehat{x}} = f(\widehat{x}, u) + K(y - h(\widehat{x})), \tag{8.2.3}$$

where K is the so-called observer gain vector which might depend on y, u and $\widehat{x}$ or may be constant. One needs to design K such that the distance $\|x(t) - \widehat{x}(t)\|$ tends to 0 when $t \to +\infty$.

In other words, setting $e = x - \widehat{x}$, the requirement is that the error dynamic,

$$\dot{e} = \dot{x} - \dot{\widehat{x}} = f(x, u) - f(\widehat{x}, u) - K(y - h(\widehat{x}))$$

to be stable.

From the above expression, it can readily be seen that this is not an easy task. For this one has to find the proper observer gain and a proper Lyapunov function in order to prove the convergence of the error dynamics. Additionally, the observability properties for nonlinear systems in general depends on the applied inputs. In other words, there may be inputs for which the system is observable while it might not be observable for other inputs. The inputs that makes a nonlinear system unobservable are called "singular inputs" [55].

However, in the case of linear observable systems the observability property hold for all inputs. Also, the observer design theory is well established in such a case. In what follows, the observer design methodology is recalled for linear systems. In effect, in such a case, we have $f(x(t), u(t)) = Ax(t) + Bu(t)$ and $y(t) = Cx(t)$ where A, B and C are square matrices of appropriate dimensions.

Here, the observer is given by:

$$\dot{\widehat{x}} = A\widehat{x} + Bu + K(y - C\widehat{x}), \tag{8.2.4}$$

and the error dynamics is given by:

$$\dot{e} = (A - KC)e.$$

In this case one has to choose the estimator gain K such that the eigenvalues of the matrix $A - KC$ lies in the left-half complex plane.

8.3 State feedback control design

Consider again the system:

$$\frac{dx(t)}{dt} = f(x(t), u(t)) \tag{8.3.1}$$

There are several control design strategies in the literature for the above systems [56]. In general, the objective of a state feedback control design is to find a function $u(x) = \alpha(x)$ such that the closed-loop system:

$$\frac{dx}{dt} = f(x, \alpha(x)) \tag{8.3.2}$$

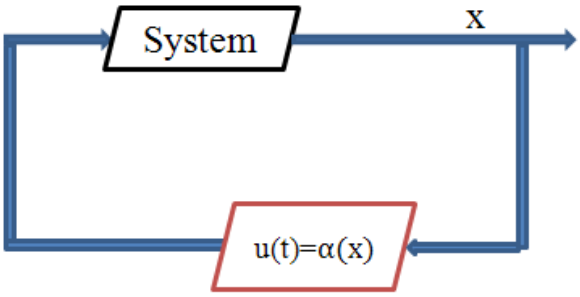

Figure 8.3: Controller design.

is stable.

Figure 8.3 illustrates a typical state feedback control loop. As in the case of observer design, nonlinear control design is not an easy matter. Generally, one has to find a proper Lyapunov function $V(x)$ such that $\frac{dV(x(t))}{dt} < 0$ in order to prove asymptotic stability. The systematic search for a candidate Lyapunov function for a general nonlinear closed-loop system is still an open problem.

8.4 Observer-based estimation for the *lac* operon

In this section, the reduced model the *lac* operon given in Chapter 3 is considered. An estimate of B and M will be provided by assuming that A is measured and that the input signal is L. For simplicity, $\tau_M = \tau_B = 0$ is assumed in equations (5.2.1-5.2.3) which gives:

$$\frac{dA}{dt} = -\widetilde{\gamma}_A A + [\alpha_A h(L) - \beta_A g(A)]B \tag{8.4.1}$$

$$\frac{dB}{dt} = -\widetilde{\gamma}_B B + \alpha_B M \tag{8.4.2}$$

$$\frac{dM}{dt} = -\widetilde{\gamma}_M M + \alpha_M f(A), \tag{8.4.3}$$

where

$$h(L) = \frac{L}{K_L + L}, \quad g(A) = \frac{A}{K_A + A}, \quad f(A) = \frac{1 + K_1 A^n}{K + K_1 A^n}.$$

First, it will be shown that the above system can be written in a state-affine form:

$$\begin{pmatrix} \frac{dA}{dt} \\ \frac{dB}{dt} \\ \frac{dM}{dt} \end{pmatrix} = \begin{pmatrix} -\widetilde{\gamma}_A & \alpha_A h(L) - \beta_A g(A) & 0 \\ 0 & -\widetilde{\gamma}_B & \alpha_B \\ 0 & 0 & -\widetilde{\gamma}_M \end{pmatrix} \begin{pmatrix} A \\ B \\ M \end{pmatrix} + \begin{pmatrix} 0 \\ 0 \\ \alpha_M f(A) \end{pmatrix},$$

which can be presented as

$$\begin{aligned} \frac{dX}{dt} &= F(u)X + \phi(y), \\ y &= A = CX, \end{aligned} \tag{8.4.4}$$

where $u = L$, $C = (1, 0, 0)$ and

$$X = \begin{pmatrix} A \\ B \\ M \end{pmatrix},$$

$$F(u) = \begin{pmatrix} 0 & \alpha_A h(L) - \beta_A g(A) & 0 \\ 0 & 0 & \alpha_B \\ 0 & 0 & 0 \end{pmatrix}.$$

Since the above system is in the state affine form, a typical observer for this kind of system is given in [57]:

$$\begin{aligned} \dot{\hat{Z}} &= F(u)\hat{Z} + S^{-1}C^T(y - C\hat{Z}), \\ \dot{S} &= -\theta S + F^T(u)S + SF(u) + C^T C. \end{aligned} \tag{8.4.5}$$

where $S(0) = I$ and $S(t)$ is a symmetric positive definite matrix. Note that since the observer gain $S^{-1}C^T$ requires the inversion of a matrix, one can avoid this inversion by witting the above observer as follows: Let $R = S^{-1}$, that is $SR = I$ and therefore $\dot{S}R = -S\dot{R}$. This led to $\dot{R} = -R\dot{S}R$. Replacing this last equality in:

$$\dot{S} = -\theta S + F^T(u)S + SF(u) + C^T C$$

one obtains

$$-R\dot{S}R = -(-\theta RSR + RF^T(u)SR + RSF(u)R + RC^T CR)$$

Hence,

$$\begin{aligned} \hat{Z} &= (F(u)\hat{X} + \phi(y)) + RC^T(y - C\hat{Z}), \\ \dot{R} &= \theta R + RF^T(u) + RF(u) - RC^T CR, \\ R(0) &= I. \end{aligned} \tag{8.4.6}$$

A simulation was carried out for the above observer. The results are shown in Figures (8.4,8.5,8.6). It can be seen that the observer converges to the true state of the system under arbitrary initial conditions.

8.5 Control design for the *lac* operon

In this section, a state feedback controller is designed for the *lac* operon. The main objective here is to regulate A to a reference value A_{ref} while maintaining all the other variables bounded. Again the reduced model of the *lac* operon is employed for this purpose. First, from the equations (8.4.1-8.4.1) $u = h(L)$ is set then,

$$\frac{dA}{dt} = -\widetilde{\gamma}_A A - B\beta_A g(A) + B\alpha_A u \tag{8.5.1}$$

$$\frac{dB}{dt} = -\widetilde{\gamma}_B B + \alpha_B M \tag{8.5.2}$$

$$\frac{dM}{dt} = -\widetilde{\gamma}_M M + \alpha_M f(A), \tag{8.5.3}$$

The objective is therefore, to design a controller u such that $A(t) \to A_{ref} = r$ when $t \to +\infty$ and r being constant. In the steady state

$$0 = \frac{dA_{ref}}{dt} = -\widetilde{\gamma}_A A_{ref} - B\beta_A g(A_{ref}) + B\alpha_A u \tag{8.5.4}$$

$$0 = -\widetilde{\gamma}_B B + \alpha_B M \tag{8.5.5}$$

$$0 = -\widetilde{\gamma}_M M + \alpha_M f(A_{ref}), \tag{8.5.6}$$

From equation (8.5.4),

$$\widetilde{\gamma}_A A_{ref} = -B\beta_A g(A_{ref}) + B\alpha_A u \tag{8.5.7}$$

$$\widetilde{\gamma}_B B = \alpha_B M \tag{8.5.8}$$

$$\widetilde{\gamma}_M M = \alpha_M f(A_{ref}). \tag{8.5.9}$$

This gives,

$$\widetilde{\gamma}_A A_{ref} = -B\beta_A g(A_{ref}) + B\alpha_A u,$$

$$B(\infty) = \frac{\alpha_B}{\widetilde{\gamma}_B \widetilde{\gamma}_M}(\alpha_M f(A_{ref})).$$

Hence,

$$u = \frac{\widetilde{\gamma}_B \widetilde{\gamma}_M \alpha_A}{\alpha_B(\alpha_M f(A_{ref}))} - (\widetilde{\gamma}_A A_{ref} + \frac{\alpha_B}{\widetilde{\gamma}_B \widetilde{\gamma}_M}(\alpha_M f(A_{ref}\beta_A g(A_{ref})). \tag{8.5.10}$$

However, since $u = h(L)$ and $h(L) = \frac{L}{K_L+L}$, then from equation 8.5.10 follows,

$$\frac{L}{K_L + L} = \frac{\widetilde{\gamma}_B \widetilde{\gamma}_M \alpha_A}{\alpha_B(\alpha_M f(A_{ref}))} - (\widetilde{\gamma}_A A_{ref} + \frac{\alpha_B}{\widetilde{\gamma}_B \widetilde{\gamma}_M}(\alpha_M f(A_{ref}\beta_A g(A_{ref})). \tag{8.5.11}$$

In other words,

$$L = \frac{uK_L}{(1-u)}.$$

On the other hand,

$$M(\infty) = \frac{\alpha_M}{\widetilde{\gamma}_M} f(A_{ref}) \tag{8.5.12}$$

$$B(\infty) = \frac{\alpha_B}{\widetilde{\gamma}_B} M(\infty). \tag{8.5.13}$$

$$\tag{8.5.14}$$

Thus from 8.5.12, one obtains,

$$M(\infty) = \frac{\alpha_M}{\widetilde{\gamma}_M} f(A_{ref}), \tag{8.5.15}$$

$$B(\infty) = \frac{\alpha_M \alpha_B}{\widetilde{\gamma}_B \widetilde{\gamma}_M} f(A_{ref}). \tag{8.5.16}$$

Note, that one has to ensure that u is less than 1, otherwise the controller will escape to infinity. This means that the controller is quite restrictive.

8.6 Simulation results

The observer and control design from section 8.4 and 8.5 are Simulated with simulink (Matlab).

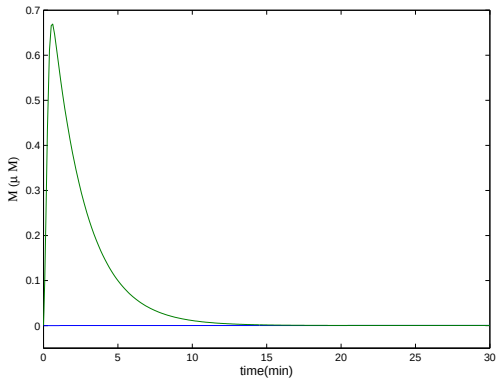

Figure 8.4: Observer design for mRNA $M\,(\mu M)$ concentration.

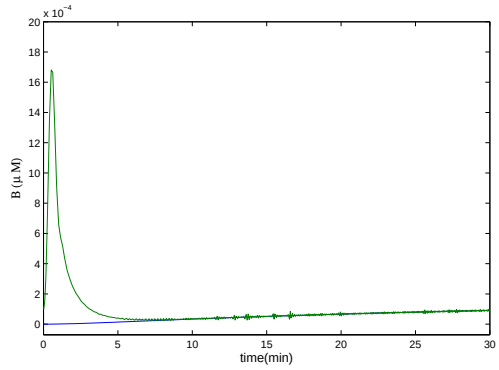

Figure 8.5: Observer design for $\beta-$galactosdase $B\,(\mu M)$ concentration.

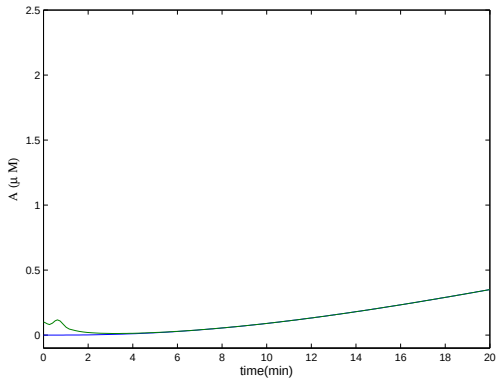

Figure 8.6: Observer design for allolactose $A\,(\mu M)$ concentration.

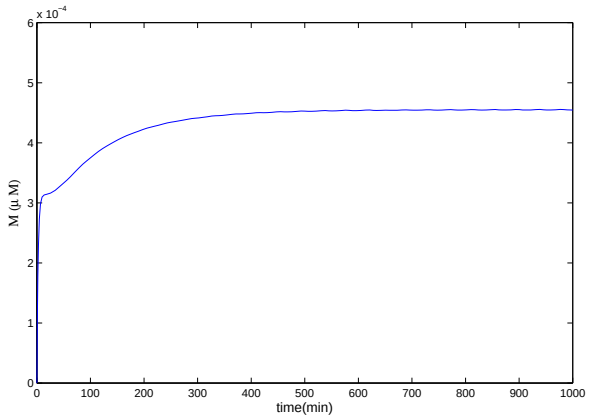

Figure 8.7: Control design for mRNA, $M\,(\mu M)$.

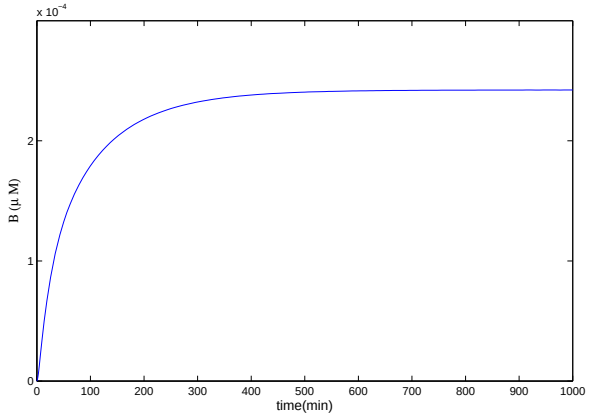

Figure 8.8: Control design for $\beta-$galactosdase, $B\,(\mu M)$.

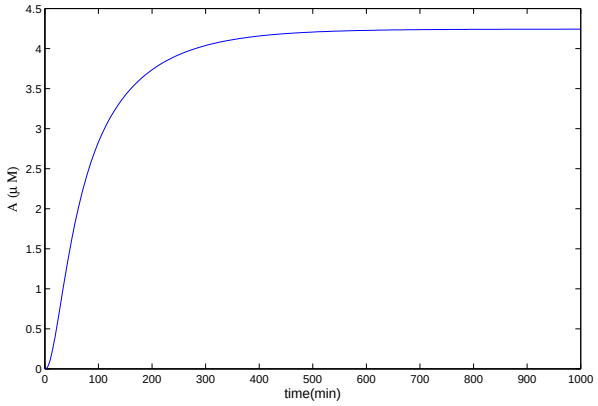

Figure 8.9: Control design for allolactose, $A\,(\mu M)$.

8.7 Summary

In the final part of this thesis, an observer design methodology is proposed in order to estimate the non-measured variables B and M of the *lac* operon by using the measurement of A and by using L as an input. For this purpose, the reduced and delay free model of the *lac* operon has been used. It is shown that this reduced model can be written in a state affine form. As a result, observer design method was used in the available literature for that purpose. Next, a controller was designed in order to regulate the A to a specific reference value. However, the proposed controller is quite restrictive. Nevertheless, as far as the author is aware, this is a first kind of work in this topic and further investigation is required in this area.

Chapter 9

Conclusion and Future Work

9.1 Conclusion

Two stochastic models (reduced and full) of the dynamics of gene regulation of the *lac* operon were developed by extending the deterministic models [11, 12] with noise terms.

The sufficient conditions of stochastic stability of the reduced and full models of the *lac* operon were obtained using Lyapunov functionals. Threshold values for the noise terms and delays were obtained. The numerical solution of the reduced and full Ito stochastic differential equations (6.2.1-6.2.3) and (7.2.1-7.2.5) respectively by the Euler Maruyama method have verified that the stability of the positive equilibrium depends on the values of the noise terms, time delays and the parameters of the system. Analytical and numerical solutions of the both models were obtained. An existence of bistable region was identified for certain lactose concentrations and the behaviour of the models investigated. The reduced and full deterministic models of the *lac* operon were simulated using Matlab with routine dde23, the evolution of the three steady states are illustrated in Chapter 4 and Chapter 5 Mostly, this work reproduced the results in [41, 42], however the evolution of unstable state is new. Finally, an estimate was made of the concentration of the mRNA (M) and the β-galactosidase (B) for the reduced model of the *lac* operon using the observer

method.

In Chapter 6 and 7, where the effect of the stochasticity on the dynamics of the reduced and full models of the *lac* operon were investigated respectively. The stochastic stability framework is useful in understanding the relative stability of equilibria point and allows to define more adequate description of the system. The stability around equilibrium in the presence of noise and time delays was investigated. The sufficient conditions of exponential mean square stability have been derived giving threshold values for the noise terms.

In the reduced model, if L lies in the bistable region the concentrations of allolactose, β- galoctosidase and mRNA can co-exist in two steady states. When there is an unstable steady state (for $L = 50$ mu M, M for example), it evolves to induced or uninduced state for the small or larger noise respectively. The model has shown that changes are most significant in allolactose when all concentrations M and B were perturbed with the same noise term. Similarly, in the full model, the concentrations of allolactose, β- galoctosidase, mRNA, lactose and permease can co-exist in two steady states if L_e lie in the bistable region. When there is an unstable steady state (for $L_e = 30$ mu M, P for example), it evolves to induced or uninduced state for the small or larger noise respectively. The model has shown that changes are most significant in allolactose and lactose when all concentrations M, B, A, L and P were perturbed with the same noise term.

The reduced model has shown that changes are most significant in allolactose when all three concentrations M, B and A were perturbed with the same noise term. In the full model, the changes of allolactose and lactose are most significant compared to the changes of other concentrations M, B, A, L and P.

The behaviour of the reduced model within the bistable region was thoroughly investigated. Near to equilibrium, when noise terms are below threshold values, the numerical simulations for values of L at or around the right boundary point of the bistable region confirm that the system can switch from uninduced to induced state even if the noise is small. Furthermore, numerical simulation shows that switching from induced to uninduced state occurs only at or around the left boundary point

for noise below threshold values, possibly due to low concentrations of lactose. When only allolactose is perturbed, a switch from uninduced state to induced (and vice versa) can occur within the bistable region when the perturbation is large (compared to threshold values for the noise terms and delays). Outside the bistable region, the concentrations oscillate around the stable state and for small concentrations of lactose the system remains uninduced. This behaviour, however, has been experimentally observed only for the artificial operon.

A very interesting result is that when only allolactose is perturbed, a switching from uninduced state to induced (and vice versa) can occur within the bistable region when the perturbation is large (compared to threshold values for the noise terms and delays). Outside the bistable region, the concentrations oscillate around the stable state and for small concentrations of lactose the system remains uninduced.

Similarly, numerical simulations for the full model were perform when values of L_e at or around the right and left boundary points of the bistable region, and confirm that the system can switch from uninduced to induced state and from induced to uninduced state respectively. However, when only allolactose is perturbed (large noise), switching inside bistable region has not been observed which is different from the reduced model. When allolactose and permease are perturbed, a switch from uninduced state to induced (and vice versa) can occur within the bistable region when the perturbation is large. Outside the bistable region, the concentrations oscillate around the stable state and for small concentrations of external lactose the system remains uninduced. The full model includes two positive feedbacks which are positive feedback regulation of mRNA production by allolactose and positive feedback lactose intake by permease as shown in Figure 4.1. Therefore, the reduced model is ignoring the positive feedback loop involving permease (Figure 5.1).

Thorough investigation of the stochastic stability of the reduced model of *lac* operon within and outside bistable region with respect to lactose concentration and noise terms demonstrates that the system behaviour is dependent on the lactose levels and perturbations. The noise has a strong effect for initial conditions close to the boundaries of the bistable region, where even small fluctuations can cause switching

between equilibrium states. Further, large perturbation of the allolactose may lead to switching inside the bistable region. As such, it was demonstrated that the stochasticity can change the behaviour in the bistable region, including switching due to the lactose concentration. While in the full model, the system behaviour is dependent on the external lactose levels and perturbations, large perturbation of the allolactose and permease may lead to switching inside the bistable region. For example, it was demonstrated that the stochasticity can change the behaviour in the bistable region, including switching due to the external lactose concentration. This has only been observed experimentally for artificial sugars.

The *lac* operon has the potential for bistability because of an inherent positive feedback loop. The bistability has been theoretically predicated by Yildirim and Mackey [11, 12] for natural inducer (lactose). This, however, has been experimentally observed only for artificial inducer [18] and the importance of noise investigated by the some authors in [39, 10].

One of the main conclusions of the thesis is that the stochasticity can change the boundaries of the bistable region in both models of the *lac* operon which cannot be obtained in the case of the deterministic models of the *lac* operon.

Finally, a design of observer is presented for the reduced model without time delay is designed to estimate the concentration of the mRNA M and the β-galactosidase B by using the measurement of A and by using L as an input. As shown in figures (Chapter 8) the observer converges to the true state of the system. Also, a state feedback controller is designed for the *lac* operon which regulates allolactose to a specific reference value while maintaining M, B are bounded. The observer method is very promising way to estimate model parameters which are difficult to measure.

9.1.1 Contributions of the thesis

- The sufficient conditions of the mean square stability of the reduced and full model of the *lac* operon were obtained using Lyapunov functional and Ito

stochastic differential equations. Threshold values for the noise terms and delays were obtained for both models. The results have verified that the stability of the positive equilibrium depends on the values of the noise terms, time delays and the parameters of the system.

- The coordinates of the state for both models move in a synchronized mode and the system shows identical behaviour. All the coordinates of the state are induced or uninduced in a synchronization behaviour.

- For low concentrations of lactose and external lactose for reduced and full model respectively, numerical simulation shows that switching from induced to uninduced state occurs only at or around the left boundary point of the bistable region.

- For large values of lactose and external lactose for reduced and full model respectively, numerical simulation shows that switching from uninduced to induced state, occurs only at or around the right boundary point of the bistable region.

- Numerical simulation for the reduced model when only allolactose was perturbed (the inner feedback loop), shows that for lactose values in the bistable region switching occurs from uninduced state to induced (and vice versa). Whereas, in the full model (two feedback loops by allolactose and permease), for values of external lactose inside bistable region switching has not been observed when only allolactose is perturbed. However, when allolactose and permease are perturbed, a switch from uninduced state to induced (and vice versa) can occur when the perturbation is large.

- The reduced model of the *lac* operon can be written in a state affine using observer design. A controller was designed in order to regulate the allolactose to a specific reference value.

9.2 Future work

This thesis has presented a model of the *lac* operon written in a state-affine form, and presented a new behaviour for the stochastic models of the *lac* operon. Promising results have been obtained, however there are some suggestions for the future work to improve the performance of the models.

- The behaviour of the *lac* operon model with and without time delays are shown in Figure 9.1 a) the reduced model of the *lac* operon with two time delays and same noise terms to all three equations ($\sigma_1 = \sigma_2 = \sigma_3 = 0.01$), Figure 9.1 b) the reduced model without time delays and with same noise terms to all three equations ($\sigma_1 = \sigma_2 = \sigma_3 = 0.01$).

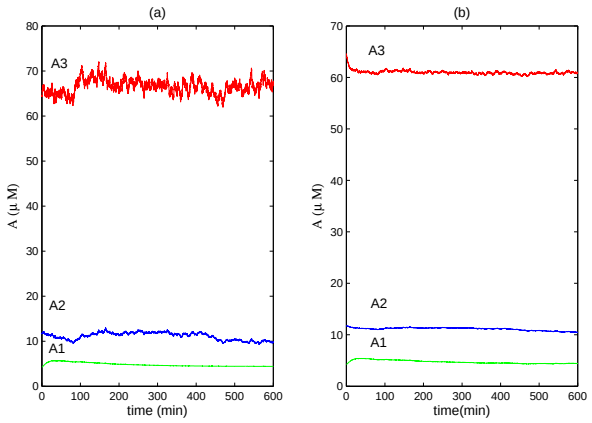

Figure 9.1: Stochastic reduced model of the *lac* operon showing allolactose when $L = 50\mu M$. a) with time delays and b) without time delay.

  The figures show that the time delays play a significant role in the dynamics and behaviour of the system. Therefore, an investigation between the delay differential equation and stochastic delay differential equations are required for the model to study how time delays affect the system's behaviour.

- From the reduced model of the *lac* operon (system 5.2.1-5.2.3), one can assume that $\tau_M = \tau_B = 0$ and the rate of loss (degradation) of mRNA is greater than the corresponding loss rates for β- galactosidase and allolactose ([58]), where

$\gamma_M > \gamma_B > \gamma_A$. Therefore the approximate relationship for the dynamics of mRNA is

$$M \simeq \gamma_M f(A). \tag{9.2.1}$$

Then, the three equations of the model reduce to two equations:

$$dB = \gamma_B[\gamma_1 f(A) - B] \tag{9.2.2}$$

$$dA = \gamma_A[f(B) - A]. \tag{9.2.3}$$

When $\gamma_B > \gamma_A$ and $B \simeq A$. The two equations (9.2.2,9.2.3) reduce to one variable system (dimensional)

$$\frac{dB}{dt} = \gamma_B[\gamma_M f(B) - B]. \tag{9.2.4}$$

Alternatively, in the case when $\gamma_A > \gamma_B$ then $A \simeq B$. The system (9.2.2,9.2.3) reduces to a one variable (dimensional)

$$\frac{dA}{dt} = \gamma_A[\gamma_M f(A) - A]. \tag{9.2.5}$$

In Equation 9.2.4 and Equation 9.2.5, one can write both equations of the form

$$\frac{dy}{dt} = \gamma[\gamma_M f(x) - x]. \tag{9.2.6}$$

Where γ denotes protein B (γ_B), or protein A (γ_A).
The one dimensional stochastic differential equation of the form

$$dx(t) = \varphi(x)dt + \sigma(x)dw(t). \tag{9.2.7}$$

Where w is an one dimensional standard Wiener process (whose increment is Gaussian process $\Delta w(t) = w(t + \Delta t) - w(t) \sim \sqrt{\Delta t}$) In Equation 9.2.6, one can examine the situation in which fluctuations appear in γ. Assume the fluctuations are Gaussian process with mean number of proteins degradation, where the standard deviation of these number is approximation to $\sqrt{x}$. The stochastic differential equation is

$$d(x) = \gamma[\gamma_1 f(x) - x] + \sigma\sqrt{x}dw. \tag{9.2.8}$$

The probability density function is a function that describes the proportional probability for this random variable. The Fokker Planck equation

$$\frac{\partial u}{\partial t} = -\frac{\partial(\varphi u)}{\partial x} + \frac{1}{2}\frac{\partial^2(\sigma^2 u)}{\partial x^2}. \tag{9.2.9}$$

One can study the stability of Ito stochastic differential equation (using 9.2.8) corresponding to Fokker Planck equation (9.2.9) that regulates the probability distribution of the random variable.

$$\frac{\partial u}{\partial t} + \frac{\partial(\gamma[\gamma_M f(x) - x])u}{\partial x} = \frac{\sigma^2}{2}\frac{\partial^2(xu)}{\partial x^2}. \tag{9.2.10}$$

The Equation 9.2.10 has a corresponding Fokker Planck equation for the evolution of the ensemble density u, this equation of the *lac* operon describes the change in probability distribution and leads to a certain partial differential equation of the probability distribution. The solution of the Fokker Planck problem is a new challenge and the next step leading to the stochastic model of the *lac* operon.

Publications of Asma Ben Halim

- Journal Papers Published:

  1. M.Angelova and A. Ben-Halim. Dynamic model of gene regulation for the *lac* operon. Journal of Physics Conf Series 286, doi: 10.1088/1742-6596/286/1/012007.

- Journal Papers in Preparation:

  1. Asma ben-Halim, Maia Angelova, Krishna Busawon and Tania Pencheva. Stochastic stability of the *lac* operon: Investigation of the bistable region. In preparation for submission in J Math Biology

  2. Asma ben-Halim, Maia Angelova, Krishna Busawon. Development of dynamic stochastic models with time delays of the *lac* operon. In preparation for submission in J Mathematical Biology

  3. Asma ben-Halim, Maia Angelova, Krishna Busawon. Observer design of the *lac* operon model. In preparation for submission for J Mathematical Biosciences

- Conference Presentations (Talks and Posters):

  Asma ben Halim. Stochastic stability of the *lac* operon. Mathematics of Human Biology 6-8 June 2012, Newcastle upon Tyne.

  Asma ben Halim. Stochastic model for the *lac* operon. Northumbria Research Conference, 11 May 2012, Newcastle upon Tyne.

  Asma ben Halim. Mathematical Modeling of Genetic regulatory Networks. Warwick Research Conference, December 2010.

- Seminars given:

  1. Dundee November 2012. Models of Multi-Stability Switches: Case Study for

the *lac* operon .

2. Northumbria March 2012, February 2013. Stability of a stochastic model for the *lac* operon.

3. MATSIQEL, Final meeting, 17 January 2014. Stochastic for the *lac* operon models.

References

[1] B. C. Goodwin. Control dynamics of -galactosidase in relation to the bacterial cell cycle. *European Journal of Biochemistry*, 10:515–522, 1969.

[2] G. Yagil and E. Yagil. On the relation between effector concentration and the rate of induced enzyme synthesis. *Biophysical Journal*, 11:11 – 27, 1971.

[3] F. Jacob and J. Monod. Genetic regulatory mechanisms in the synthesis of proteins. *Journal of molecular biology*, 3:318–356, 1961.

[4] J. S. Griffith. Mathematics of cellular control processes ii. positive feedback to one gene. *Journal of Theoretical Biology*, 20(2):209 – 216, 1968.

[5] Arthur B. Pardee, Francois Jacob, and Jacques Monod. The genetic control and cytoplasmic expression of inducibility in the synthesis of beta-galactosidase by e. coli. *Journal of Molecular Biology*, 1(2):165 – 178, 1959.

[6] J. D. Murray. *Mathematical Biology I. An Introduction*, volume 17. Springer, New York, 3 edition, 2002.

[7] J. M. Bower and B. Hamid. *Computational Modeling of Genetic and Biochemical Networks (Computational Molecular Biology)*. The MIT Press, 2004.

[8] E. Klipp, R. Herwig, A. Kowald, C. Wierling, and H. Lehrach. *Systems Biology in Practice: Concepts, Implementation and Application*. Wiley-VCH, 2005.

[9] A. Babloyantz and M. Sanglier. Chemical instabilities of all-or-none type in beta-galactosidase induction and active transport. *FEBS Lett.*, 23:364–366, 1972.

[10] E. M. Ozbudak, M. Thattai, H. N. Lim, B. I. Shraiman, and O. A. Van. Multistability in the lactose utilization network of escherichia coli. *Nature*, 427:737–40, 2004.

[11] N. Yildirim and M. C. Mackey. Feedback regulation in the lactose operon: A mathematical modeling study and comparison with experimental data. *Biophys. J*, 84:2841–2851, 2003.

[12] N. Yildirim, M. Santilln, D . Horike, and M. C. Mackey. Dynamics and bistability in a reduced model of the lac operon. *Chaos*, 14:279–292, 2004.

[13] Jose. M. Vilar, Calin. C. Guet, and Stanislas. Leibler. Modeling network dynamics: the lac operon, a case study. *The Journal Of Cell Biology*, 161:471–476, 2003.

[14] Andrzej. M. Kierzek, Jolanta. Zaim, and Piotr. Zielenkiewicz. The effect of transcription and translation initiation frequencies on the stochastic fluctuations in prokaryotic gene expression. *Journal of Biological Chemistry.*

[15] D. J. Wilkinson. *Stochastic Modelling for Systems Biology (Chapman & Hall/CRC Mathematical & Computational Biology).* Chapman and Hall/CRC, 1 edition, 2006.

[16] Joseph M. Mahaffy and Emil Simeonov Savev. Stability analysis for a mathematical model of the lac operon. *Q. Appl. Math.*, LVII(1):37–53, 1999.

[17] M. Santilln and M. C. Mackey. Influence of catabolite repression and inducer exclusion on the bistable behavior of the lac operon. *Biophysical Journal*, 86:1282–1292, 2004.

[18] A. Novick and M. Weiner. Enzyme induction as an all-or-none phenomenon. *Proceedings of the National Academy of Sciences*, 43(7):553–566, 1957.

[19] M. Santilln, M. C. Mackey, and E. S. Zeron. Origin of Bistability in the lac Operon. *Biophysical Journal*, 92:3830–3842, 2007.

[20] M. Santilln. Bistable Behavior in a Model of the lac Operon in Escherichia coli with Variable Growth Rate. *Biophysical Journal*, 94:2065–2081, 2008.

[21] E.M. Ozbudak, M. Thattai, I. Kurtser, A.D. Grossman, and A. van Oudenaarden. Regulation of noise in the expression of a single gene. *Nat Genet*, 31:69–73, 2002.

[22] Michael. B. Elowitz, Arnold. J. Levine, Eric. D. Siggia, and Peter. S. Swain. Stochastic gene expression in a single cell. *Science*, 297:1183–1186, 2002.

[23] M. A. Gilbson and E. M. Jolsness. Computational modeling of genetic and biochemical networks (computational molecular biology), james m. b and hamid. b. In *Modeling of Activity of Single Gene*, pages 4–48. The MIT Press, 2001.

[24] M. Ptashne. *A genetic switch: phage lambda revisited*. Cold Spring Harbor Laboratory Press, 2004.

[25] M. Santillan and M. Mackey. Dynamic regulation of the tryptophan operon: A modeling study and comparison with experimental data. *Proceedings of the National Academy of Sciences of the United States of America*, 98(4):1364–1369, 2001.

[26] J. D. Murray. *Mathematical Biology: I. An Introduction (Interdisciplinary Applied Mathematics) (Pt. 1)*. Interdisciplinary applied mathematics. Springer, 3rd edition, 2007.

[27] R.D. Levine. *Molecular Reaction Dynamics*. Cambridge University Press, 2005.

[28] Marcello Farina and Maria Prandini. Hybrid models for gene regulatory networks: The case of lac operon in e. coli. volume 4416, pages 693–697, 2007.

[29] E. Almaas, B. Kovacs, T. Vicsek, Z. N. Oltvai, and A-L. L. Barabasi. Global organization of metabolic fluxes in the bacterium Escherichia coli. *Nature*, 427:839–843, 2004.

[30] J. M. Mahaffy. Cellular control models with linked positive and negative feedback and delays. ii. linear analysis and local stability. *Journal of Theoretical Biology*, 106:103–118, 1984.

[31] M. Santilln and M. C. Mackey. Quantitative approaches to the study of bistability in the lac operon of escherichia coli. *Journal of the Royal Society Interface the Royal Society*, 5 Suppl 1:S29–S39, 2008.

[32] S. Nikolov, J. Vera, V. Kotev, O. Wolkenhauer, and V. Petrov. Dynamic properties of a delayed protein cross talk model. *Biosystems*, 91:51–68, 2008.

[33] A. Maia and A. H. Asma. Dynamic model of gene regulation for the lac operon. *Journal of Physics: Conference Series*, 286(1):012007, 2011.

[34] Jerome. T. Mettetal, Dale. Muzzey, Juan. M. Pedraza, Ertugrul. M. Ozbudak, and Alexander. van Oudenaarden. Predicting stochastic gene expression dynamics in single cells. *Proceedings of the National Academy of Sciences of the United States of America*, 103(19):7304–7309, 2006.

[35] J. Paulsson. Models of stochastic gene expression. *Physics of Life Reviews*, 2:157–175, 2005.

[36] H. H. McAdams and A. Arkin. Stochastic mechanisms in geneexpression. *Proceedings of the National Academy of Sciences of the United States of America*, 94:814–819, 1997.

[37] Peter. S. Swain, Michael. B. Elowitz, and Eric. D. Siggia. Intrinsic and extrinsic contributions to stochasticity in gene expression. *Proceedings of the National Academy of Sciences*, 99:12795–12800, 2002.

[38] T. A. Carrier and J. D. Keasling. Investigating autocatalytic gene expression systems through mechanistic modeling. *J Theor Biol*, 201:25–36, 1999.

[39] Milan. Van Hoek and Paulien. Hogeweg. The effect of stochasticity on the lac operon: An evolutionary perspective. *PLoS Comput Biol*, 3:1071–1082, 2007.

[40] M. J. A. Van Hoek and P. Hogeweg. In silico evolved lac operons exhibit bistability for artificial inducers but not for lactose. *Biophys J*, 91:2833–2843, 2006.

[41] Anna. Ochab-Marcinek. Predicting the asymmetric response of a genetic switch to noise. *J Theor Biol*, 254:37–44, 2008.

[42] Anna. Ochab-Marcinek. Extrinsic noise passing through a michaelis-menten reaction: a universal response of a genetic switch. *J Theor Biol*, 263:510–20, 2010.

[43] Hunter. B. Fraser, Aaron. E. Hirsh, Guri. Giaever, Jochen. Kumm, and Michael. B. Eisen. Noise minimization in eukaryotic gene expression. *PLoS Biol*, 2:e137, 2004.

[44] M. Stamatakis and N. V. Mantzaris. Comparison of deterministic and stochastic models of the lac operon genetic network. *Biophysical Journal*, 96:887 – 906, 2009.

[45] B. S. Chen and Y. T. Chang. A systematic molecular circuit design method for gene networks under biochemical time delays and molecular noises. *BMC Systems Biology*, 2:103, 2008.

[46] V. B. Kolmanovskii and V. R. Nosov. *Stability of functional differential equations* . Academic press, NewYork, 1986.

[47] L. Shaikhet. Stability in probability of nonlinear stochastic systems with delay. *Mathematical Notes*, 57:103–106, 1995.

[48] L. Shaikhet. *Lyapunov Functionals and Stability of Stochastic Difference Equations*. Springer-Verlag, London, 2011.

[49] M. Carletti. Mean-square stability of a stochastic model for bacteriophage infection with time delays. *Mathematical Biosciences*, 210:395 – 414, 2007.

[50] D. H. Ballard. *An introduction to natural computation*. MIT Press, 1999.

[51] Tian. Tianhai, Burrage. Kwvin, M. Burrage. Pamela, and Carletti. Margherita. Stochastic delay differential equations for genetic regulatory networks. *Journal of Computational and Applied Mathematics*, 205:696–707, 2007.

[52] R. Kalman. On the general theory of control systems. *Ire Transactions on Automatic Control*, 4:110–110, 1959.

[53] D.G. Luenberger. Observer the state of a linear systems. *Trans.Mil.Electron, IEEE Transactions on*, MIL-8:74–80, 1964.

[54] M. Darouach. Existence and design of functional observers for linear systems. *Automatic Control, IEEE Transactions on*, 45(5):940–943, 2000.

[55] J.-P. Gauthier, H. Hammouri, and S. Othman. A simple observer for nonlinear systems applications to bioreactors. *Automatic Control, IEEE Transactions on*, 37(6):875–880, 1992.

[56] Wei Ren. Cooperative control design strategies with local interactions. In *Networking, Sensing and Control, 2006. ICNSC '06. Proceedings of the 2006 IEEE International Conference on*, pages 451–456, 2006.

[57] H. Hammouri and J. de Leon Morales. Observer synthesis for state-affine systems. In *Decision and Control, 1990., Proceedings of the 29th IEEE Conference on*, pages 784–785 vol.2, 1990.

[58] C. Mackey. Michael, Tyran-Kaminska. Marta, and Yvinec. Romain. Molecular distributions in gene regulatory dynamics. *Journal of Theoretical Biology*, 274:84 – 96, 2011.

[59] P. Smith. *Nonlinear ordinary differential equations: an introduction to dynamical systems*, volume 2. Oxford University Press, 1999.

[60] D.K. Arrowsmith and C.M. Place. *Dynamical Systems: Differential Equations, Maps, and Chaotic Behaviour*. Chapman Hall/CRC Mathematics Series. Chapman & Hall, 1992.

[61] Peter J. Olver. *Applications of Lie Groups to Differential Equations*. sv, ny, 1986.

[62] A. Bacciotti and L. Rosier. *Liapunov Functions and Stability in Control Theory*. Lecture Notes in Control And Iinformation Sciences. SPRINGER VERLAG GMBH, 2001.

[63] Thomas L. Vincent and Walter J. Grantham. *Nonlinear and Optimal Control Systems*. John Wiley & Sons, Inc., New York, NY, USA, 1st edition, 1999.

[64] R. S. Liptser and A. N. Shiriaev. *Statistics of random processes / R. S. Liptser, A. N. Shiryayev ; translated by A. B. Aries*. Springer-Verlag, New York, 1977.

Appendix A

Mathematical tools

A.1 Steady state

The notion of steady states (fixed points) is important for dynamic systems. Steady states are determined by the fact that values of all state variables remain constant in time, thus the behaviour after an adequately long time is often stationary. Although the concept of stationary states is mathematical, it is important in kinetic models since it points to typical behavioural modes of the system investigated and the respective mathematical problems that are frequently easier to solve. Differential equations are the description of the change of the state (see Section 3.2.3) of variables; for this the modelling of biological systems is to characterize the dependence of certain properties on time and space [8].

Klipp et al. [8] have explained the steady state for the system of first order of nonlinear ordinary differential equations (ODEs) as follows,

$$\dot{x} = f(x).$$

Steady state points are obtained by solving $f(x_*) = 0$, or equivalently $\dot{x} = 0$ (the value of x satisfy $f(x_*) = 0$). The disturbance about the steady state points is $x = x_* + X$, then a linearization is given by $\dot{X} = J.X$, where

$$J = (\frac{\partial f_i}{\partial x_j})_{(i,j)}.$$

Below are the definitions of stable and asymptotically stable solutions for the system of first order ordinary differential equations:

Definition 1. *[59], The steady state x_* of the system $\dot{x} = f(x)$ is said to be stable if for every $\delta > 0$, $t_0 \geq 0$, there exits a $\sigma > 0$ such that every solution $x(t)$ having initial conditions within $\| x(t_0) - x_* \| < \sigma \Rightarrow \| x(t) - x_* \| < \delta$, for all $t \geq t_0$.*

Definition 2. *[59], The steady state x_* of the system $\dot{x} = f(x)$ is said to be asymptotically stable if it is stable and there exists $\sigma_0 > 0$ such that $\| x(t_0) - x_* \| < \sigma_0$, then $x(t)$ approaches x_* as t tends to infinity.*

The steady state is locally stable if the Jacobian J has eigenvalues with negative real parts. The steady state is unstable if at least one eigenvalue has a positive real part (Lyapunov's first order). Thus, if the steady state is stable, the dynamic system returns to this state; if unstable, the system leaves this state.

Thus, although solutions near a stable equilibrium may drift slightly farther away, they must remain relatively close. In the case of asymptotic stability, they will eventually return to equilibrium ([60, 61]). This is illustrated in Figure A.1.

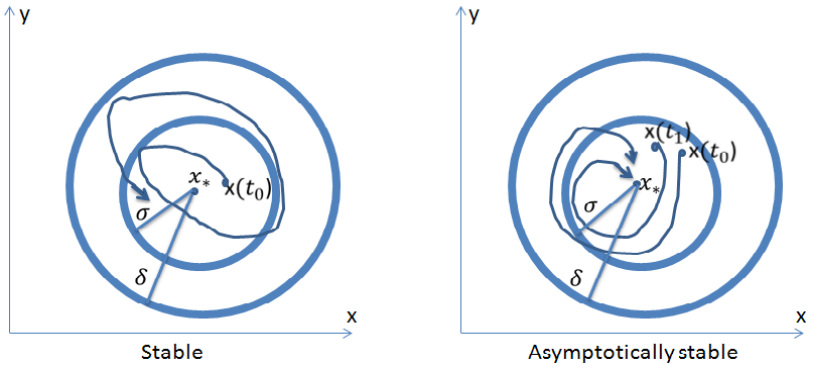

Figure A.1: Schematic representations of stability and asymptotic stability with an equilibrium point.

For a system of n differential equations, the characteristic of the stability is through the eigenvalues λ, which are the roots of the characteristic polynomial,

$$\lambda^n + a_1\lambda^{n-1} + ... + a_{n-1}\lambda + a_n = 0, \quad a_i = 0, 1, 2, ..., n$$

This is a polynomial of degree n. One method to understand the concept of stable state and analyse the stability problem is using the Routh-Hurwitz conditions, which are the necessary and sufficient conditions for λ to fulfil [6].

$$\Delta_1 = a_1 > 0$$

$$\Delta_2 = \begin{pmatrix} a_1 & a_3 \\ 1 & a_2 \end{pmatrix} > 0.$$

$$\Delta_3 = \begin{pmatrix} a_1 & a_3 & a_5 \\ 1 & a_2 & a_4 \\ 0 & a_1 & a_3 \end{pmatrix} > 0, ...\Delta_n > 0.$$

$$\Delta_4 = \begin{pmatrix} a_1 & a_3 & a_5 & . & . \\ 1 & a_2 & a_4 & . & . \\ . & . & . & . & . \\ 0 & 0 & . & . & a_k \end{pmatrix} > 0, ...k = 1, ...n$$

A.2 Lyapunov function

The concept of a Lyapunov function is widely known, and one of the most important methods in the analysis of dynamical systems. Lyapunov function proves the stability of equilibria points in nonlinear systems. There are two approaches to study the stability of continuous dynamical systems, known as Lyapunov's first order (indirect method) and the Lyapunov's second order (direct method). The first method, as mentioned in A.1, but is unsatisfactory when the linearized system has imaginary eigenvalues. The second method enables one to prove the stability of an equilibrium of a nonlinear system without integrating the differential equation and this is a great advantage in this case of nonlinear systems. By using the direct method for any differential equations, one is able to find Lyapunove function ($V(x)$) such that $V(x) > 0, \quad x \neq 0$, along the trajectories $\frac{d}{dt}V(x(t))$ is smaller than zero $V(x) < 0, \quad x \neq 0$. There are many different types for Lyapunov theorems; see for instance [62, 63].

A.3 Stochastic stability

The stochastic behaviour is accounted for by adding a noise term to the deterministic differential equations. Noise is usually present in any real life system, so it is possible to study how random noise can change the behaviour in the dynamical models. The noise term can be constructed using the Wiener process [64].

Consider the stochastic functional differential equations of the form,

$$\begin{aligned} x_t = \quad & x_0 + \int_0^t f(s, x_s)ds + \sum_{j=1}^{n} \int_0^t g_j(s, x_s)dw_j(s), \quad s \geq 0 \\ x_0 = \quad & \varphi = \{\varphi(\theta) : \theta \in J,\ J = [-\tau, 0], \tau \geq 0\}. \end{aligned} \tag{A.3.1}$$

Here $(w_1(t), ..., w_n(t))$ be an n-dimensional standard Wiener process (whose increment is Gaussian process $\Delta w_j(t) = w_j(t + \Delta t) - w_j(t) \sim \sqrt{\Delta t}N(0, 1)$) on the probability space $[\Omega, \xi, \{\xi_t\}_{0 \leq t < \infty}, P]$ with filtration $\{\xi_t, t \geq 0\}$. Let $C = C(J, R^m)$ indicates the family of all continuous functions from J to R^m with the supremum norm $\|\varphi\| = \sup_{\theta \in J}|\varphi(\theta)|$, where $f : R^+ \times C \to R^m$, $g : R^+ \times C \to R^{m \times n}$ and $x_s = \{x(s + \theta) : \theta \in J\}$ is a C valuated random process and $x_0 \in \digamma$. Here $\digamma$ is the space of ξ_0-adapted function $\varphi \in C$, such that the solution of (A.3.1) satisfies $E|\varphi|^2 < \infty$, where E is the mathematical expectation [46, 47].

Theorem A.3.1. *Assume there exist a continuous functional $K(t, \varphi) \in C^{2,1}$ such that for any solution of (A.3.1) the following inequalities hold*

$$\begin{aligned} W_1|\varphi|^2 \leq K(t, \varphi) \leq W_2|\varphi|^2 \\ LK(t, \varphi) \leq -W_3|\varphi|^2. \end{aligned} \tag{A.3.2}$$

Then the trivial solution is exponentially mean square stable.

Here $C^{2,1}$ is the Banach space of all positive and continuous functions $K(t, \varphi)$ for $t \geq 0$, W_1, W_2 and W_3 are positive constants. The functions are twice continuously differentiable with respect to x and have one bounded derivative with respect to t. Then, the generating operator L for K of Equation A.3.1 is

$$LK(t, \varphi) = \frac{\partial K(t, \varphi)}{\partial t} + f^T(t, \varphi)\frac{\partial K(t, \varphi)}{\partial x} + \frac{1}{2}Trace[g^T(t, \varphi)\frac{\partial^2 K(t, \varphi)}{\partial x^2}g(t, \varphi)].$$